COORDINATION AND CYCLOMETALLATED RUTHENIUM COMPLEXES WITH SOME HYDRAZONE LIGANDS

A THESIS

SUBMITTED FOR THE DEGREE OF

DOCTOR OF PHILOSOPHY

By

NAGARAJU KOPPANATHI

SCHOOL OF CHEMISTRY

UNIVERSITY OF HYDERABAD

HYDERABAD – 500 046

INDIA

OCTOBER 2013

Dedicated to

My Parents,
Teachers
and friends

CONTENTS

STATEMENT

I hereby declare that the matter embodied in this thesis entitled "**Coordination and Cyclometallated Ruthenium Complexes with Some Hydrazone Ligands"** is the result ofthe investigation carried out by me in the School of Chemistry, University of Hyderabad,under the supervision of **Prof. Samudranil Pal**.

In keeping the general practice of reporting scientific observation, due acknowledgement has been made wherever the work described is based on findings of other investigations. Any omission which might have occurred by oversight or error is regretted.

October 2013 **K Nagaraju**

UNIVERSITY OF HYDERABAD
Prof. Samudranil Pal

SCHOOL OF CHEMISTRY
HYDERABAD 500 046, INDIA

Fax: +91-40-2301-2460, Phone: +91-40-2313-4829, E-mail: spal@uohyd.ac.in

25th October, 2013

CERTIFICATE

Certified that the work embodied in the thesis entitled "**Coordination and Cyclometallated Ruthenium Complexes with Some Hydrazone Ligands**" has been carried out by **Mr. K Nagaraju** under my supervision and the same has not been submitted elsewhere for any degree.

Prof. Samudranil Pal
(Thesis Supervisor)

Dean
School of Chemistry
University of Hyderabad

ACKNOWLEDGEMENTS

With high regards and profound respect, I wish to express my deep sense of gratitude to **Prof. Samudranil Pal** for his guidance, encouragement and valuable suggestions throughout my research work. It is a great privilege for me to work with him throughout the course of my work and quite helpful in improving my confidence, patience and communication skills.

I thank Prof. M. V. Rajasekharan, Dean, School of Chemistry, for providing me the facilities needed for my research. I extend my sincere thanks to former Deans and all the faculty members for their cooperation on various aspects.

I am deeply indebted to all my teachers right from my school to University for the support and training I received throughout my academic career.

I am thankful to my former lab-mates Dr. Raji Raveendran, Dr. Anindita Sarkar Dr. Tulika Ghosh and Dr. Swamy Malothu for their cooperation in the lab. I acknowledge help from my present lab-mates: A.R. Balavardhana Rao, K. Sathish Kumar G. Narendra Babu and Dr. Rupesh N. Prabhu. All of them have been helpful in creating a pleasant work atmosphere.

I would like to express my sincere gratitude to *all my friends in School of Chemistry (present and former)* and friends in University of Hyderabad. All of them have been very kind, generous, affectionate and helpful.

Friends are naturally lot and it is indeed a difficult task to mention them all here. I acknowledge whole-heatedly each and every one of them. Especially Ramesh, Rambabu, GDP, Kishor, Ramakrishna Nandamuri, Murali, Giri, Balaram and Ramesh Kola for many reasons. I specially thank my beloved 'TV-room' friends GB, Vijji, Nagarajuna, PSR, Bharani, Narayana, Vijji (macha), Srinu. K, Chandu and Ashok for making my stay in the campus unforgettable.

I also thank all the non-teaching staff of the School of Chemistry for their help in many ways. It is my privilege to acknowledge Suresh (EPR), Mr. Vara Prasad, Mr. Bhaskar Rao, Mrs. Asia Parwez, Dr. P. Raghavaiah, Kumar, Mr. Shetty, Mr. Venkataramana, Mr. Durgesh, Mr. Chittibabu and Mr. Venkateswararao.

I thank Council of Scientific and Industrial Research (CSIR, New Delhi) and Department of Science and Technology (DST, New Delhi) for financial support. I thank Department of Science and Technology (New Delhi) for the Single Crystal X-ray Diffractometer Facility at the University of Hyderabad and UGC for providing many other research facilities.

Lastly, I would like to express my heartfelt thanks to my parents Venkateswara Rao K, Vedavati and my wife Girija and daughter Pravalika for their enormous love, kindness, faith on me. I specially thank my sister (Kumari), brother-in-law (Narayana Rao), sweety, sunny and my brother Gopalakrishna for their love and affection along this journey. Thank you

Nagaraju Koppanathi

SYNOPSIS

Chapter 1

In this chapter, the relevance of ruthenium coordination complexes has been briefly elaborated. The objectives of the present investigation in the context of known ruthenium Schiff base complexes have been stated.

Chapter 2

Ruthenium(III) complexes, $[Ru(L^n)_2]ClO_4$ with *N*-(2-pyridyl)-*N′*-(5-*R*-salicylidene)-hydrazines (HL^n; *R* = H, Cl, Br, Me and OMe) have been synthesized (Scheme 1). Microanalysis (C,H,N), magnetic susceptibility and various spectroscopic (IR, UV-Vis and EPR) measurements have been used for

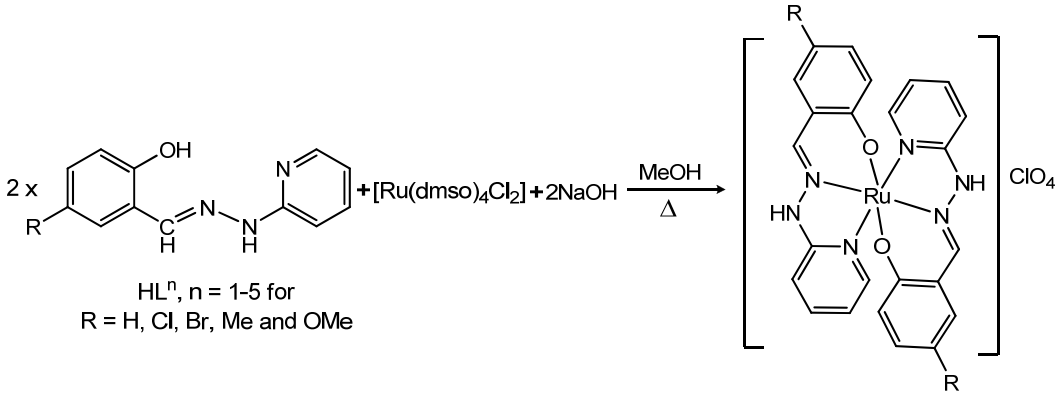

Scheme 1

the characterization of these complexes. The molecular structures of all the complexes except for the complex where *R* = Br have been confirmed by single crystal X-ray diffraction study. The metal centres in these complex cations are in distorted octahedral N_4O_2 coordination sphere assembled by the pyridine-N, the imine-N and the phenolate-O donor $(L^n)^-$ ligands. Intermolecular hydrogen-bonding assisted supramolecular structures formed by the solvated complexes range from dimeric to one-dimensional chain to two-dimensional sheet structures.

Chapter 3

Reactions of $[Ru(PPh_3)_3Cl_2]$ with 1-pyrenaldehyde 4-*R*-benzoylhydrazones (H_2pnbh*R*, where *R* = H, Me, OMe, Cl and NO_2) in presence of NaOAcafford *ortho*-metallated ruthenium(III) complexes of formula *trans*-[Ru(pnbh*R*)$(PPh_3)_2$Cl] (**1**–**5**)(Scheme 2). The complexes have been characterized

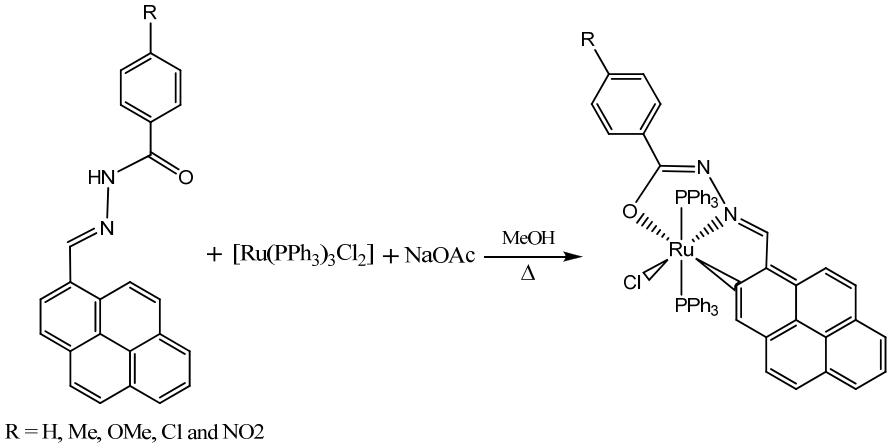

Scheme 2

by elemental analysis, magnetic susceptibility, spectroscopic (IR, UV-Vis and EPR) and cyclic voltammetric measurements. Molecular structure of **2** (*R* = Me) determined by single crystal X-ray crystallography shows a distorted octahedral $CNOClP_2$ coordination sphere around the trivalent metal centre assembled by the 1-pyrenyl *ortho*-C, azomethine-N and amidate-O donor pnbhMe^{2-}, two mutually *trans* PPh_3 and the chloride. Electronic spectra of **1**–**5** in dichloromethane display several strong bands within 555−276 nm due to ligand to metal charge transfer and ligand centred transitions. The complexes are one-electron paramagnetic (μ_{eff} = 1.90−1.99 μ_B) and display rhombic EPR spectra in frozen (130 K) dichloromethane-toluene (1:1). Cyclic voltammograms of the complexes in dimethylformamide display a ligand substituent sensitive metal centred one electron reduction couple in the $E_{1/2}$ range −0.24 to −0.31 V (vs. Ag/AgCl).

Chapter 4

In methanol, reactions of $[Ru(PPh_3)_3Cl_2]$, 1-naphthaldehyde 4-*R*-benzoylhydrazones (H_2nabh*R*, where *R* = H, Me, OMe, Cl and NO_2) and NaOAc in 1:1:2 mole ratio provide *ortho*-metallated ruthenium(III) complexes of general formula *trans*-[Ru(nabh*R*)$(PPh_3)_2$Cl] (**1**–**5**) in 50–58% yields (Scheme 3). Elemental analysis, magnetic susceptibility, spectroscopic (IR, UV-Vis and EPR)

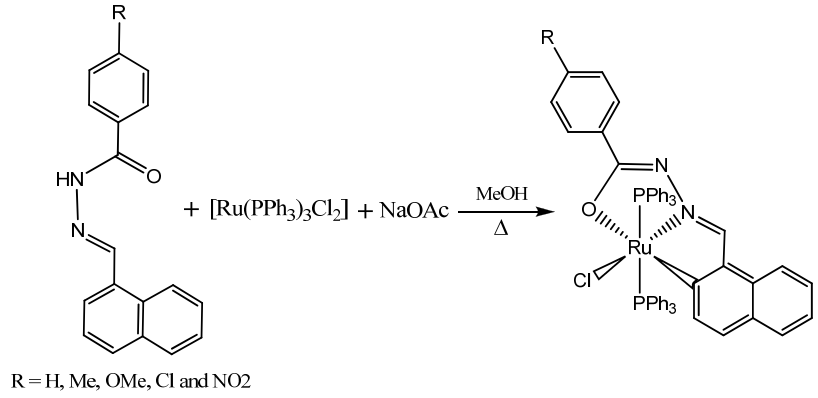

Scheme 3

and cyclic voltammetric measurements were used to characterize the complexes. Single crystal X-ray structures of **1** (*R* = H), **2** (*R* = Me) and **5** (*R* =NO_2) show pincer like coordination mode of nabhR^{2-}. The 1-naphthalenyl *ortho*-C, the azomethine-N and the amidate-O donor nabhR^{2-}, two mutually *trans* PPh_3 and the chloride assemble a distorted octahedral *trans*-$CNOClP_2$ coordination sphere around the trivalent metal centre. In the electronic spectra, dichloromethane solutions of **1**–**5** display multiple strong bands within 506−272 nm due to ligand to metal charge transfer and intraligand transitions. The room temperature (298 K) magnetic moments (μ_{eff}) of **1**–**5** are within 1.92−1.99 μ_B and they display rhombic EPR spectra in frozen (130 K) dichloromethane-toluene (1:1). Cyclic voltammetry with dimethylformamide solutions of the complexes reveals ligand substituent sensitive Ru(III)→Ru(II) reduction and Ru(III)→Ru(IV) oxidation in

the potential ranges −0.27 to −0.36 V and 0.94 to 1.13 V (vs. Ag/AgCl), respectively.

Chapter 5

Reactions of $[Ru(PPh_3)_3Cl_2]$, H_2L^n (thiobenzhydrazones, n = 1–4) and NaOAc in 1:2:2 mole ratio in methanol produces ruthenium(II) complexes of formula *cis*-$[Ru(PPh_3)_2(HL^n)_2]$ (**1**–**4**) in ~80% yields (Scheme 4). Microanalysis

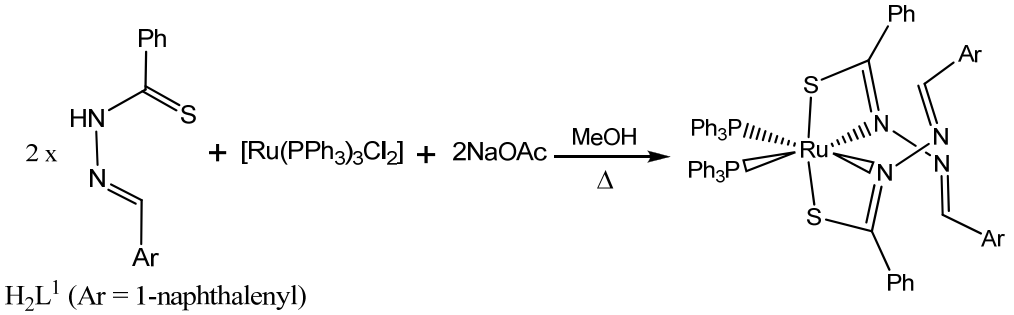

H_2L^1 (Ar = 1-naphthalenyl)
H_2L^2 (Ar = 9-anthracenyl)
H_2L^3 (Ar = 9-phenanthryl)
H_2L^4 (Ar = 1-pyrenyl)

cis-$[Ru(HL^n)_2(PPh_3)_2]$
(n = 1-4)

Scheme 4

(C,H,N),magnetic susceptibility, solution conductivity, spectroscopic (IR, UV-Vis and NMR) and cyclic voltammetric measurements have been used for the characterization of **1**–**4**. The complexes are non-electrolytic and diamagnetic. In the electronic spectra of the complexes, multiple absorptions within 505–245 nm due to metal-to-ligand and ligand centred transitions have been observed. Molecular structures of **3** and **4** have been determined by X-ray crystallography. In each of **3** and **4**, two thioamidate-N,S coordinating $(HL^n)^-$ and two mutually *cis* oriented PPh_3 molecules assemble a $N_2S_2P_2$ coordination sphere around the metal centre. Cyclic voltammograms of **1**–**4** show an oxidation response within $E_{1/2}$ = 0.76–0.86 V (ΔE_p = 90–100 mV) vs. Ag/AgCl.

Chapter 1

Introduction

In this chapter, the relevance of ruthenium coordination complexes has been briefly elaborated. The objectives of the present investigation in the context of known ruthenium Schiff base complexes have been stated.

1.1. Interest in Ruthenium Chemistry

Coordination chemistry was founded by Alfred Werner (1866–1919). For his seminal contribution he was awarded the Nobel Prize in 1913. Since then this branch of inorganic chemistry has grown tremendously and expanded to different areas such as polymers, oligomers, dendrimers, catalysis, organometallic chemistry etc. In the beginning, complexes of first transition metals were studied extensively, while the complexes of the second and the third transition series metal ions did not get much attention.

Ruthenium is a second transition series metal and its coordination chemistry was not explored much. Ruthenium chemistry is being studied extensively only during the last three decades. Before this period very few ruthenium complexes were known. Some of them are ruthenium red,[1a] $[Ru(bpy)_3]^{2+}$,[1b] $[Ru(phen)_3]^{2+}$, Creutz-Taube complexes[1c] etc. Now a vast literature on ruthenium chemistry is available. Ruthenium has $4d^75s^1$ electronic configuration and hence it has the widest range of oxidation states (from −2 in $[Ru(CO)_4]^{2-}$ to 8 in RuO_4) among all elements of the periodic table. Its complexes in each electronic configuration can adopt a variety of coordination geometries. Interconversion of different oxidation states are usually done by using different redox reagents. The ability of ruthenium to assume a wide range of oxidation states and coordination geometries provides inimitable opportunities for the application of its complexes in wide range of

research areas. The unique properties and the wide range of applications led to the continuous quest for new ruthenium complexes with diverse types of ligands. The goal is to change the coordination environment around the metal centre and fine-tune the physical and the chemical properties of the complex. The ultimate objective is to generate new materials of improved efficiency in their various applications.

1.2. Some applications

1.2.1 Biological applications

Ruthenium polypyridyl complexes are well known as probes for the elucidation of structural and electron transfer properties of proteins and DNA.[2] There are innumerable reports on the DNA binding and cleavage studies with such polypyridyl complexes. Some of the ruthenium complexes are very noteworthy for their promise in the development of several types of pharmaceutical drugs particularly as anticancer agents.[3,4]

1.2.2. Catalytic applications

Recently metal-catalyzed reactions have evolved as a new area in inorganic and organic synthesis. Variety of synthetic methods have been reported using mainly group 8 transition metal complexes in stoichiometric or catalytic amounts.[5] Ruthenium complexes with carbonyl, oxo, tertiary phosphines, arenes, cyclopentadienyl and dienes have been shown to serve as efficient catalysts.[6-9] These complexes are utilized in metathesis, Murai coupling, oxidation,[11] isomerisation,[12] nucleophilic addition to C–C and C–heteroatom multiple bonds,[13] hydrogenation[14] and constructing C–C bonds.[10] At present ruthenium complexes are being widely applied in tandem catalytic[15] processes in which the catalyst supports several functions resulting into sequential modification of a substrate.

The homogeneous catalytic hydrogenation of aldehydes and ketones is of considerable interest in connection with industrially important reactions such as those involved in the production of alcohols and other useful products.[16] Furthermore, this reaction may also be of use in synthetic organic chemistry and as a simple model for the widely publicized CO hydrogenation reaction and its implications in Fischer-Tropsch and related chemistry.[17] Literature reports related to homogeneous catalysts for the hydrogenation of aldehydes and ketones to corresponding alcohols are still relatively scare.[18] Some of the ruthenium complexes known to reduce aldehydes and ketones are $RuH_2(CO)_2(PPh_3)_2$,[19] $RuCl_2(PPh_3)_3$,[20] $RuCl_2(CO)_2(PPh_3)_2$,[21] $RuH_2(PPh_3)_4$.[22]

Ruthenium complexes are by far the best water oxidation catalysts. Particularly ruthenium polypyridyl complexes have been shown to be very efficient.[23,24] In 1982 T. J. Meyer group reported a diruthenium(II) bipyridine complex, $[(bpy)_2(H_2O)Ru(\mu\text{-}O)Ru(H_2O)(bpy)_2]^{4+}$ capable of oxidizing water catalytically. In that same year, a cationic ruthenium complex $[Ru(pap)_2(H_2O)(py)]^{2+}$ (pap = 2-phenylazopyridine, py = pyridine) that acts as homogeneous water oxidation catalyst was reported by A. Chakravorty and co-workers. Ruthenium amine complexes are also known to act as water oxidation catalysts.[25] Few of them are ruthenium red,[25a] $[(NH_3)_5Ru^{III}(\mu\text{-}O)Ru^{III}(NH_3)_5]^{4+}$ [25b] and $[(NH_3)_3Ru^{III}(\mu\text{-}Cl)_3Ru^{II}(NH_3)_3]^{2+}$ [25c]

1.2.3. Cyclometallation

The chemistry of cyclometallated complexes is undoubtedly one of the most studied areas of organometallic chemistry.[26-28] The term cyclometallation is used to describe the process in which a ligand undergoes an intramolecular (or more rarely, intermolecular) metallation with the formation of metal-carbon σ bond. One way of obtaining a cyclometallated complex is by the intramolecular C–H activation in a fragment of the coordinated ligand by transition metal.

Metallation of the *ortho*-position of aryl-substituted ligands termed as *ortho*-metallation has been most frequently described, but the wider scope of these reactions is recognized as cycloclometallation.[29] Cyclometallation has become an important concept in organometallic chemistry and are successfully used in organic synthesis especially in catalysis.[30,31] One of the important application of ruthenium in cyclometallation chemistry is to activate the inert C–H bond of ligands and form cycloruthenates. (Figure 1.1).

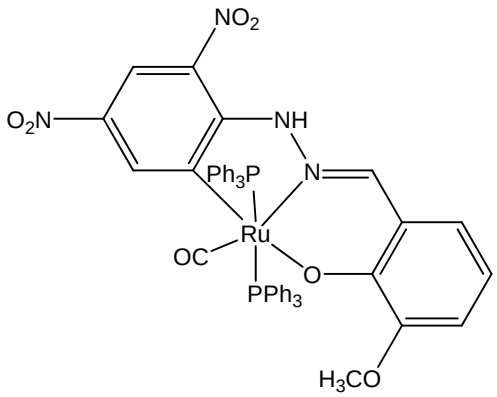

Figure 1.1

1.3. Ruthenium Schiff Base Chemistry

Metal complexes with Schiff bases have been studied extensively due to their attractive chemical and physical properties.[29b,32] They also exhibit a wide range of applications in numerous scientific areas.[33] Generally Schiff bases are prepared by condensation reaction of carbonyl compounds with amines in different solvents. The presence of dehydrating agent normally favours the formation of imines in good yields. The common structural feature of these compounds with the general formula $R_1R_2C=NR^1$, (where R_1, R_2 and R^1 are alkyl, aryl, etc) is the azomethine group (>C=N–). These compounds named after Hugo Schiff, a German chemist, exhibit rich coordination chemistry with transition metals. Schiff bases are also

1.3.1. Ruthenium complexes with amine based Schiff bases

Ruthenium complexes with Schiff bases prepared from salicylaldehyde and different amines have been the most well studied species. Amines like aniline, benzylamine, ethylenediamine, cyclohexene-1,2-diamine etc. were used to

prepare bidentate, tridentate and tetradentate Schiff bases. Hexa-coordinated ruthenium(II) complexes[37] of the type [Ru(X)(CO)(L)(EPh_3)] (where L = Schiff base anion; X = H or Cl; E = P or As) were prepared by performing the reaction between [RuHX(CO)(EPh_3)$_3$] and the corresponding bidentate Schiff base (prepared by condensation of *o*-hydroxyacetophenone with aniline). Ruthenium complexes containing oxygen and nitrogen as donor atoms were found to be very efficient catalysts in oxidation of alcohols.[38] One of such ruthenium Schiff base complexes is illustrated in Figure 1.2.

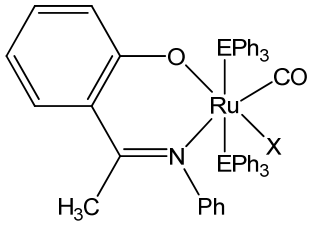

E = P or As

Figure 1.2

The well known tetradentate H_2salen is one of the first Schiff bases used to explore the ruthenium coordination chemistry. H_2salen coordinates through two imine nitrogen and two phenolic oxygen atoms. It has been reported that different types of ruthenium(II) $(salen)^{2-}$ complexes act as very good catalysts in organic synthesis such as olefination of a wide variety of aldehydes in homogeneous phase. They also exhibit very high catalytic activity and excellent selectivity. Catalytic amount of ruthenium complexes with chiral $(salen)^{2-}$ type ligands $(salen^*)^{2-}$ [Ru(salen*)(PPh_3)$_2$][39] was used in the enantioselective intramolecular cyclopropanation of *cis*-substituted allylic diazoacetates. An example for these catalysts is shown in Figure 1.3.

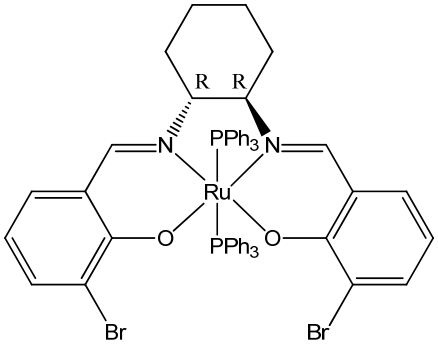

Figure 1.3

Ruthenium complexes with Schiff bases containing S-donor atom show significant antifungal, antibacterial and anticancer activities. A series of new hexa-coordinated ruthenium(III) complexes of the type [Ru(X)(2-atmp-ba)(EPh_3)] were prepared by reacting [$RuX_2(EPh_3)_3$] with the tetradentate Schiff base H_2atmpba. (= N, N'-bis(2-aminothiophenol)benzoylacetone; X = Cl or Br; E = P or As) These complexes exhibit excellent antimicrobial activities against microorganisms like E. coli, S. aureus, D. typhi and A. hydrophila.[40] One of the representative complexes from this series is shown in Figure 1.4.

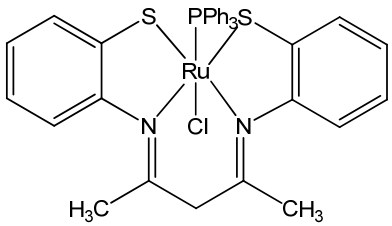

Figure 1.4

1.3.2. Ruthenium complexes with acid hydrazide based Schiff bases

This type of Schiff bases can be readily prepared by condensation of the aldehydes or ketones with acid hydrazides. These are characterized by the presence of >C=N–NH–C(=O)– functional group and have a strong tendency to

bind to transition metals. Acid hydrazones are known to exhibit amide-imidol tautomerism in solution state. By attaining imidol form, the effective conjugation along hydrazone skeleton is increased thereby giving rise to an efficient electron delocalization. Coordination complexes of aroylhydrazones have been reported to act as enzyme inhibitors and have useful pharmacological applications.[41-44] In recent years, a large number of reports on metal complexes of aroylhydrazones have appeared. However, ruthenium complexes with aroylhydrazones are very few in literature. Some important examples of ruthenium aroylhydrazone complexes are described below.

The benzoylhydrazone Schiff bases (HL) were easily prepared in good yield by the condensation of various thiophene aldehydes with benzhydrazide in an equimolar ratio. These ligands were reacted with $[RuHCl(CO)(AsPh_3)_3]$ in the presence of base to afford new ruthenium complexes having general formula, $[Ru(L)(CO)Cl(AsPh_3)_2]$. These complexes were demonstrated as efficient catalysts for the one-pot conversion of various aldehydes to their corresponding primary amides.[45] One of the ruthenium complexes utilized for this conversion is shown Figure 1.5.

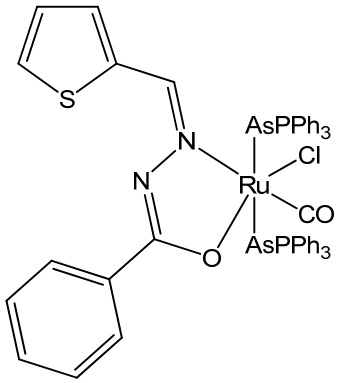

Figure 1.5

Considerable attention has been paid towards the reactions of transition metals with aroylhydrazones leading to the formation of metal-carbon bond *via* C–H activation. Such organometallic complexes have considerable importance as they often serve as models for reactive intermediates in metal-mediated transformation in organic synthesis. The C–H bond is much stronger than the M–C bond and the thermodynamic barrier for homolytic cleavage of a C–H bond is high. Recently from our laboratory we have reported such *ortho*–metallated ruthenium complexes. One example is outlined below (Figure 1.6).[46]

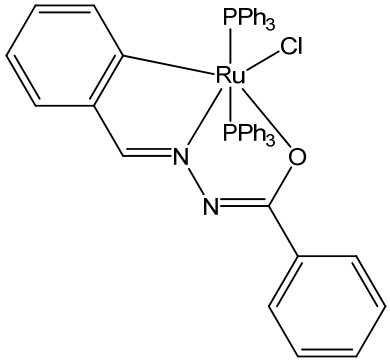

Figure 1.6

1.3.3. Ruthenium complexes with semicarbazide based Schiff bases

The coordination chemistry of ruthenium with semicarbazones has been unexplored until recently. The benzaldehyde semicarbazone and its derivatives coordinate to the ruthenium centre in different coordination modes. The coordination modes can be controlled by various parameters like experimental conditions, substitutions on benzaldehyde and the type of ruthenium starting material. These Schiff bases coordinate to ruthenium mainly in three different modes (i) tridentate through *ortho*–C, imine–N and amidate–O donor atoms to form 5,5-membered fused chelate ring complexes (ii) bidentate through imine–N

and amidate–O donor atoms to form a stable 5-membered chelate complexes and (iii) bidentate through semicarbazate–N,O donor atoms to form unusual 4-membered chelate complexes. One example for the ruthenium complex with 4-nitrobenzaldehyde semicarbazone is given below. Here, the ligand $(L–NO_2)^{2–}$ coordinates to ruthenium centre through tridentate–C,N,O donor atoms forming 5,5-membered fused chelate ring complex. The general formula is *trans*–$[Ru(L–NO_2)(PPh_3)_2Cl]$[47] (Figure 1.7).

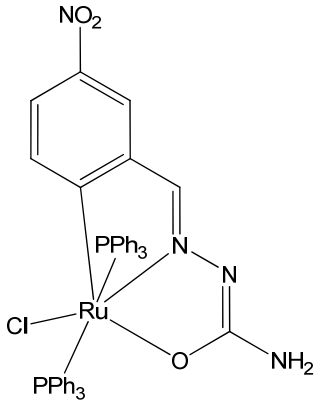

Figure 1.7

1.3.4. Ruthenium complexes with thiosemicarbazide based Schiff bases

The chemistry of the transition-metal complexes with thiosemicarbazones has received considerable attention primarily because of their biological (antibacterial, antimalarial, antiviral, and antitumor) activities.[48] Thiosemicarbazones were conveniently prepared by the condensation of aldehydes/ketones with thiosemicarbazide in good yields. General formula of thiosemicarbazones is >C=N–NH–C(=S)–. They can easily coordinate to transition metals. These are versatile ligands and exhibit thioamide-iminothiol tautomerism in solution. Thiosemicarbazones form a special class of mixed hard-soft oxygen/nitrogen-sulfur chelating ligands that show different coordination

modes towards metal ions in their complexes. The thiosemicarbazonate can act as a monodentate ligand that bind to the metal ion through the S–atom, as a bidentate ligand that coordinate to the metal ion through the S–atom and one of the N–atoms of the hydrazine moiety to form a 4- or a 5-membered chelate ring or a tridentate ligand that bind to the metal ion through the S–atom, the imine–N and the *ortho*–C of the aldimine moiety and form 5,5-membered fused chelate rings.

Reactions of benzaldehyde thiosemicarbazones (H_2LR, where 2H stand for the hydrazinic proton and the phenyl proton at the *ortho* position, with respect to the imine function and R (= H, OMe, CH_3, Cl, and NO_2) for the para substituent) with $[Ru(PPh_3)_2(CO)_2Cl_2]$ carried out in refluxing ethanol afford monomeric complexes of type $[Ru(HLR)(PPh_3)_2(CO)H]$. The thiosemicarbazonate ligand is coordinated to the ruthenium center as a monoanionic bidentate N,S–donor forming a 4-membered chelate ring. When the reactions of the thiosemicarbazones with $[Ru(PPh_3)_2(CO)_2Cl_2]$ were carried out in refluxing toluene, a family of dimeric complexes of type $[Ru_2(LR)_2(PPh_3)_2(CO)_2]$ was obtained. Each thiosemicarbazonate ligand is coordinated to one of the two ruthenium atoms as a dianionic tridentate C,N,S-donor forming 5,5-membered fused chelate rings, and at the same time the S–atom is also bonded to the second ruthenium center. The representative complexes[49] are shown in Figure 1.8.

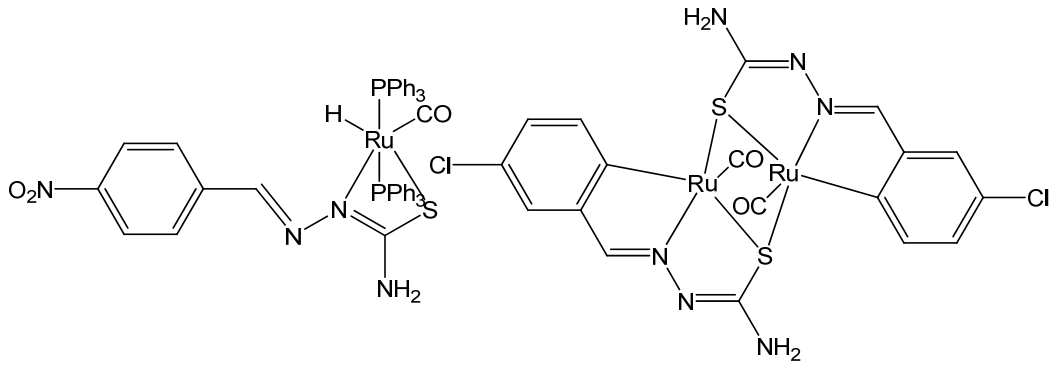

Figure 1.8

1.4. About the Present Investigation

In the previous sections, we have briefly discussed different types of ruthenium complexes with amine, acid hydrazide, semicarbazide and thiosemicarbazide based Schiff bases and some of their applications. There are essentially no reports on coordination complexes of ruthenium with some hydrazine based Schiff bases such as salicylaldehyde-pyridine-2-hydrazone and aroylhydrazones/thiobenzhydrazones of polycyclic aromatic aldehydes. In the present work, we have explored the ruthenium coordination chemistry with some of the above mentioned Schiff bases (Figure 1.9). The details of our observations are discussed in the following chapters.

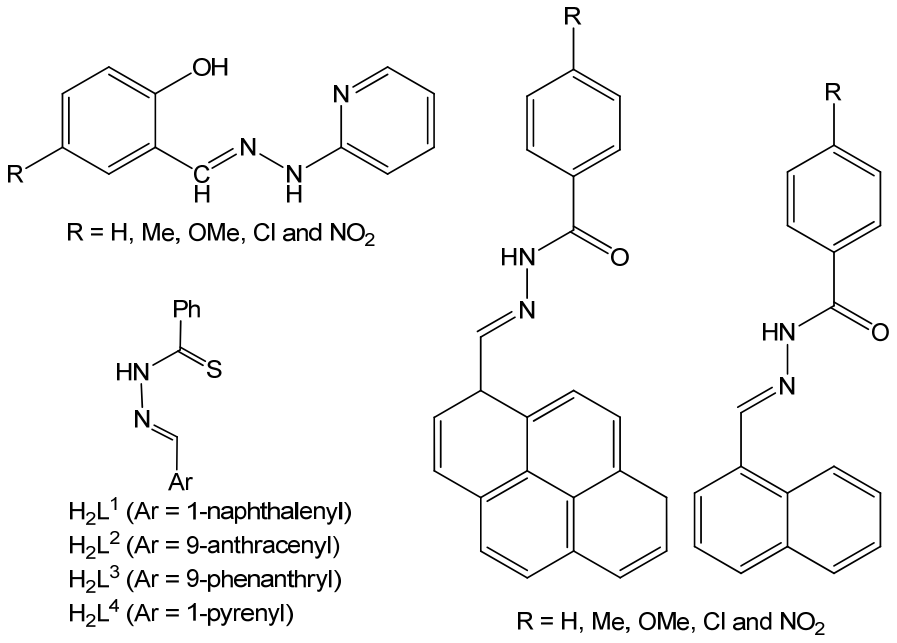

Figure 1.9

1.5. References

[1] (a) A. joly, C. R. *Acad. Sci.* 115 **(**1892) 1299. (b) F. H. Brusttall, J. Chem. Soc. (1936) 173. (c) C. Creutz, H. Taube, *J. Am. Chem. Soc.* 95 (1973) 1086.

[2] P. J. Carter, C. C. Cheng, H. H. Thorp, *J. Am. Chem. Soc.* 120 (1998) 632. (b) D. R. Frasca, M. J. Clarke, *J. Am. Chem. Soc.* 121 **(**1999) 8523.

[3] (a) B. K. Keppler, Metal Complexes in Cancer Chemotherapy, Wiley-VCH, Weinhein, 1993. (b) N. Farrell, Bioorganometallics, ed. G. Jaouen, Wiley-VCH, weinhein, 2005. (c) I. Haidue, C. Silvestru, *Coord. Chem. Rev.* 99 (1990) 253.

[4] (a) P. J. Dyson, G. Sava, J. Chem. Soc., *Dalton Trans.* (2006) 1929. (b) A. Bergamo, G. Sava, J. Chem. Soc., *Dalton Trans.* (2007) 1267.

[5] (a) J. H. Bateson, M. B. Mitchell, Organometallic Reagents in Organic Synthesis, Academic Press: London, 1994. (b) Oraganometallics in Synthesis, M. Ed. Schlosser, John Wiley & Sons, Chichester, 1994. (c) F. J. McQuillin, D. G. Parker, G. R. Stephenson, Transition Metal Organometallics for Synthesis, Cambridge University Press, Cambridge, 1991. (d) A. Yamamoto, Organotransition Metal Chemistry. Fundamental Concepts and Applications, Wiley, New York, 1986. (e) H. M. Coquhoun, J. Holton, D. J. Thompson, M. V. Twigg, New Pathways for Organic Synthesis, Plenum Press: New York, 1984. (f) S. G. Davies, Organotransition Metal Chemistry. Applications to Organic Synthesis, Pergamon Press: Oxford, 1982. (g) E. Negishi, Organometallics in Organic Synthesis, John Wiley & Sons, New York, 1980.

[6] T. Naota, H. Takaya, S. I. Murahashi, *Chem. Rev.* 98 (1998) 2599.

[7] B. M. Trost, F. D. Toste, A. B. Pinkerton, *Chem. Rev.* 101 (2001) 2067.

[8] M. Bresson, N. d'Allessandro, L. Liberatore A. Morvillo, *Coord. Chem. Rev.* 185-186 (1999) 385.

[9] S. Murai, N. Chatani, F. Kakiuchi, *Pure Appl. Chem.* 69 (1997) 589.

[10] (a) T. Mirsudo, S. W. Zhang, M. Nagao, Y. Watanabe, J. Chem. Soc., *Chem. Commun.* (1991) 598. (b) N. Chatani, H. Inoue, T. Ikeda, S. Murai, *J. Org. Chem.* 65 (2000) 4913. (c) C. S. Yi, N. Liu, *J. Organomet. Chem.* 553 (1980) 157. (d) E. Galardon, P. Le Maux, G. Simonneaux, *Tetrahedron* 56 (2000) 615. (e) J. W. Faller, Parr, *Organometallics* 19 (2000) 1820. (f) T. Midsudo, M. Takagi, S. W. Zhang, Y. Watanabe, *J. Organomet. Chem.* 423 (1992) 405. (g) M. Yamaguchi, Y. Kido, K. Omata, M. Harama, *Synlett.* (1995) 1181. (h) S. Murai, F. Kakiuchi, S. Sekine, Y. Tanaka, A. Kamatani, M. Sonoda, N. Chatani, *Nature* 366 (1993) 529. (i) F. Kakiuchi, Y. Yamamoto, N. Chatani, S. Murai, *Chem. Lett.* (1996) 111. (j) R. Grigg, V. Savig, *Tetrahedron Lett.* 38 (1997) 5737. (k) T. Takemori, H. Suzuki, M. Tanaka, *Organometallics* 15 (1996) 4346. (l) S. Cenini, F. Ragaini, S. Tollare, D. Paone, *J. Am. Chem. Soc. 188* (1996) 11964. (m) W. A. Hermann, W. C. Schattenmann, O. Nuyken, S. C. Glander, *Angew. Chem. Int. ed.* 36 (1997) 2121. (n) Y. S. Shon, T. R. Lee., *Tetrahedron Lett.* 38 (1997) 1283. (o) M. J. Marsella, H. D. Maynard, R. H. Grubbs, *Angew. Chem. Int. Ed.* 36 (1997) 1101.(p) S. H. Kim, N. Bowden, R. H. Grubbs, *J. Am. Chem. Soc.* 116 (1994) 10801. (q) A. Demonceau, C. A. Lemoine, A. F. Noels., I. T. Chizhevsky, P. V. Sorokin, *Tetrahedron Lett.* 36 (1995) 8419. (r) T. Kondo, N. Suzuki, T. Okada, T. Mitsudo, *J. Am. Chem. Soc.* 119 (1997) 6187. (s) J. W. Steed, D. A. Tocher, R. D. Rogers, J. Chem. Soc., *Chem. Commun.* (1996) 1589. (t) H. Nakamatsu, S. Blechert, *Angew. Chem. Int. Ed.* 41 (2002) 794. (u) J.C. Sworen, J. H. Pawlow, W. Case, J. Lever, K. B. Wagener, *J. Mol. Catal., A: Chem.* 194 (2003) 69.

[11] (a) S. I. Murashi, T. Naota, Y. Oda, N. Hirai, *Synlett.* (1995) 733. (b) G. Barak, J. Dakka, Y. Sasson, *J. Org. Chem.* 53 (1988) 3553. (c) M.

Matsumoto, S. J. Ito, J. Chem. Soc., *Chem. Commun.* (1981) 907. (d) M. Matsumoto, S. J. Ito, *Synth. Commun.* 14 (1984) 697.

[12] (a) T. N. Mitchel, F. Giessemann, *Synlett.* (1996) 473. (b) T. Mitsudo, S. –W. Zhang, N.Satake, T. Kondo, Y. Watanabe, *Tetrahedron Lett.* 33 (1992) 5533.

[13] (a) C. Ruppin, P. H. Dixneuf, S. Lecolier, *Tetrahedron Lett.* 29 (1998) 5365. (b) J. Fournier, C. Bruneau, P. H. Dixneuf, S. Licolier, *J. Org. Chem.* 56 (1991) 4456. (c) S. I. Murahashi, T. Naota, E. Saito, *J. Am. Chem. Soc.* 108 (1986) 7846.

[14] J. F. Knifton, *J. Org. Chem.* 41 (1976) 1200. (b) T. Ohta, T. Miyake, H. Takaya, J. Chem. Soc., *Chem. Commun.* (1992) 1725. (c) H. Takaya, T. Ohta, R. Noyori, *Tetrahedron Lett.* 31 (1990) 7189. (d) T. Ohkuma, H. Ikehira, T. Ikariya, R. Noyori, *Synlett.* (1997) 467.

[15] (a) W. J. Zuercher, M. Hashimoto, R. H. Grubbs, *J. Am. Chem. Soc.* 118 (1996) 6634. (b) D. E. Fogg, D. Amoroso, S. D. Drouin, J. Snelgrove, J. Conrad, F. Zamanian, *J. Mol. Catal. 190A* (2002) 177.

[16] (a) R. L. Pruett, *Adv. Organomet. Chem.* 17 (1979) 1-60. (b) B. Cornils, A. Mullen, *Hydrocarbon Process*, 59 (1980) 93. (c) C. Masters, "Homogeneous Transition-Metal Catalysis-A Gentle Art", Chapman Hall: London, (1981) 102. (d) J. B. Cropley, L. M. Burgess, R. A. Loke, Chemtech (1984) 374.

[17] (a) C. Masters, *Adv. Organomet. Chem. 17* (1979), 61. (b) R. P. A. Sneeden, In "Comprehensive Organometallic Chemistry", G. Wilkinson, F. G. A. Stone, E. W. Abel, Eds; Pergamon Press: London, 1982, Vol. 8, Chapter 50.2.

[18] G. Mestroni, A. Camus, G. Zassinovich, In "Aspects of Homogeneous Catalysis", R. Ugo, Ed; D. Reidel, Dordrecht, The Netherlands, 1981, Vol. 4, pp 71-98.

[19] R. A. Sanchez-Delgado, J. S. Bradley, G. Wilkinson, J. Chem. Soc., *Dalton Trans.* (1976) 399.

[20] (a) J. Tsuji, H. Suzuki, *Chem. Lett.*, (1977) 1085. (b) W. M. U. S. Kruse, *Patent 4024193*, 1977.

[21] W. Strohmeier, H. Steigerwald, *J. Organomet. Chem.* 129 (1977) C43.

[22] D. J. Cole-Hamilton, G. Wilkinson, *New. J. Chim.* 1 (1977) 141.

[23] (a) W. Ruttinger, G. C. Dismukes, *Chem. Rev.* 97 (1997) 1. (b) M. Yagi, M. Kaneko, *Chem. Rev.* 101 (2001) 21. (c) Y. Gao, R. H. Crabtree, G. W. Brudvig, *Inorg. Chem.* 51 (2012) 4043.

[24] (a) S. W. Gersten, G. J. Samuels, T. J. Meyer, *J. Am. Chem. Soc.* 104 (1982) 4029. (b) J. A. Gilbert, D. s. Eggleston, W. R. Murphy Jr., D. A. Geselowitz, S. W. Gersten, D. J. Hodgson, T. J. Meyer, *J. Am. Chem. Soc.* 107 (1985) 3855. (c) J. R. Schoonover, J. F. Ni, L. Roecker, P. S. White, T. J. meyer, *Iorg. Chem.* 35 (1996) 5885. (d) S. Goswami, A. R. Chakravarty, A. Chakravarty, J. Chem. Soc., *Chem. Commun.* (1982) 1288.

[25] (a) M. Yagi, S. Tokita, K. Nagoshi, I. Ogino, M. Kaneko, J. Chem. Soc., *Faraday Trans. 92* (1996) 2457. (b) K. Nagoshi, M. Yagi, M. Kaneko, Bull. *Chem. Soc. Jpn.* 73 (2000) 2193. (c) M. Yagi, Y. Osawa, N. Sukegawa, M. Kaneko, *Langmuir* 15 (1999) 7406.

[26] M. Albrecht, *Chem, Rev.* 110 (2010) 576.

[27] F. Mohr, S. H. Priver, S. K. Bhargava and M. A. Bennet, *Coord. Chem. Rev.* 250 (2006) 1851.

[28] A. Diez, E. Lalinde and M. T. Moreno, *Coord. Chem. Rev.* 255 (2011) 2426.

[29] (a) M. I. Bruce, Angew. Chem. *Int. Ed. Engl.* 16 (1977) 73. (b) R. Raveendran, S. Pal, *Inorg. Chem. Acta* 359 (2006) 3212.

[30] F. Barigelletti, J. D. Sandrini, M. Maestri, V. Balzani, A. Von Zelewsky, L. Chassot, P. Jolliet, U. Maeder, *Inorg. Chem.* 27 (1988) 3644.

[31] (a) V. Ritleng, C. Sirlin, M. Pfsffer, *Chem. Rev.* 102 (2002) 1731. (b) P. G. Bomben, K. C. D. Robson, B. D. Koivisto, C. P. Berlinguette, *Coord. Chem. Rev. 256* (2012) 1438. (c) D. Morales-Morales, *Rew. Soc. Quim. Mex.* 48 (2004) 338.

[32] (a) S. N. Pal, S. Pal, *Inorg. Chem.* 40 (2001) 4807. (b) S. N. Pal, S. Pal, *Z. Anorg. Allg. Chem.* 628 (2002) 2091. (c) S. N. Pal, S. Pal, J. Chem. Soc., *Dalton Trans.* (2002) 2102. (d) S. N. Pal, S. Pal, *Eur. J. Inorg. Chem.* (2003) 4244. (e) R. Raveendran, S. Pal, *Polyhedron* 24 (2005) 57.

[33] (a) R. N. Prabhu, D. Pandiarajan, R. Ramesh, *J. Organomet. Chem.* 694 (2009) 4170. (b) R. N. Prabhu, R. Ramesh, *J. Organomet. Chem.* 718 (2012) 43.

[34] P. G. Cozzi, *Chem. Soc. Rev.* 33 (2004) 410.

[35] F. Calderazzo, C. Floriani, R. Henzi, F. L. Eplattenier, *J. Chem. Soc. A* (1969) 1378.

[36] (a) K. S. Finny, G. W. Everett, *Inorg. Chim. Acta* 11 (1974) 185. (b) G. Henrich-Olive, S. Olive, *J. Mol. Catal.* 1 (1976) 121. (c) J. R. Thornback, G. Wilkinson, J. Chem. Soc., *Dalton Trans.* (1978) 110. (d) K. S. Murray, A. M. van den Bergen, B. O. West, *Aust. J. Chem.* 31 (1978) 203.

[37] P. Viswanathamurthi, R. Karvembu, V. Tharaneeswaran, K. Natarajan, *J. Chem. Sci.* 117 (2005) 235.

[38] (a) R. I. Kureshy, N. H. Khan, S. H. R. Abdi, *J. Mol. Catal.* 96 (1995) 117. (b) A. M. EI-Hendawy, A. H. Alkubaisi, EI-Ghany, A. EI-Kourashy, M. M. Shanab, *Polyhedron* 12 (1993) 2343. (c) A. M. EI-Hendawy, EI-Ghany, A. EI-Kourashy, M. M. Shanab, *Polyhedron* 11 (1992) 523. (d) G. Bhowon, Li Khan, H. Wah, R. Narain, *Polyhedron* 18 (1999) 341.

[39] G-Y. Li, J. Zhang, P. W. H. Chan, Z-J. Xu, N. Zhu, C-M. Che, *Organometallics* 25 (2006) 1676.

[40] R. Prabhakaran, A. Geetha, K. Natarajan, *J. Inorg. Biochem.* 98 (2004) 2131.

[41] N. Galic, B. Peric, B. Koji-Prodi, Z. cimerman, *J. Molecular Structure* 559 (2001) 187.

[42] A. A. Salem, *J. Microchem.* 60 (1998) 51.

[43] B. Tang, M. Du, Y. Wang, *Analyst* 123 (1998) 283.

[44] R. S. Baliogar, V. K. Revankar, *J. Serb. Chem. Soc.* 71 (2006) 1301.

[45] R. N. Prabhu, R. Ramesh, *RSC Adv.* 2 (2012) 4515.

[46] (a) R. Raveendran, S. Pal, *J. Organomet. Chem.* 692 (2007) 824. (b) R. Raveendran, S. Pal, *J. Organomet. Chem.* 694 (2009) 1482.

[47] F. Basuli, S–M. Peng, S. Bhattacharya, *Inorg. Chem.* 40 (2001) 1126.

[48] (a) F. A. French, E. Blanz Jr, *J. Med. Chem.* 13 (1970) 1117. (b) K. C. Agrawal, A. C. Sartorelli, *Prog. Med. Chem.* 15 *(*1978) 321. (c) J. P. Scovill, D. L. Klayman, C. F. Franchino, *J. Med. Chem.* 25 (1982) 1261. (d) A. Papageorgiou, Z. Iakovidou, D. Mourelatos, E. Mioglou, L. Boutis, A. Kotsis, D. Kovala-Demertzi, D. X. Domopoulou, M. A. Demertzis, *Anticancer Res.* 17 *(*1997) 247. (e) M. C. Miller III, C. N. Stineman, J. R. Vance, D. X. West, I. H. Hall, *Anticancer Res.* 18 (1998) 4131. (f) D. Kovala-Demertzi, J. R. Miller, N. Kourkoumelis, S. K. Hajikakou, M. A. Demertzis, *Polyhedron* 18 (1999) 1005. (g) Z. Iakovidou, A. Papageorgiou, M. A. Demertzis, E. Mioglou, D. Mourelatos,A. Kotsis, P. N. Yadav, D. Kovala-Demertzi, *Anticancer Drugs* 12 (2001) 65.

[49] S. Dutta, F. Basuli, A. Castineiras, S-M, Peng, G-H, Lee, S. Bhattacharya, *Eur. J. Inorg. Chem.* (2008) 4538.

Chapter 2

Ruthenium(III) complexes with *N*-(2-pyridyl)-*N′*-(5-*R*-salicylidene)hydrazines: Synthesis, physical properties and structural studies

Ruthenium(III) complexes, $[Ru(L^n)_2]ClO_4$ with *N*-(2-pyridyl)-*N′*-(5-*R*-salicylidene)-hydrazines (HL^n; *R* = H, Cl, Br, Me and OMe) have been synthesized. Microanalysis (C,H,N), magnetic susceptibility and various spectroscopic (IR, UV-Vis and EPR) measurements have been used for the characterization of these complexes. The molecular structures of all the complexes except for the complex where *R* = Br have been confirmed by single crystal X-ray diffraction study. The metal centres in these complex cations are in distorted octahedral N_4O_2 coordination sphere assembled by the pyridine-N, the imine-N and the phenolate-O donor $(L^n)^-$ ligands. Intermolecular hydrogen-bonding assisted supramolecular structures formed by the solvated complexes range from dimeric to one-dimensional chain to two-dimensional sheet structures.

2.1. Introduction

In this chapter the ruthenium coordination chemistry with the Schiff bases *N*-(2-pyridyl)-*N′*-(5-*R*-salicylidene)-hydrazines (HL^n, H represents the dissociable phenolic-OH proton) derived from 2-hydrazinopyridine and 5-*R*-salicylaldehydes (*R* = H, Cl, Br, Me and OMe) has been described. The main reason for the choice of this type of ligands is their ability to behave as noninnocent ligands [1–3]. The Schiff base system HL^n (Figure 2.1) contains a diimine fragment, which is π-acidic in nature. The tridentate mono-anionic pyridine-N, imine-N and phenolate-

O donor ligand $(L^n)^-$ can form 5,6-membered fused chelate rings with the metal ion. Herein, the details of synthesis, characterization and properties of a series of mononuclear ruthenium(III) complexes of general formula $[Ru(L^n)_2]ClO_4$ are reported. Molecular structures of all the complexes except for one have been confirmed by single crystal X-ray structure determination.

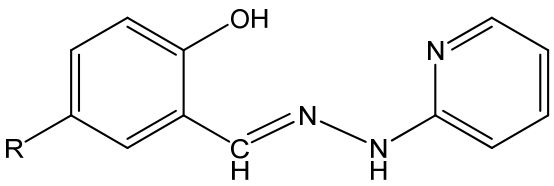

HL^n, n = 1-5 for
R = H, Cl, Br, Me and OMe

Figure 2.1

2.2. Experimental Section

2.2.1. Materials

The Schiff bases HL^n were synthesized from equimolar amounts of 2-hydrazinopyridine and 5-substituted salicylaldehydes by following procedures similar to that reported earlier [4,5]. $[Ru(dmso)_4Cl_2]$ was prepared using a literature procedure [6]. All other chemicals and solvents were of analytical grade available commercially and were used without further purification.

2.2.2. Physical measurements

Elemental (C,H,N) analysis data were obtained with the help of a Thermo Finnigan Flash EA1112 series elemental analyzer. A Digisun DI-909 conductivity meter was used to measure the solution electrical conductivities. Magnetic susceptibilities with powdered samples of the complexes were measured with a Sherwood Scientific balance. Diamagnetic corrections calculated from Pascal's

constants [7] were used to obtain the molar paramagnetic susceptibilities. A Shimadzu LCMS 2010 liquid chromatograph mass spectrometer was used for the purity verification. A Jeol SX 102/DA-6000 mass spectrometer was used for the FAB mass spectroscopic experiment. Infrared spectra were recorded by using KBr pellets on a Jasco-5300 FT-IR spectrophotometer. A Shimadzu UV-3600 UV-VIS-NIR spectrophotometer was used to collect the electronic spectra. X-band EPR measurements were performed on a Jeol JES-FA200 spectrometer.

2.2.3. Synthesis of complexes

All the complexes (**1-5**) were prepared in 32-40% yield by following the same procedure. Details are given only for a representative case.

2.2.4. Synthesis of $[Ru(L^1)_2]ClO_4$ (1)

Solid $[Ru(dmso)_4Cl_2]$ (200 mg, 0.41 mmol) was added to a clear methanol solution (20 ml) of HL^1 (175 mg, 0.82 mmol) and NaOH (33 mg, 0.83 mmol). The mixture was refluxed for ½ h and then cooled to room temperature. The orange-red crystalline material formed was collected by filtration, washed with methanol and finally dried in air (yield, 100 mg). 0.2 ml of 70% perchloric acid was dissolved in 10 ml methanol. 1.6 ml of this acid solution was added to a suspension of the orange-red crystalline material in 20 ml of methanol. A clear reddish brown solution was formed. It was allowed to evaporate slowly at room temperature. After about 5 days reddish brown crystalline material deposited was collected by filtration and dried in air. Yield was 90 mg (35%).

The other four complexes having the same general formula $[Ru(L^n)_2]ClO_4$ (**2**, **3**, **4** and **5** where n = 2, 3, 4 and 5 for *R* = Cl, Br, Me and OMe, respectively) were synthesized in 32−40% yields from $[Ru(dmso)_4Cl_2]$ and the appropriate Schiff base (HL^n) by following procedures similar to that described for **1**.

2.2.5. X-ray crystallography

Single crystals of **1**, **2**, **4** and **5** were grown by slow evaporation of their methanol solutions. Despite our several attempts by various ways we were not able to get X-ray quality crystals of **3**. The complexes crystallize as **1**·1.5CH_3OH, **2**·CH_3OH, **4**·2H_2O and **5**·H_2O·CH_3OH. A Bruker-Nonius SMART APEX CCD single crystal diffractometer, equipped with a graphite monochromator and a Mo $K\alpha$ fine-focus sealed tube (λ = 0.71073 Å) was used to determine the unit cell parameters and to collect the intensity data at 298 K for **1**·1.5CH_3OH. The SMART software was used for data acquisition and the SAINT-Plus software was used for data extraction [8]. The absorption corrections were performed with the help of the SADABS program [9]. Determination of the unit cell parameters and the intensity data collection for **2**·CH_3OH were performed on an Enraf-Nonius Mach-3 single crystal diffractometer using graphite monochromated Mo $K\alpha$ radiation (λ = 0.71073 Å) by the ω-scan method at 298 K. Intensities of three check reflections were measured after every 1.5 h during the data collection to monitor the crystal stability. There was no decay during the 55 h of exposure to X-ray. An empirical absorption correction was performed based on the Ψ-scans [10] of four reflections. Calculations for data reduction and absorption correction were done using the WinGX package [11]. The unit cell parameters and the intensity data at 298 K for **4**·2H_2O and **5**·H_2O·CH_3OH were obtained on an Oxford Diffraction Xcalibur Gemini single crystal X-ray diffractometer using graphite monochromated Mo Kα radiation (λ = 0.71073 Å). The CrysAlisPro software [12] was used for data collection, reduction and absorption correction. The structures of all four complexes were solved by direct method and refined on F^2 by full-matrix least-squares procedures. The non-hydrogen atoms in all the structures were refined using anisotropic thermal parameters. For each of **4**·2H_2O

Table 2.1. Selected crystallographic data

Complex	**1**·1.5CH_3OH	**2**·CH_3OH	**4**·2H_2O	**5**·H_2O·CH_3OH
Empirical formula	$RuC_{25.5}H_{26}N_6O_{7.5}Cl$	$RuC_{25}H_{22}N_6O_7Cl_3$	$RuC_{26}H_{28}N_6O_8Cl$	$RuC_{27}H_{30}N_6O_{10}Cl$
Formula weight	673.04	725.91	689.06	735.09
Crystal system	triclinic	orthorhombic	triclinic	triclinic
Space group	$P\bar{1}$	*P*bna	$P\bar{1}$	$P\bar{1}$
a (Å)	9.490(2)	12.576(3)	10.6285(3)	11.129(6)
b (Å)	11.564(3)	18.181(3)	12.3351(3)	12.332(5)
c (Å)	13.149(4)	25.213(4)	22.4176(6)	12.822(7)
α (°)	80.726(6)	90	92.807(2)	110.55(4)
β (°)	74.177(5)	90	98.220(2)	90.92(4)
γ (°)	87.600(8)	90	91.797(2)	103.61(4)
V (Å^3)	1370.2(6)	5765(2)	2903.16(13)	1591.8(13)
Z	2	8	4	2
ρ (g cm^{-3})	1.631	1.673	1.577	1.534
μ (mm^{-1})	0.728	0.877	0.691	0.639
Reflections collected	12250	5632	20105	10685
Reflections unique	4762	5064	10225	5529
Reflections ($I \geq 2\sigma(I)$)	4446	1955	8512	2378
Parameters	378	381	785	412
*R*1, *wR*2 ($I \geq 2\sigma(I)$)	0.0468, 0.1234	0.0617, 0.0930	0.0459, 0.1159	0.0994, 0.1841
*R*1, *wR*2 (all data)	0.0489, 0.1259	0.2204, 0.1319	0.0587, 0.1241	0.2005, 0.2383
GOF (F^2)	1.070	0.982	1.080	0.963
Largest peak and hole (*e* Å^{-3})	1.419, −1.402	0.521, –0.456	1.565, –0.769	0.941, −0.611

and **5**·H_2O·CH_3OH, the H-atoms of the lattice water molecules were located in a difference map and refined with geometric restraints and U_{iso}(H) = 1.5U_{iso}(O). The H-atoms of the ligands and methanol molecules if any in all the structures were included in the structure factor calculations at idealized positions by using a riding model. The SHELX-97 programs [13] available in the WinGX package [11] were used for structure solution and refinement. The ORTEP6a [14], Platon [15] Mercury [16] packages were used for molecular graphics. Selected crystallographic data are summarized in Table 2.1.

2.3. Results and discussion

2.3.1. Synthesis and characterization

The Schiff bases (HL^n) were prepared in 55−60% yields by condensation reactions of 2-hydrazinopyridine with equimolar amount of 5-*R*-salicylaldehydes (n = 1, 2, 3, 4 and 5 for *R* = H, Cl, Br, Me and OMe, respectively) in refluxing methanol [4,5]. The purity of all the Schiff bases were checked by LC-MS and elemental analysis. The reactions of [Ru(dmso)$_4$Cl$_2$], HL^n and NaOH (1:2:2 mole ratio) in methanol provides orange-red microcrystalline materials. Treatment of this orange-red material with two equivalents of perchloric acid in methanol provides the complexes **1**−**5** in moderate yields. The elemental analysis data (Table 2.2) are in good agreement with the general formula of these complexes as [Ru(L^n)$_2$]ClO_4. The room temperature magnetic moments are within 1.83−1.99 μ_B. These values confirm the +3 oxidation state and the low-spin character of the metal centre in each complex. Molar conductivity values (Table 2.2) of **1**−**5** in acetonitrile implicate their 1:1 electrolytic behaviour.

The orange-red precursors of **1**−**5** are insoluble in common organic solvents such as dichloromethane, chloroform, methanol, ethanol and acetonitrile. However, they are slightly soluble in dimethylformamide and dimethylsulfoxide

to provide yellow-orange solutions. In solution, they are very unstable and converted to some intractable green species. The elemental analysis data of orange-red precursors indicate 1:2 metal-to-ligand ratio. All five precursors are paramagnetic and in frozen (130 K) dimethylformamide-toulene (1:1) they display rhombic EPR spectra typical of low-spin ruthenium(III) species. The highest mass (m/z = 525) in the LC mass spectra of **1** and its precursor in dimethylformamide and that (m/z = 594) in the FAB mass spectra of **2** and its precursor in *m*-nitrobenzylalcohol indicate the complex cation $[Ru(L^n)_2]^+$ in both **1**, **2** and their orange-red precursors. Thus these orange-red materials could be the chloride salts of $[Ru(L^n)_2]^+$. However, metathesis reactions of these solids with excess sodium perchlorate do not provide $[Ru(L^n)_2]ClO_4$ (**1**−**5**). These are obtained only by treating these materials with perchloric acid. It may be noted that the Schiff bases derived from 2-hydrazinopyridine and 5-*R*-salicylaldehyde are known to exhibit amino-imino tautomerism involving its 2-pyridine−NH− fragment [4]. Thus there is a possibility that these are neutral $[Ru(L^n)_2]$ where one ligand is monoanionic amino tautomer and the other ligand is dianionic imino tautomer. Efforts are going on to grow single crystals of these materials during their formation to confirm their identity.

Table 2.2. Elemental analysis and molar conductivity[a] data of $[Ru(L^n)_2]ClO_4$

$[Ru(L^n)_2]ClO_4$	Found (calc) (%)			$\Lambda_M(\Omega^{-1}\ cm^2\ mol^{1-})$
	C	H	N	
$[Ru(L^1)_2]ClO_4$	45.81 (46.10)	3.08 (3.23)	13.16 (13.45)	137
$[Ru(L^2)_2]ClO_4$	41.32 (41.53)	2.43 (2.62)	11.85 (12.11)	118
$[Ru(L^3)_2]ClO_4$	36.65 (36.81)	2.21 (2.32)	10.52 (10.74)	136
$[Ru(L^4)_2]ClO_4$	47.65 (47.80)	3.78 (3.71)	12.64 (12.87)	130
$[Ru(L^5)_2]ClO_4$	45.22 (45.57)	3.36 (3.53)	12.15 (12.27)	135

[a] acetonitrile

2.3.2. Infrared Spectral properties

Infrared spectra of **1**−**5** were collected in the range 4000−400 cm^{-1}. Several sharp bands of various intensities are observed within ~1625−400 cm^{-1}. Except for few characteristic bands, assignment of the remaining has not been attempted. The strong band observed in the range 1614−1622 cm^{-1} is attributed to the C=N stretch of the ligand by comparing with the spectra of similar complexes [23−34]. The very strong broad band and the sharp medium intensity band at ~1100 and ~620 cm^{-1}, respectively are diagnostic of the perchlorate counteranion in **1**−**5**. Except for these two bands the spectrum of each of the orange-red precursors is very similar to that of the corresponding **1**−**5**. A representative spectrum is depicted in Figure 2.2.

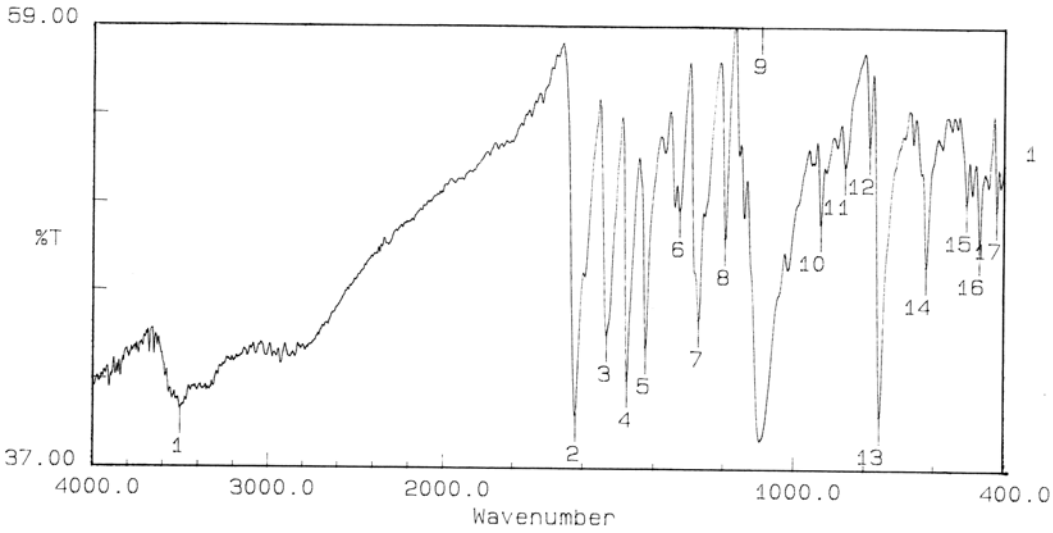

Figure 2.2. Infrared spectrum of $[Ru(L^1)_2]ClO_4$] (**1**).

2.3.3. Electronic spectral properties

Electronic spectra of **1**−**5** were collected using their acetonitrile solutions. The spectral profiles are very similar. Spectroscopic data are listed in Table 2.3

and a representative spectrum is shown in Figure 2.3. All the spectra display three strong absorption bands in the range 940−490 and three very strong bands within

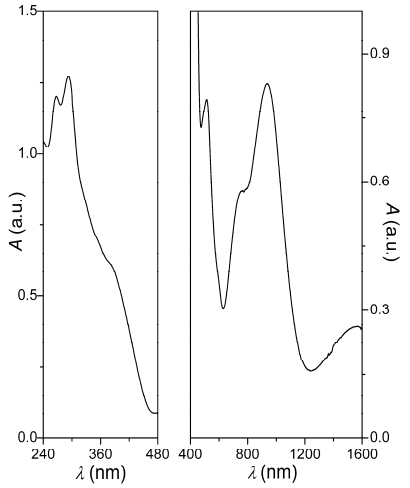

Figure 2.3. Electronic spectrum of $[Ru(L^5)_2]ClO_4$ (**5**) in acetonitrile

Table 2.3. Electronic spectroscopic[a] data of $[Ru(L^n)_2]ClO_4$

$[Ru(L^n)_2]ClO_4$	λ_{max} (nm) ($10^{-4} \times \varepsilon$ (M^{-1} cm^{-1}))
$[Ru(L^1)_2]ClO_4$	808 (2.3), 570sh (3.4), 490sh (4.4), 365 (25.5), 293 (35.4), 255 (35.2)
$[Ru(L^2)_2]ClO_4$	850 (2.7), 581sh (1.9), 500 (3.1), 368 (37.4), 290 (59.0), 259 (68.8)
$[Ru(L^3)_2]ClO_4$	838 (2.5), 580sh (2.6), 498 (3.5), 367 (28.1), 290 (42.5), 260 (51.0)
$[Ru(L^4)_2]ClO_4$	850 (3.0), 578sh (2.1), 498 (3.3), 367 (27.0), 293 (47.8), 260 (48.2)
$[Ru(L^5)_2]ClO_4$	940 (3.9), 760sh (2.7), 515 (3.7), 385 (28.0), 293 (59.4), 268 (56.2)

385−255 nm due to charge transfer and ligand centred transitions. The spectra of the complexes in the near infrared region above 1600 nm could not be recorded due to solvent background noise. However, **5** shows essentially one half of an

absorption band at ~1565 nm (Figure 2.3) and the remaining complexes show the tail of an absorption at ~1600 nm. This absorption is likely to be due to one of the two lowest energy ligand-field transitions possible for distorted octahedral ruthenium(III) complexes (*vide infra*).

2.3.4. EPR spectral properties

EPR spectra of **1**−**5** in dimethylformamide-tolune (1:1) were collected at 130 K. The *g*-values are summarized in Table 2.4 and a representative spectrum is shown in Figure 2.4. All the complexes display three distinct signals typical of distorted octahedral ruthenium(III) species. The spectra were analysed with the help of the *g*-tensor theory of low-spin d^5 metal ion complexes to appraise the extent of distortion in terms of axial (Δ) and rhombic (V) components [17]. Taking into account the two rigid meridionally spanning pyridine-N, imine-N and phenolate-O donor $(L^n)^-$ ligands around the metal centre it is very likely that in these complexes the axial (Δ) distortion is tetragonal compression operative along the N(imine)−Ru−N(imine) axis [7]. The X-ray structures of the complexes also corroborate this supposition (*vide infra*). This axial component splits the t_2 level into 'a' and 'e' and the rhombic component again splits 'e' into two non-degenerate levels (Figure 2.4). Thus two ligand-field transitions ν_1 and ν_2 are possible within these three levels. The distortion parameters (Δ and V) and the transition energies (ν_1 and ν_2) listed in Table 2 were calculated using the EPR *g*-values and the spin-orbit coupling constant of ruthenium(III) as 1000 cm^{-1} [18]. The axial component (Δ = 5.56 x 10^{-3} to 6.24 x 10^{-3} cm^{-1}) is significantly larger than the rhombic component (V = 0.91 x 10^{-3} to 1.19 x 10^{-3} cm^{-1}) for all the complexes. The calculated ν_1 and ν_2 values are within the ranges 5000−5650 cm^{-1} (2000−1770 nm) and 6420−7090 cm^{-1} (1558−1410 nm), respectively. Due to the limitation in the spectral measurements the wavelength range of the ν_1 band could

not be scanned (*vide supra*). However, the tail observed at ~1600 nm in the electronic spectra of **1**−**5** is attributed to the ν_2 band (Figure 2.3).

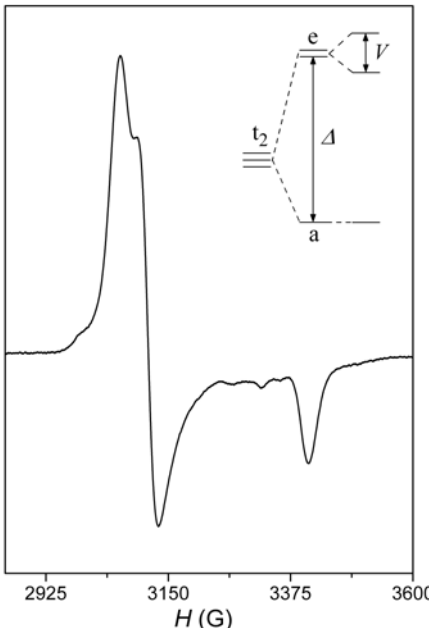

Figure.2.4. EPR spectrum of $[Ru(L^1)_2]ClO_4$ (**1**) in frozen (130 K) dimethylformamide-toluene (1:1) solution and the t_2 level splitting pattern.

Table 2.4. EPR *g*-values,[a] distortion parameters and near-IR transitions[b]

Complex	g_1	g_2	g_3	Δ/λ	V/λ	ν_1/λ	ν_2/λ
$[Ru(L^1)_2]ClO_4$ (**1**)	2.14	2.10	1.92	5.94	1.19	5.33	6.82
$[Ru(L^2)_2]ClO_4$ (**2**)	2.13	2.09	1.91	5.56	1.11	5.00	6.42
$[Ru(L^3)_2]ClO_4$ (**3**)	2.13	2.10	1.92	5.89	0.91	5.39	6.67
$[Ru(L^4)_2]ClO_4$ (**4**)	2.12	2.09	1.92	5.86	0.94	5.35	6.65
$[Ru(L^5)_2]ClO_4$ (**5**)	2.11	2.08	1.93	6.24	1.11	5.65	7.09

[a] In dimethylformamide-toluene (1:1) at 130 K.

[b]Calculated using spin-orbit coupling constant (λ) of Ru(III) as 1000 cm^{-1}.

2.3.5. Description of X-ray structures

Complexes **1**, **2**, **4** and **5** crystallizes from methanol as **1**·1.5CH_3OH, **2**·CH_3OH, **4**·2H_2O and **5**·H_2O·CH_3OH, respectively (Table 2.1). The asymmetric units of **1**, **2** and **5** contain one complex molecule and the corresponding solvent molecules. On the other hand, the asymmetric unit of **4**·2H_2O contains two essentially identical complex molecules and four water molecules. The molecular structures of the four complex cations are illustrated in Figures 2.5 and 2.6. The bond parameters related to the metal ions are listed in Tables 2.5 and 2.6. Each meridionally spanning pyridine-N, imine-N and phenolate-O donor ligand forms a five- and a six-membered chelate ring. Two such ligands assemble a distorted octahedral N_4O_2 coordination sphere around the metal centre in each complex. The *cis* bond angles spread over the range of 79.39(14)−100.15(14)^o, while the *trans* bond angles are within 169.99(13)−178.9(3)^o. The average bite angles for the five- and six-membered rings are 80^o and 93^o, respectively. The Ru−N(pyridine), the Ru−N(imine) and the Ru−O(phenolate) bond lengths are within the ranges 2.024(8)−2.068(4) Å, 1.982(8)−2.013(3) Å and 1.960(6)−1.996(7) Å, respectively. The Ru−N(pyridine) bond lengths are significantly longer compared to the Ru−N(imine) bond lengths. This difference is likely to be due to the rigidity of the tridentate ligand and the better π-back-bonding in the Ru−N(imine) bond than that in the Ru−N(pyridine) bond [7]. The average of all the *trans* O(phenolate)−Ru−N(pyridine) bonds is longer by about 0.14 Å than the average of all the *trans* N(imine)−Ru−N(imine) bonds (Tables 2.5 and 2.6). Thus in these complex cations the axial component of the distorted RuN_4O_2 coordination sphere is tetragonal compression operative along the N(imine)−Ru−N(imine) axis. On the whole, all the bond lengths are comparable with the bond lengths reported for ruthenium(III) complexes having the similar coordinating atoms [19,20,21−28].

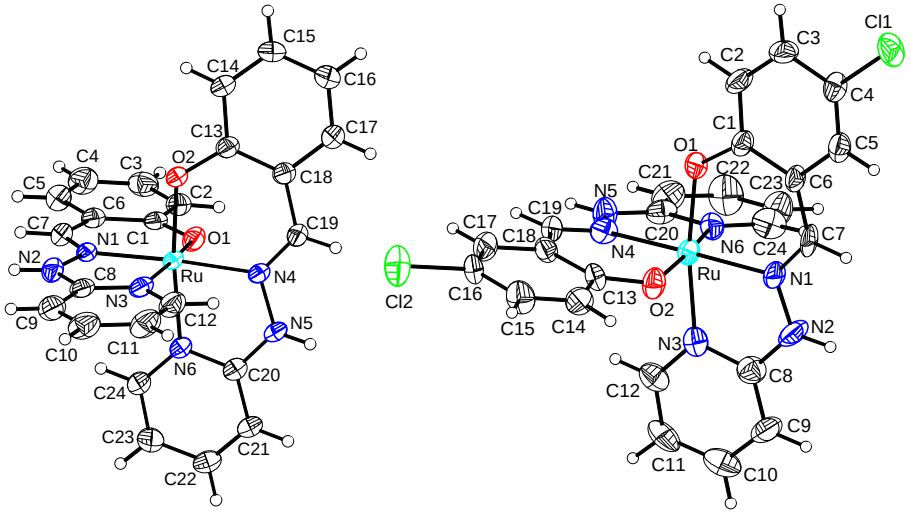

(a) **(b)**

Figure 2.5. Structures of (a) $[Ru(L^1)_2]^+$ and (b) $[Ru(L^2)_2]^+$ with the atom labeling schemes. All non-hydrogen atoms are represented by their 40% probability thermal ellipsoids.

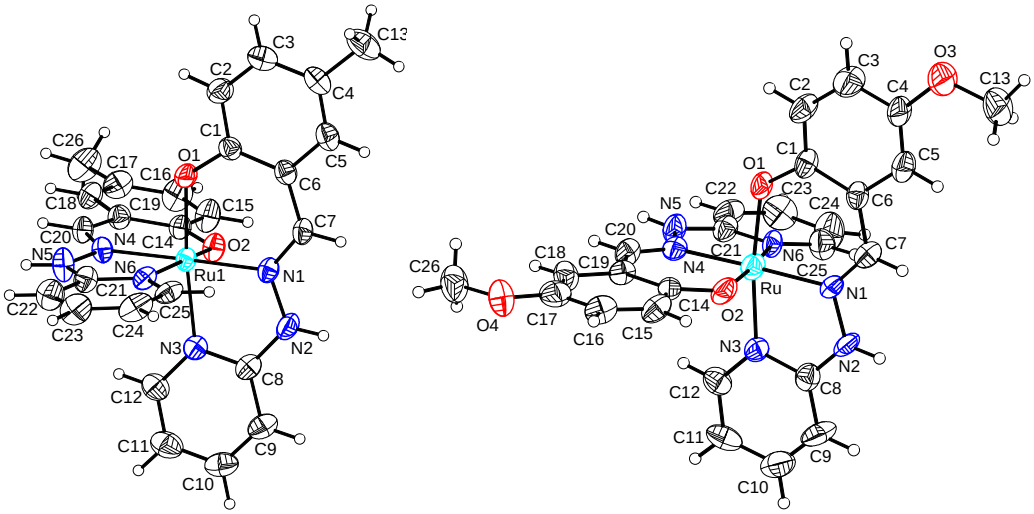

(a) **(b)**

Figure 2.6. Structures of (a) $[Ru(L^4)_2]^+$ and (b) $[Ru(L^5)_2]^+$ with the atom labeling schemes. All non-hydrogen atoms are represented by their 40% probability thermal ellipsoids.

Table 2.5. Selected bond lengths (Å) and angles (°) for **1**·1.5CH_3OH, **2**·CH_3OH and **5**·H_2O·CH_3OH

Complex	**1**·1.5CH_3OH	**2**·CH_3OH	**5**·H_2O·CH_3OH
Ru–O(1)	1.971(2)	1.960(6)	1.996(7)
Ru–O(2)	1.993(2)	1.968(6)	1.963(7)
Ru–N(1)	1.999(3)	2.008(6)	1.985(7)
Ru–N(3)	2.053(3)	2.039(8)	2.025(8)
Ru–N(4)	2.000(3)	1.992(7)	1.982(8)
Ru–N(6)	2.048(3)	2.039(8)	2.024(8)
O(1)–Ru–O(2)	93.61(10)	95.0(2)	93.0(3)
O(1)–Ru–N(1)	93.5(1)	93.1(3)	92.5(3)
O(1)–Ru–N(3)	171.93(10)	171.2(3)	171.7(3)
O(1)–Ru–N(4)	88.40(11)	88.0(3)	89.3(3)
O(1)–Ru–N(6)	89.26(11)	90.5(3)	89.8(3)
O(2)–Ru–N(1)	90.30(10)	88.1(3)	88.9(3)
O(2)–Ru–N(3)	90.57(10)	89.5(2)	90.0(3)
O(2)–Ru–N(4)	92.55(10)	92.2(3)	92.7(3)
O(2)–Ru–N(6)	171.54(10)	170.5(3)	172.6(3)
N(1)–Ru–N(3)	79.57(11)	79.5(3)	79.8(3)
N(1)–Ru–N(4)	176.47(9)	178.9(3)	177.6(3)
N(1)–Ru–N(6)	97.47(11)	99.3(3)	97.9(3)
N(3)–Ru–N(4)	98.31(11)	99.4(3)	98.3(3)
N(3)–Ru–N(6)	87.58(12)	86.1(3)	88.3(3)
N(4)–Ru–N(6)	79.56(11)	80.3(3)	80.4(3)

Table 2.6. Selected bond lengths (Å) and angles (°) for **4**·2H_2O

Molecule 1		Molecule 2	
Ru(1)–O(1)	1.994(3)	Ru(2)–O(3)	1.995(3)
Ru(1)–O(2)	1.992(3)	Ru(2)–O(4)	1.990(3)
Ru(1)–N(1)	2.002(3)	Ru(2)–N(7)	2.013(3)
Ru(1)–N(3)	2.068(4)	Ru(2)–N(9)	2.049(3)
Ru(1)–N(4)	2.011(3)	Ru(2)–N(10)	2.004(3)
Ru(1)–N(6)	2.061(4)	Ru(2)–N(12)	2.048(3)
O(1)–Ru(1)–O(2)	94.44(14)	O(3)–Ru(2)–O(4)	93.56(13)
O(1)–Ru(1)–N(1)	93.09(13)	O(3)–Ru(2)–N(7)	92.56(12)
O(1)–Ru(1)–N(3)	171.55(13)	O(3)–Ru(2)–N(9)	171.73(12)
O(1)–Ru(1)–N(4)	87.20(13)	O(3)–Ru(2)–N(10)	89.99(12)
O(1)–Ru(1)–N(6)	90.54(14)	O(3)–Ru(2)–N(12)	89.43(13)
O(2)–Ru(1)–N(1)	90.28(13)	O(4)–Ru(2)–N(7)	89.48(12)
O(2)–Ru(1)–N(3)	89.48(14)	O(4)–Ru(2)–N(9)	89.80(13)
O(2)–Ru(1)–N(4)	92.12(13)	O(4)–Ru(2)–N(10)	92.86(12)
O(2)–Ru(1)–N(6)	169.99(13)	O(4)–Ru(2)–N(12)	171.97(12)
N(1)–Ru(1)–N(3)	79.39(14)	N(7)–Ru(2)–N(9)	79.90(14)
N(1)–Ru(1)–N(4)	177.55(14)	N(7)–Ru(2)–N(10)	176.42(14)
N(1)–Ru(1)–N(6)	98.13(14)	N(7)–Ru(2)–N(12)	97.84(13)
N(3)–Ru(1)–N(4)	100.15(14)	N(9)–Ru(2)–N(10)	97.39(14)
N(3)–Ru(1)–N(6)	86.76(14)	N(9)–Ru(2)–N(12)	88.24(13)
N(4)–Ru(1)–N(6)	79.44(14)	N(10)–Ru(2)–N(12)	79.68(13)

2.3.6. Hydrogen bonding and supramolecular assembly

Extended microporous networks of transition metal complexes produced *via* various non-covalent intermolecular interactions driven supramolecular assembly are of considerable interest for their potential use as functional materials [29−34]. In each crystal structure described here, the constituent complex molecule as well as the trapped solvent molecules contain several hydrogen bond donor and acceptor sites. We have investigated the intermolecular hydrogen-bonding and the resulting supramolecular assembly patterns in all four structures. As expected both complex and the lattice solvent molecules are involved in several intermolecular hydrogen bonds that are primarily charge assisted type [35,36]. All these hydrogen bond parameters are listed in Table 2.7 the resulting self-assembled supramolecular structures (Figures 2.7 and 2.8) of the four solvated complexes are described below.

In the crystal lattice, **1**·1.5CH_3OH exists as discrete dimeric units (Figure. 2.7a). Two complex cations are involved in a pair of reciprocal N−H···O(phenolate) hydrogen bonds and form a dimer. Two full occupancy methanol molecules are at the two sides of this dimer through two more N−H···O(methanol) interactions. Each of these two methanol molecules is connected to a perchlorate via O−H···O(perchlorate) interaction. The methyl-C of the half occupancy methanol resides on a crystallographic inversion centre. Two of these half occupancy methanol molecules are connected to both ends of the long dimeric unit via bifurcated O−H···O,O(percholate) hydrogen bonds (Figure 2.7a).

2·CH_3OH forms a two-dimensional sheet structure because of N−H···O and O−H···O hydrogen bonds (Figure 2.7b). Each complex cation is flanked by a perchlorate and a methanol molecule due to involvement of the N−H groups of the two ligands in hydrogen bonds with perchlorate-O and methanol-O atoms. The same O-atom of the perchlorate acts as acceptor in the O−H···O interaction

with the OH group of a symmetry related methanol molecule. As a result, a one-dimensional chain of complex cations bridged by $O_3ClO\cdots HOCH_3$ units is formed. The parallel chains are connected by C−H···Cl interactions involving the methanol methyl group and the Cl-atom *para* to the phenolate-O of one of the two ligands. These inter-chain C−H···Cl interactions assemble the two-dimensional sheet structure of **2**·CH_3OH (Figure 2.7b). There is no other significant interaction between these parallel sheet structures.

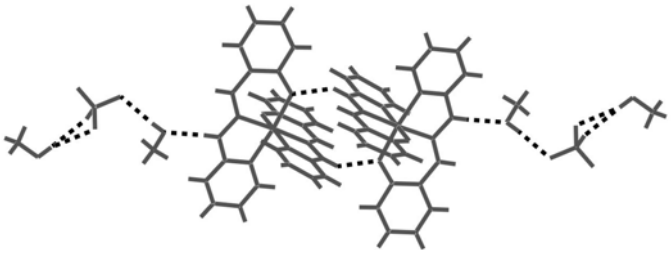

(a)

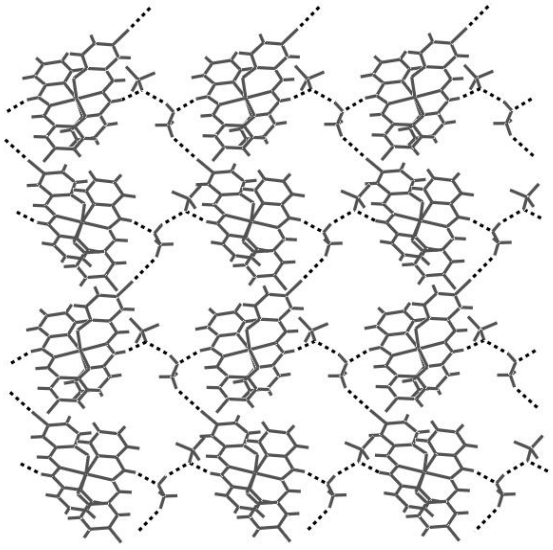

(b)

Figure 2.7. Hydrogen bond assisted (a) dimerisation of $[Ru(L^1)_2]ClO_4\cdot 1.5CH_3OH$ (**1**·$1.5CH_3OH$) and (b) two-dimensional sheet structure of $[Ru(L^2)_2]ClO_4\cdot CH_3OH$ (**2**·CH_3OH).

The supramolecular assembly pattern of **4**·2H_2O is rather intricate compared to that of the other three solvated complexes (Figures 2.7a b). This is due to the presence of two complex molecules and four water molecules in the asymmetric unit and hence a large number of hydrogen bonds (Table 2.7). Four water molecules are connected to the two complex molecules through four N−H···O hydrogen bonds. Each water molecule is also connected to four symmetry related complex cations through O−H···O(phenolate) hydrogen bonds. Except for one, the other three water molecules also act as hydrogen bond donor to two perchlorate O-atoms. These eleven hydrogen bonds assemble a two-dimensional sheet structure in the crystal lattice of **4**·2H_2O (Figure 2.7a). These parallel sheets are not connected by any other weak interaction.

Complex **5** crystallizes as **5**·H_2O·CH_3OH. This solvated species shows five intermolecular hydrogen bonds. These are two N−H···O, two O−H···O and a bifurcated O−H···O,O interactions (Table 2.7, Figure 2.7b). As observed in **1**, here also the complex cation exists as a dimer due to a pair of reciprocal N−H···O(phenolate) hydrogen bonds. The other two N−H groups on the two sides of this dimeric unit bind two water molecules through N−H···O(water) interactions. One methanol molecule is connected to each complex cation through an O−H···O interaction involving the O-atom of the OMe substituent of one of the two ligands. Each perchlorate is connected to two complex cation bound water molecules through an O−H···O(perchlorate) and a bifurcated O−H···O,O(perchlorate) hydrogen bonds. Thus cyclic $\{(H_2O)_2(ClO_4)_2\}_2^{2-}$ clusters are formed. These clusters bridge the dimeric units of the methanol containing complex cations and form a one-dimensional chain structure (Figure 2.7b). No other significant intermolecular interaction between these parallel chains is detected.

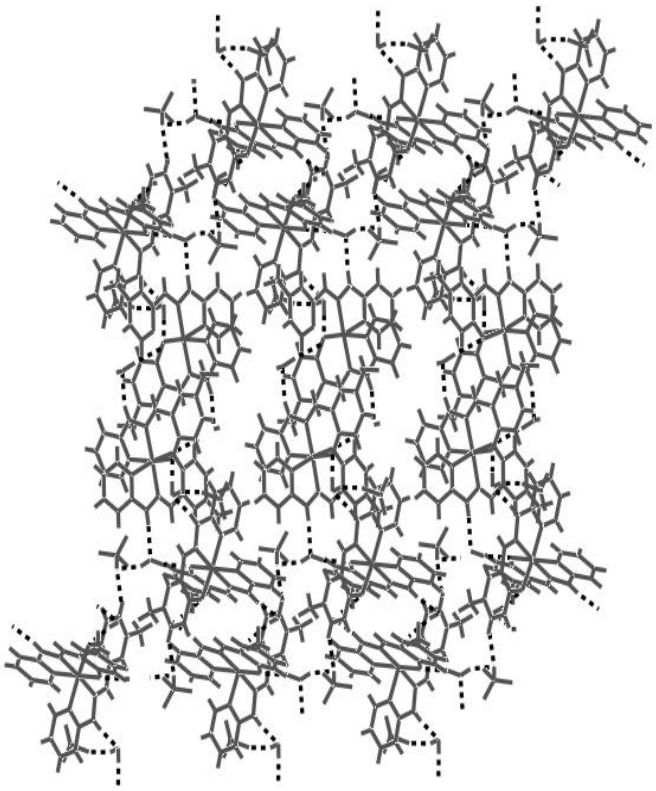

(a)

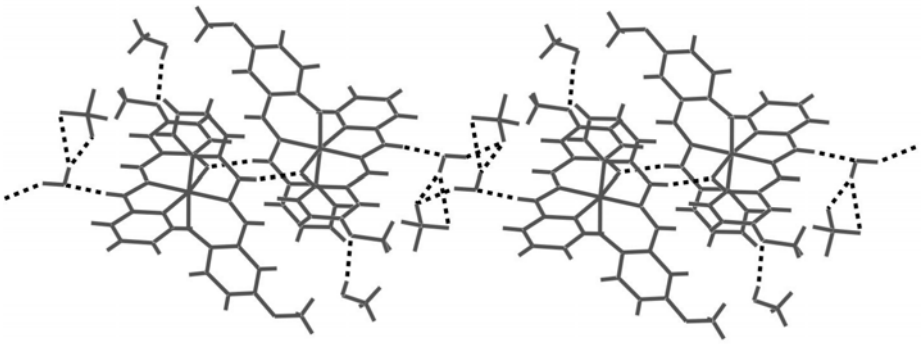

(b)

Figure 2.8. Hydrogen bond assisted (a) two-dimensional sheet structure of $[Ru(L^4)_2]ClO_4 \cdot 2H_2O$ (**4**$\cdot 2H_2O$) and (b) one-dimensional chain structure of $[Ru(L^5)_2]ClO_4 \cdot H_2O \cdot CH_3OH$ (**5**$\cdot H_2O \cdot CH_3OH$).

Table 2.7. Hydrogen bonding parameters (Å and ^{o})

Complex	D–H···A	H···A (Å)	D···A (Å)	D–H···A (^{o})
1·1.5CH_3OH	N(2)−H(2A)···O(2)^{i}	2.10	2.805(3)	138.7
	N(5)−H(5A)···O(7)^{ii}	1.97	2.788(5)	157.5
	O(7)−H(7A)···O(5)	2.27	3.091(7)	176.1
	O(8)−H(8)···O(4)	2.65	3.338(15)	142.7
	O(8)−H(8)···O(6)	2.40	3.201(14)	164.5
2·CH_3OH	N(2)–H(2A)···O(7)	1.88	2.708(12)	161.6
	N(5)–H(5A)···O(3)	2.05	2.852(10)	155.8
	O(7)–H(7A)···O(3)^{iii}	2.02	2.811(12)	160.7
	C(25)–H(25A)···Cl(2)^{iv}	2.67	3.538(16)	150.1
4·2H_2O	N(2)−H(2A)···O(13)	1.95	2.799(5)	171.0
	N(5)−H(5A)···O(14)	1.99	2.813(7)	159.1
	N(8)−H(8A)···O(15)	1.99	2.839(6)	171.0
	N(11)−H(11A)···O(16)	1.93	2.778(5)	170.5
	O(13)−H(53A)···O(3)^{v}	1.95(2)	2.889(5)	166(6)
	O(13)−H(53B)···O(9)	2.09(2)	3.015(9)	161(5)
	O(14)−H(54B)···O(1)^{vi}	2.24(2)	3.192(7)	168(8)
	O(15)−H(55A)···O(9)	2.11(1)	3.025(10)	155(3)
	O(15)−H(55B)···O(4)^{vii}	2.12(1)	3.084(7)	166(5)
	O(16)−H(56A)···O(2)^{viii}	1.94(2)	2.886(5)	165(5)
	O(16)−H(56B)···O(5)^{ix}	1.99(2)	2.924(10)	163(6)
5·H_2O·CH_3OH	N(2)−H(2A)···O(9)	1.98	2.834(12)	174.1
	N(5)−H(5A)···O(1)^{x}	2.00	2.759(9)	146.7
	O(9)−H(9A)···O(8)^{xi}	2.40(16)	3.09(2)	127(15)
	O(9)−H(9B)···O(8)	2.57(7)	3.50(3)	161(16)
	O(9)−H(9B)···O(6)	2.59(9)	3.46(2)	149(14)
	O(10)−H(10A)···O(3)	2.59	3.40(3)	169.5

Symmetry transformations used: (i) −x+2, −y+1, −z; (ii) −x+1, −y+1, −z+1; (iii) x+1, y, z; (iv) −x+1/2, y+1/2, −z+1/2; (v) x−1, y, z; (vi) −x, −y+2, −z+1; (vii) −x+1, −y+1, −z; (viii) x+1, y, z; (ix) −x+1, −y+1, −z+1; (x) −x, −y+1, −z+1; (xi) −x+1, −y, −z+1.

2.4. Conclusion

A series of five ruthenium(III) complexes with the phenolate-O, the imine-N and the pyridine-N donor deprotonated Schiff bases derived from 2-hydrazinopyridine and 5-substituted salicylaldehydes have been synthesized and characterized. The one-electron paramagnetic complexes display rhombic EPR spectra at $g_{av} \approx 2.04$ indicating a distorted octahedral coordination environment around low-spin ruthenium(III). Single crystal X-ray structures of four solvated complexes substantiate the distortion of the RuN_2O_4 coordination sphere. Intermolecular hydrogen bonding driven supramolecular assembly of these solvated complexes leads to dimeric, one-dimensional chain and two-dimensional sheet structures in the crystal lattice.

2.5. References

[1] V. Arion, K. Wieghardt, T. Weyhermueller, E. Bill, V. Leovac, A. Rufinska, *Inorg. Chem.* 36 (1997) 661.

[2] U. Knof, T. Weyhermüller, T. Wolter, K. Wieghardt, E. Bill, C. Butzlaff, A.X. Trautwein, *Angew. Chem. Int. Ed. Engl.* 32 (1993) 1635.

[3] A. Mukhopadhyay, S. Pal, *Eur. J. Inorg. Chem.* (2009) 4141.

[4] M.F. Zady, J.L. Wong, *J. Org. Chem.* 41 (1976) 2491.

[5] J.L. Wong, M.F. Zady, *J. Org. Chem.* 40 (1975) 2512.

[6] I.P. Evans, A. Spencer, G. Wilkinson, *J. Chem. Soc., Dalton Trans.* (1973) 204.

[7] S.N. Pal, S. Pal, *J. Chem. Soc., Dalton Trans.* (2002) 2102.

[8] SMART version 5.630 and SAINT-plus version 6.45, Bruker-Nonius Analytical X-ray Systems Inc., Madison, WI, USA, 2003.

[9] G.M. Sheldrick, SADABS, Program for Area Detector Absorption Correction, University of Göttingen, Göttingen, Germany, 1997.

[10] A.C.T. North, D.C. Philips, F.S. Mathews, *Acta Crystallogr., Sect. A* 24 (1968) 351.

[11] L.J. Farrugia, *J. Appl. Crystallogr.* 32 (1999) 837.

[12] CrysAlisPro version 1.171.33, Oxford Diffraction Ltd., Abingdon, Oxfordshire, UK, 2007.

[13] G.M. Sheldrick, SHELX-97, Structure Determination Software, University of Göttingen, Göttingen, Germany, 1997.

[14] P. McArdle, *J. Appl. Crystallogr.* 28 (1995) 65.

[15] A.L. Spek, Platon, A Multipurpose Crystallographic Tool, Utrecht University, Utrecht, The Netherlands, 2002.

[16] C.F. Macrae, I.J. Bruno, J.A. Chisholm, P.R. Edgington, P. McCabe, E. Pidcock, L. Rodriguez-Monge, R. Taylor, J. van de Streek, P.A. Wood, *J. Appl. Cryst.* 41 (2008) 466.

[17] S. Bhattacharya, A. Chakravorty, *Proc. Indian Acad. Sci. (Chem. Sci.)* 95 (1985) 159.

[18] C. Daul, A. Goursot, *Inorg. Chem.* 24 (1985) 3554.

[19] S.N. Pal, S. Pal, *Inorg. Chem.* 40 (2001) 4807.

[20] S.N. Pal, S. Pal, Eur. *J. Inorg. Chem.* (2003) 4244.

[21] R. Raveendran, S. Pal, *Inorg. Chim. Acta* 359 (2006) 3212.

[22] R. Raveendran, S. Pal, *J. Organomet. Chem.* 692 (2007) 824.

[23] R. Raveendran, S. Pal, *Polyhedron* 27 (2008) 655.

[24] R. Raveendran, S. Pal, *Eur. J. Inorg. Chem.* (2008) 5540.

[25] R. Raveendran, S. Pal, *J. Organomet. Chem.* 694 (2009) 1482.

[26] A.A. Batista, S.A. Onofre, S.L. Queiroz, G. Oliva, M.R.M. Fontes, O.R. Nascimento, *J. Braz. Chem. Soc.* 8 (1997) 641.

[27] F. Laurent, E. Plantalech, B. Donnadieu, A. Jiménez, F. Hernández, M. Martínez-Ripoll, M. Biner, A. Llobet, *Polyhedron* 18 (1999) 3321.

[28] M. Scarpellini, J.C. Toledo Jr., A. Neves, J. Ellena, E.E. Castellano, D.W. Franco, *Inorg. Chim. Acta* 357 (2004) 707.

[29] A.D. Bond, W. Jones, In: W. Jones, C.N.R. Rao (Eds.), Supramolecular Organization and Materials Design, Cambridge University Press, Cambridge, 2001, pp. 391−443.

[30] M. Nishio, *Cryst. Eng. Comm.* 6 (2004) 130.

[31] S. Kitagawa, R. Matsuda, *Coord. Chem. Rev.* 251 (2007) 2490.

[32] M.P. Suh, Y.E. Cheon, E.Y. Lee, *Coord. Chem. Rev.* 252 (2008) 1007.

[33] S. Pal, Rev. *Inorg. Chem.* 29 (2009) 111.

[34] T.–F. Liu, J. Lü, R. Cao, *Cryst. Eng. Comm.* 12 (2010) 660.

[35] P. Gilli, V. Bertolasi, V. Ferretti, G. Gilli, *J. Am. Chem. Soc.* 116 (1994) 909.

[36] S. Das, S. Maloth, S. Pal, *Eur. J. Inorg. Chem.* 27 (2011) 4270.

Chapter 3

Ortho-metallation of 1-pyrenyl in 1-pyrenaldehyde 4-*R*-benzoylhydrazones: Cycloruthenates(III) with CNO-pincer like ligands

Reactions of $[Ru(PPh_3)_3Cl_2]$ with 1-pyrenaldehyde 4-*R*-benzoylhydrazones (H_2pnbh*R*, where *R* = H, Me, OMe, Cl and NO_2) in presence of NaOAc afford *ortho*-metallated ruthenium(III) complexes of formula *trans*-$[Ru(pnbhR)(PPh_3)_2Cl]$ (**1**–**5**). The complexes have been characterized by elemental analysis, magnetic susceptibility, spectroscopic (IR, UV-Vis and EPR) and cyclic voltammetric measurements. Molecular structure of **2** (*R* = Me) determined by single crystal X-ray crystallography shows a distorted octahedral $CNOClP_2$ coordination sphere around the trivalent metal centre assembled by the 1-pyrenyl *ortho*-C, azomethine-N and amidate-O donor pnbhMe^{2-}, two mutually *trans* PPh_3 and the chloride. Electronic spectra of **1**–**5** in dichloromethane display several strong bands within 555−276 nm due to ligand to metal charge transfer and ligand centred transitions. The complexes are one-electron paramagnetic (μ_{eff} = 1.90−1.99 μ_B) and display rhombic EPR spectra in frozen (130 K) dichloromethane-toluene (1:1). Cyclic voltammograms of the complexes in dimethylformamide display a ligand substituent sensitive metal centred one electron reduction couple in the $E_{1/2}$ range −0.24 to −0.31 V (vs. Ag/AgCl).

3.1. Introduction

Compared to the vast literature on ruthenium(II) complexes having M−C bond [1−7], ruthenium(III) complexes of that kind are a handful [8−27]. For the

past few years our group has been working on cyclometallated palladium and ruthenium complexes with aroylhydrazones of various monocyclic and polycyclic aromatic aldehydes [26−32]. It has been found that this pincer like [32−35] aryl-C, azomethine-N and amidate-O donor ligand system is very efficient to stabilize ruthenium not only in the trivalent state but also makes its tetravalent state accessible [26,27]. The aroylhydrazones of benzaldehyde and acetophenone can afford only *ortho*-metallated complexes [26−29]. On the other hand, aroylhydrazones of polycyclic aromatic aldehydes provide both *ortho* and *peri* positions of the polycyclic aryl moiety as the potential metallation site depending upon the position of the azomethine functionality on it [30−32]. Recently we have reported some cyclopalladated complexes with aroylhydrazones of indole-3-aldehyde and 4-*R*-1-naphthaldehydes [30,32]. In each type of complexes, the tridentate ligand forms 6,5-membered fused chelate rings due to regioselective *peri* palladation of its polycyclic aryl (indole-3 and 1-naphthalenyl) fragment. In the present work, we have reported the results in our investigation on the ruthenium coordination chemistry with 1-pyrenaldehyde 4-*R*-benzoylhydrazones (H_2pnbh*R*). The objectives were to explore the possibility of C−H activation and formation of cyclometallated species, stabilization of ruthenium(III) and regioselective metallation of the 1-pyrenyl moiety if any. In this effort, we have isolated a series of *ortho*-metallated ruthenium(III) complexes of formula *trans*-[Ru(pnbh*R*)(PPh_3)$_2$Cl] (Scheme 1). In the following account, we have described synthesis, characterization and physical properties of these complexes. X-ray crystal structure of one representative complex has been also reported.

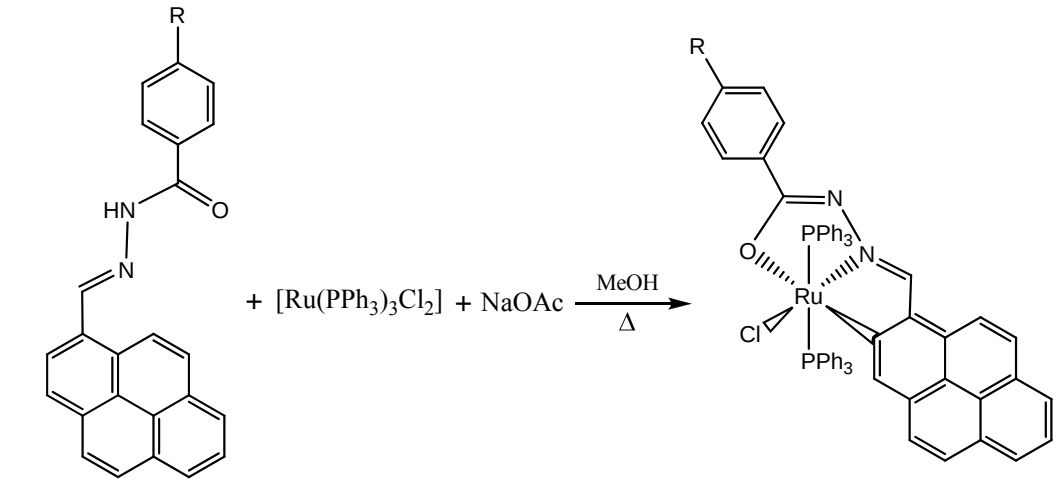

R = H, Me, OMe, Cl and NO2

Scheme 3.1

3.2. Experimental section

3.2.1. Materials

$[Ru(PPh_3)_3Cl_2]$ was prepared by following a reported procedure [36]. All other chemicals were of analytical grade available commercially and were used as supplied without further purification. The solvents used were purified by following standard methods [37].

3.2.2. Physical measurements

Microanalysis (C, H, N) were performed by using a Thermo Finnigan Flash EA1112 series elemental analyzer. Magnetic susceptibilities were measured with the help of a Sherwood scientific balance. Diamagnetic corrections calculated from Pascal's constants [38] were used to obtain the molar susceptibilities. A Digisun DI-909 conductivity meter was used to measure the solution electrical conductivities. The infrared spectra were obtained by using KBr pellets on a Jasco-5300 FT-IR spectrophotometer. A Shimadzu LCMS 2010

liquid chromatograph mass spectrometer was used for the purity verification of the Schiff bases. The electronic spectra were recorded on a Cary 100 Conc UV/vis spectrophotometer. A Jeol JES-FA200 spectrometer was used to record the X-band EPR spectra. The NMR spectra were obtained with the help of a Bruker 400 MHz NMR spectrometer. A CH-Instruments model 620A electrochemical analyzer was used for cyclic voltammetric experiments with dimethylformamide solutions of the complexes containing tetrabutylammonium perchlorate (TBAP) as the supporting electrolyte. The three electrode measurements were carried out at 298 K under dinitrogen atmosphere with a platinum disk working electrode, a platinum wire auxiliary electrode and an Ag/AgCl reference electrode. Under identical condition the $E_{1/2}$ value of the Fc^{+}/Fc couple was observed at 0.42 V.

3.2.3. Synthesis of H_2pnbhH

Benzoylhydrazine (177 mg, 1.3 mmol) was added to an ethanol solution (20 ml) of 1-pyrenaldehyde (300 mg, 1.3 mmol). The mixture was boiled under reflux for 3 h and then cooled to room temperature. The pale yellow solid separated was collected by filtration, washed with ethanol and finally dried in air. The yield was 420 mg (92%).

The same procedure described above was used for the synthesis of each of the four remaining Schiff bases (H_2pnbh*Me*, H_2pnbh*OMe*, H_2pnbh*Cl* and H_2pnbh*NO_2*) in ~90% yield from one mole equivalent each of 1-pyrenaldehyde and the corresponding 4-substituted benzoylhydrazine.

3.2.4. Synthesis of [Ru(pnbhH)(PPh_3)$_2$Cl] (1)

Solid [Ru(PPh_3)$_3Cl_2$] (200 mg, 0.21 mmol) was added to a methanol solution (30 ml) of H_2pnbh*H* (73 mg, 0.21 mmol) and NaOAc (35 mg, 0.43 mmol). The mixture was refluxed for 30 min. and then cooled to room temperature. The red solid deposited was collected by filtration and dried in air.

This material was dissolved in minimum amount of dichloromethane and transferred to a silica gel column packed with dichloromethane. The first moving yellow band eluted with dichloromethane/*n*-hexane (2:3) was discarded. The following red band containing the complex (**1**) was eluted using the same dichloromethane/*n*-hexane mixture but in the ratio 3:2. The red solution thus obtained was evaporated to dryness and the complex was collected as a dark red solid. The yield was 140 mg (62%).

The other four complexes **2**–**5** having the general formula [Ru(pnbh*R*)(PPh_3)$_2$Cl] **2** (*R* = Me), **3** (*R* = OMe), **4** (*R* = Cl) and **5** (*R* = NO_2)) were synthesized in 56–64% yields using [Ru(PPh_3)$_3$$Cl_2$], NaOAc and the corresponding Schiff bases (in 1:2:1 mole ratio) by following procedures very similar to that described above for **1** (*R* = H).

3.2.5. X-ray crystallography

Single crystals of [Ru(pnbh*Me*)(PPh_3)$_2$Cl] (**2**) were grown by slow evaporation of its dichloromethane-acetonitrile (1:1) solution. Unit cell parameters and intensity data at 298 K were obtained on an Oxford Diffraction Xcalibur Gemini single crystal X-ray diffractometer fitted with graphite monochromated Mo Kα radiation (λ = 0.71073 Å). The CrysAlisPro software [39] was used for data collection, reduction and absorption correction. The structure was solved by direct method and refined on F^2 by full-matrix least-squares procedures. All non-hydrogen atoms were refined with anisotropic thermal parameters. A riding model was used to include the hydrogen atoms in the structure factor calculations. The SHELX-97 programs [40] provided in the WinGX package [41] were used for structure solution and refinement. The Platon [42] and the Mercury [43] packages were used for molecular graphics. Selected crystallographic data are summarized in Table 3.1.

Table 3.1. Selected crystallographic data for *trans*-[Ru(pnbh*Me*)(PPh_3)$_2$Cl] (**2**)

Empirical formula	$RuC_{61}H_{46}N_2OP_2Cl$
Formula weight	1021.46
Crystal system	Monoclinic
Space group	$P2_1/c$
a (Å)	15.0653(4)
b (Å)	14.8940(4)
c (Å)	22.3055(5)
β (°)	94.404(2)
V (Å^3)	4990.2(2)
Z	4
ρ (g cm^{-3})	1.360
μ (mm^{-1})	0.476
Reflections collected	18056
Reflections unique	8773
Reflections ($I \geq 2\sigma(I)$)	6451
Parameters	614
$R1$, $wR2$ ($I \geq 2\sigma(I)$)	0.0434, 0.0926
$R1$, $wR2$ (all data)	0.0688, 0.1046
GOF (F^2)	1.032
Largest diff. peak and hole (e Å^{-3})	0.594 and -0.356

3.3. Results and discussion

3.3.1. Synthesis and characterization

The Schiff bases H_2pnbh*R* (*R* = H, Me, OMe, Cl and NO_2) were obtained in very good yields (~90%) in the condensation reactions of 1-pyrenaldehyde and the corresponding 4-*R*-benzoylhydrazines in 1:1 mole ratio in ethanol. The

identity and structures of the Schiff bases were established by elemental analysis and spectroscopic (infrared, electronic, mass and ^{1}H NMR) measurements. These characterization data are summarized in Tables 3.2-3.4. A representative proton NMR spectrum shown in Figure 3.1

Table 3.2. Elemental analysis and LCMS[a] data for the Schiff bases (H_2pnbh*R*)

H_2pnbh*R*	Found (calc) (%)			*m/z*
	C	H	N	$(M+1)^+$
H_2pnbh*H*	82.65 (82.73)	4.58 (4.63)	8.12 (8.04)	349
H_2pnbh*Me*	82.72 (82.84)	5.12 (5.01)	7.81 (7.73)	363
H_2pnbh*OMe*	79.12 (79.34)	4.91 (4.80)	7.36 (7.41)	379
H_2pnbh*Cl*	75.41 (75.28)	3.85 (3.95	7.21 (7.32)	382
H_2pnbh*NO*$_2$	73.12 (73.26)	3.81 (3.85)	10.56 (10.69)	393

[a] In dichloromethane.

Table 3.3. Electronic spectroscopic[a] data for the Schiff bases (H_2pnbh*R*)

H_2pnbh*R*	λ_{max} (nm) ($10^{-4} \times \varepsilon$ (M^{-1} cm^{-1}))
H_2pnbh*H*	400 (2.35), 380[b] (3.42), 370 (3.52), 295[b] (2.47), 286 (2.66)
H_2pnbh*Me*	401 (2.04), 381[b] (3.06), 369 (3.26), 298[b] (2.18), 282 (2.63)
H_2pnbh*OMe*	401 (2.03), 381[b] (3.04), 369 (3.25), 297[b] (2.21), 282 (2.62)
H_2pnbh*Cl*	401 (2.34), 381[b] (2.34), 371 (3.38), 296[b] (2.36), 286 (2.56)
H_2pnbh*NO*$_2$	402 (2.40), 382 (3.08), 368[b] (2.84), 293[b] (2.74), 284 (2.83)

[a] In dichloromethane.

[b] Shoulder.

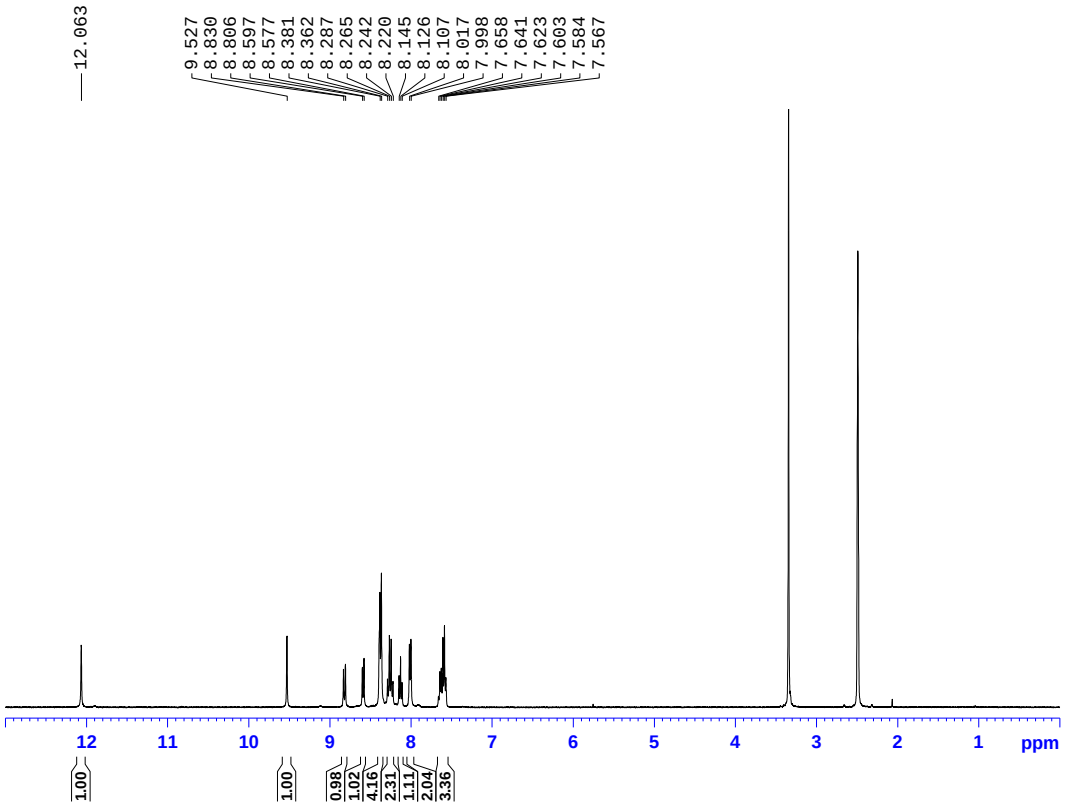

Figure 3.1 Proton NMR spectrum of H_2pnbhH

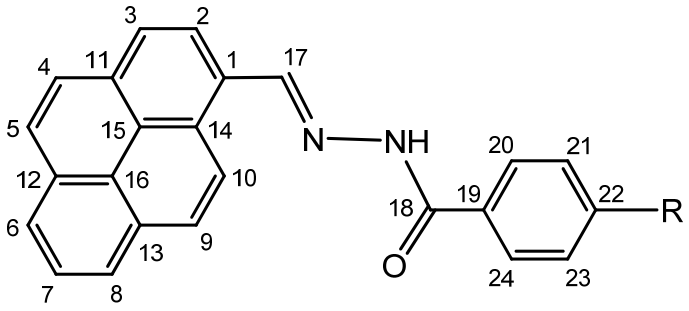

H_2pnbh*R*

Table 3.4. ^{1}H NMR data for the Schiff bases (H_2pnbh*R*) in $(CD_3)_2SO$

Ligand	δ (ppm) (J (Hz))
H_2pnbh*H*	12.06 (s, 1H, NH); 9.53 (s, 1H, H^{17}); 8.82 (9) (d, 1H, H^2); 8.59 (8) (d, 1H, H^3); 8.37 (8) (d, 4H, H^4, H^5, H^9, H^{10}); 8.28 (9), 8.23 (9) (AB pattern, q, 2H, H^6, H^8); 8.13 (8) (t, 1H, H^7); 8.01 (7) (d, 2H, H^{20}, H^{24}); 7.61 (m, 3H, H^{21}, H^{22}, H^{23})
H_2pnbh*Me*	11.99 (s, 1H, NH); 9.52 (s, 1H, H^{17}); 8.81 (9) (d, 1H, H^2); 8.58 (8) (d, 1H, H^3); 8.37 (8) (d, 4H, H^4, H^5, H^9, H^{10}); 8.27 (9), 8.23 (9) (AB pattern, q, 2H, H^6, H^8); 8.12 (8) (t, 1H, H^7); 7.92 (8) (d, 2H, H^{20}, H^{24}); 7.39 (8) (d, 2H, H^{21}, H^{23}); 2.45 (s, 3H, Me)
H_2pnbh*OMe*	11.94 (s, 1H, NH); 9.51 (s, 1H, H^{17}); 8.81 (9) (d, 1H, H^2); 8.57 (8) (d, 1H, H^3); 8.36 (8) (d, 4H, H^4, H^5, H^9, H^{10}); 8.26 (9), 8.22 (9) (AB pattern, q, 2H, H^6, H^8); 8.12 (8) (t, 1H, H^7); 8.00 (8) (d, 2H, H^{20}, H^{24}); 7.12 (9) (d, 2H, H^{21}, H^{23}); 3.86 (s, 3H, OMe)
H_2pnbh*Cl*	12.12 (s, 1H, NH); 9.51 (s, 1H, H^{17}); 8.82 (9) (d, 1H, H^2); 8.58 (8) (d, 1H, H^3); 8.37 (8) (d, 4H, H^4, H^5, H^9, H^{10}); 8.28 (9), 8.23 (9) (AB pattern, q, 2H, H^6, H^8); 8.13 (8) (t, 1H, H^7); 8.03 (8) (d, 2H, H^{20}, H^{24}); 7.67 (8) (d, 2H, H^{21}, H^{23})
H_2pnbh*NO*$_2$	12.33 (s, 1H, NH); 9.53 (s, 1H, H^{17}); 8.83 (9) (d, 1H, H^2); 8.59 (8) (d, 1H, H^3); 8.41 (m, 6H, H^4, H^5,H^6, H^8, H^9, H^{10}); 8.29 (8), 8.24 (8) (~AB pattern, q, 4H, H^{20}, H^{24}, H^{21}, H^{23}); 8.14 (8) (t, 1H, H^7)

Reactions of $[Ru(PPh_3)_3Cl_2]$, the corresponding H_2pnbh*R* and NaOAc in 1:1:2 mole ratio in methanol under aerobic conditions produce red colored complexes of formula *trans*-[Ru(pnbh*R*)$(PPh_3)_2$Cl] (**1**–**5**) in 56−64% yields. The elemental analysis data (Table 3.5) of the complexes are in good agreement with the above general molecular formula. All of **1**–**5** are one-electron paramagnetic.

The room temperature (298 K) magnetic moments are within 1.90–1.99 μ_β. These values suggest the low-spin trivalent oxidation state of ruthenium in each of **1**–**5**. In all probability the oxygen in air oxidizes the metal centre during the synthesis of the complexes from $[Ru(PPh_3)_3Cl_2]$. All the complexes are highly soluble in dichloromethane, chloroform, dimethylsulfoxide and dimethylformamide and provide red solutions. In solution, they behave as non-electrolyte.

Table 3.5. Elemental analysis data of *trans*-[Ru(pnbh*H*)$(PPh_3)_2$Cl]

Complex	Found (calc) (%)		
	C	H	N
trans-[Ru(pnbh*H*)$(PPh_3)_2$Cl]	71.38 (71.51)	4.51 (4.40)	2.71 (2.78)
trans-[Ru(pnbh*Me*)$(PPh_3)_2$Cl]	71.56 (71.71)	4.61 (4.54)	2.65 (2.74)
trans-[Ru(pnbhO*Me*)$(PPh_3)_2$Cl]	70.81 (70.61)	4.41 (4.47)	2.65 (2.70)
trans-[Ru(pnbhCl)$(PPh_3)_2$Cl]	68.95 (69.15)	4.23 (4.16)	2.61 (2.69)
trans-[Ru(pnbh*NO*$_2$)$(PPh_3)_2$Cl]	68.57 (68.45)	4.18 (4.12)	3.86 (3.99)

3.3.2. Infrared Spectral properties

Infrared spectra of the Schiff bases and the complexes (**1**–**5**) were recorded using KBr pellets. The Schiff bases display the N–H and C=O stretches of the amide functionality in the ranges 3222–3162 and 1663–1633 cm^{-1}, respectively. A medium to strong band observed within 1605–1592 cm^{-1} is assigned to the C=N stretching vibration of the Schiff bases. Complexes **1**–**5** do not display any band associated with the amide N–H and C=O groups. Thus the amide functionality of the tridentate ligand (pnbhR^{2-}) is deprotonated in the complexes. A medium intensity band observed in the range 1582–1574 cm^{-1} for **1**–**5** is attributed to the metal coordinated C=N stretching vibration of pnbhR^{2-}. Each of **1**–**5** shows three strong bands at ~743, ~693 and ~517 cm^{-1} typical of

metal bound PPh_3 [20–22,25–27]. A representative spectrum is shown in Figure 3.2.

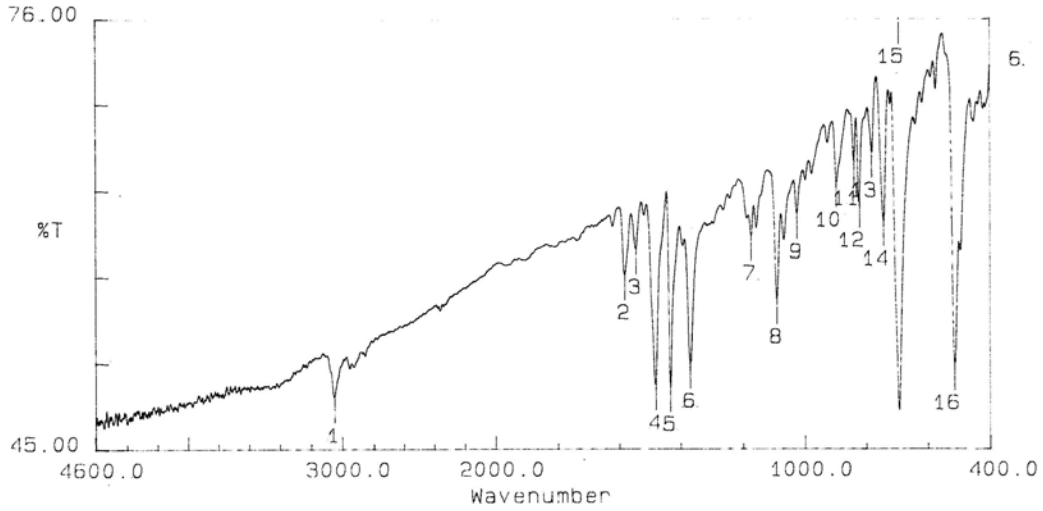

Figure 3.2. Infrared spectrum of *trans*-[Ru(pnbh*H*)$(PPh_3)_2$Cl] (**1**)

3.3.3. Electronic spectral properties

Electronic spectral profiles of **1–5** obtained using the corresponding dichloromethane solutions are very similar. A representative spectrum is shown in Figure 3.3. The spectral data are listed in Table 3.6. The complexes display several strong to very strong absorptions in the wavelength range 555–276 nm. The electronic spectra of all the Schiff bases (H_2pnbh*R*) in dichloromethane were also recorded for comparison. The spectra of H_2pnbh*R* are also very similar and display two groups of intense absorptions centred at ~370 and ~285 nm Table 3.6. The spectrum of H_2pnbh*H* is shown in Figure 3.3. Below 400 nm the spectral profiles of the complexes are somewhat similar to those of the Schiff bases. Thus the absorptions observed above 400 nm for **1–5** are assigned to ligand-to-metal

charge transfer transitions and the absorptions observed below 400 nm are primarily due to ligand centred transitions [20–22,25–27]

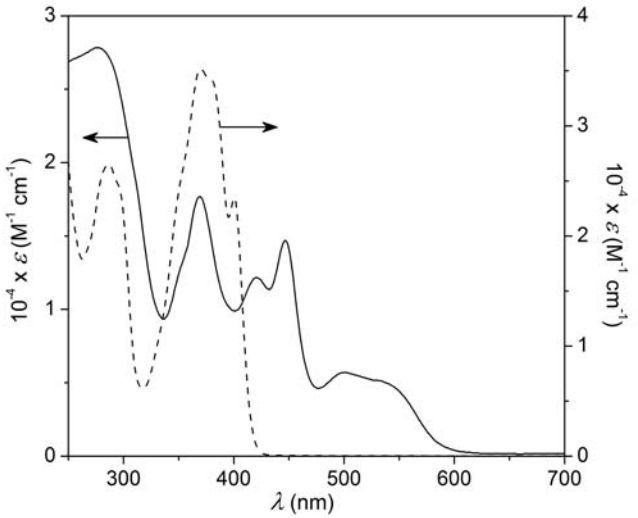

Figure 3.3. Electronic spectra of H_2pnbh*H* (----) and *trans*-[Ru(pnbh*H*)$(PPh_3)_2$Cl] (**1**) (—) in dichloromethane

Table 3.6. Electranic spectroscopic[a] data of *trans*-[Ru(pnbh*R*)$(PPh_3)_2$Cl]

Complex	λ_{max} (nm) ($10^{-4} \times \varepsilon$ (M^{-1} cm^{-1}))
trans-[Ru(pnbh*H*)$(PPh_3)_2$Cl]	535[b] (0.51), 501 (0.57), 447 (1.47), 421 (1.22), 369 (1.77), 276 (2.78)
trans-[Ru(pnbh*Me*)$(PPh_3)_2$Cl]	536[b] (0.50), 500 (0.56), 446 (1.44), 420 (1.19), 369 (1.73), 313[b] (1.65), 279 (2.32)
trans-[Ru(pnbh*OMe*)$(PPh_3)_2$Cl]	537[b] (0.47), 497 (0.57), 445 (1.37), 419 (1.15), 370 (1.65), 312[b] (1.65), 279 (2.37)
trans-[Ru(pnbh*Cl*)$(PPh_3)_2$Cl]	537[b] (0.50), 500 (0.58), 449 (1.44), 423 (1.21), 370 (1.68), 312[b] (1.66), 279 (2.18)
trans-[Ru(pnbhNO_2)$(PPh_3)_2$Cl]	555[b] (0.51), 518 (0.55), 452 (1.05), 409[b] (1.15), 371 (1.41), 280 (2.30)

[a] In dichloromethane.

[b] Shoulder.

3.3.4. EPR spectral properties

The one-electron paramagnetic complexes are EPR active. All the complexes in dichloromethane-toluene (1:1) solution display an isotropic spectrum with g ≈ 2.12 at room temperature (298 K). However, the spectra of **1–5** in frozen (130 K) solution show three distinct EPR signals. The spectrum of **3** is illustrated in Figure 3.4 and the *g*-values for all five complexes are listed in Table 3.7. Such EPR spectra are typical of rhombically distorted octahedral low-spin ruthenium(III) species [11,14,18,20–23,26,27]. Considering the type of ligands in each of these quaternary complexes (**1–5**) and hence the stereochemistry of the molecule, rhombic distortion of the coordination sphere around the metal centre from ideal octahedral geometry is quite anticipated. The molecular structure of *trans*-[Ru(pnbh*Me*)(PPh_3)$_2$Cl] (**2**) determined by X-ray crystallography (*vide infra*) corroborates the observed EPR characteristics.

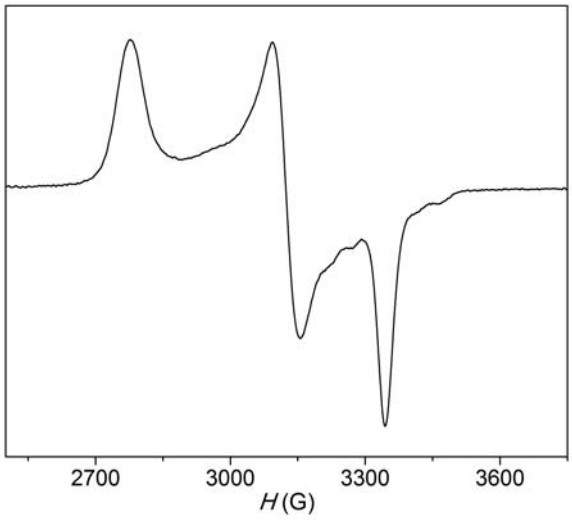

Figure 3.4. EPR spectrum of *trans*-[Ru(pnbh*OMe*)(PPh_3)$_2$Cl] (**3**) in frozen (130 K) dichloromethane-toluene (1:1) solution.

Table 3.7. EPR spectroscopic data[a] of *trans*-[Ru(pnbh*R*)(PPh_3)$_2$Cl]

Complex	g_1	g_2	g_3
trans-[Ru(pnbh*H*)(PPh_3)$_2$Cl]	2.36	2.09	1.95
trans-[Ru(pnbh*Me*)(PPh_3)$_2$Cl]	2.36	2.09	1.96
trans-[Ru(pnbh*OMe*)(PPh_3)$_2$Cl]	2.35	2.09	1.96
trans-[Ru(pnbh*Cl*)(PPh_3)$_2$Cl]	2.36	2.10	1.95
trans-[Ru(pnbh*NO$_2$*)(PPh_3)$_2$Cl]	2.36	2.09	1.95

[a] In dichloromethane-toluene (1:1) at (130 K)

3.3.5 X-ray structure of trans-[Ru(pnbhMe)(PPh_3)$_2$Cl] (2)

The X-ray molecular structure of *trans*-[Ru(pnbh*Me*)(PPh_3)$_2$Cl] (**2**) is depicted in Figure 3.5. All the bond lengths and angles involving the metal centre and the coordinating atoms are listed in Table 3.8. These bond parameters indicate a distorted octahedral $CNOP_2Cl$ coordination sphere around the ruthenium atom. The meridionally spanning pnbhMe^{2-} coordinates the metal centre through the 1-pyrenyl *ortho*-C, the azomethine-N and the amidate-O atoms and forms 5,5-fused chelate rings. The chlorine atom completes a CNOCl square-plane around the metal centre and the two PPh_3 molecules occupy the two axial positions. Both bite angles (77.38(11)^o) and (74.34(9)°) in the 5,5-fused chelate rings of **2** are comparable with those reported for trivalent ruthenium complexes containing similar fused chelate rings formed by C,N,O-donor pincer like ligands [11,22,26,27]. The remaining *cis* angles are in the range 84.10(6)–106.58(9)°. The P(1)–Ru–P(2) angle (178.01(3)°) formed by the two mutually *trans* PPh_3 molecules is very close to the ideal value, while *trans* N(1)–Ru–Cl angle (173.84(8)°) is somewhat shorter than that. In contrast, due to steric requirement the *trans* C(1)–Ru–O angle (150.65(11)°) formed by the two ends of the C,N,O-donor pnbhMe^{2-} is significantly shorter than 180°. The two very similar *trans*

oriented Ru–P bond lengths are somewhat longer than the Ru–Cl bond length but significantly longer than the bond lengths between the metal centre and the coordinating atoms from pnbh*Me*$^{2-}$ (Table 3.8). On the whole, the Ru to the aryl-C, the azomethine-N, the amidate-O and the Cl-atom bond lengths and the two Ru–P bond lengths are within the ranges observed for ruthenium(III) complexes having similar coordinating atoms [11,22,23,26,27].

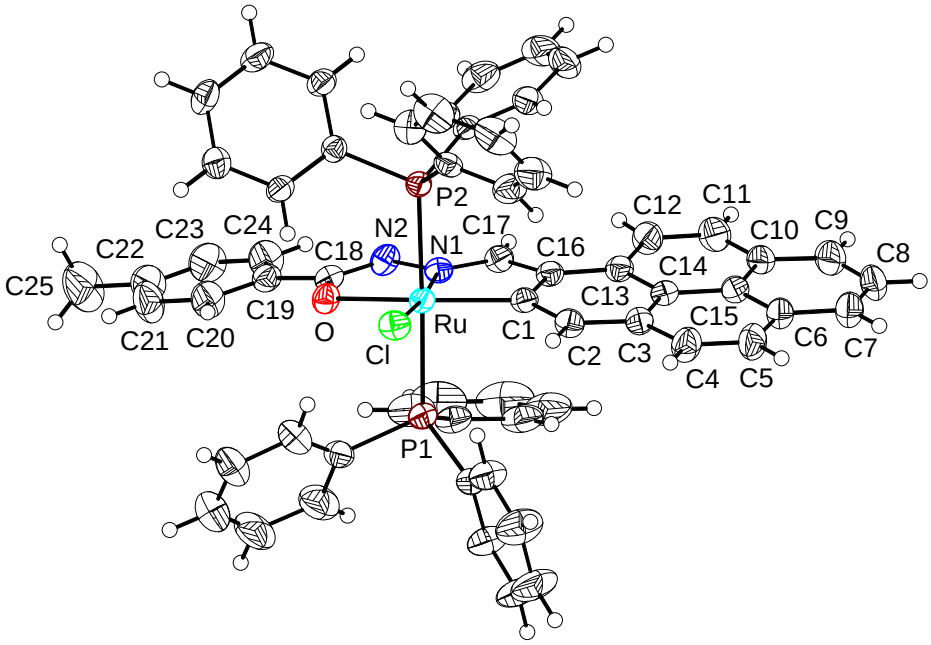

Figure 3.5. X-ray molecular structure of *trans*-[Ru(pnbh*Me*)(PPh_3)$_2$Cl] (**2**) with the atom labeling schemes. Carbon atoms of the PPh_3 molecules are not labeled for clarity. All non-hydrogen atoms are represented by their 40% probability thermal ellipsoids.

Table 3.8. Selected bond lengths (Å) and angles (°) for *trans*-[Ru(pnbh*Me*)(PPh_3)$_2$Cl] (**2**)

Ru−C(1)	2.048(3)	Ru−N(1)	2.025(3)
Ru−O	2.132(2)	Ru−Cl	2.3651(8)
Ru−P(1)	2.4030(9)	Ru−P(2)	2.3941(9)
C(1)−Ru−N(1)	77.38(11)	C(1)−Ru−O	150.65(11)
C(1)−Ru−Cl	106.58(9)	C(1)−Ru−P(1)	88.89(9)
C(1)−Ru−P(2)	92.39(9)	N(1)−Ru−O	74.34(9)
N(1)−Ru−Cl	173.84(8)	N(1)−Ru−P(1)	91.30(7)
N(1)−Ru−P(2)	87.49(7)	O−Ru−Cl	102.27(6)
O−Ru−P(1)	84.10(6)	O−Ru−P(2)	94.04(6)
Cl−Ru−P(1)	93.47(3)	Cl−Ru−P(2)	87.63(3)
P(1)−Ru−P(2)	178.01(3)		

3.3.6. Electron transfer properties

Electron transfer behaviour of **1**–**5** were studied using cyclic voltammetry. All the complexes in dimethylformamide display a reduction and a couple of irreversible oxidation responses on the cathodic and anodic sides, respectively of Ag/AgCl reference electrode. The reduction response of **4** is illustrated in Figure 3.6. All the potential data are summarized Table 3.9. The one electron nature of the reduction response has been inferred by comparing the current heights with known one electron transfer processes under identical condition [26,27]. The trend in the $E_{1/2}$ values of this reduction reflects the effect of the electronic nature of the substituent (*R*) on the aroyl fragment of pnbhR^{2-}. There is a satisfactory linear relationship between the $E_{1/2}$ values and the Hammett constants [44] of the substituents (Figure 3.6). The free Schiff bases do not display any such response in this potential range under identical condition. Thus the electron transfer process

observed for **1**–**5** is assigned to the ruthenium(III)-ruthenium(II) reduction couple. At present we are not sure about the nature of the two irreversible oxidation responses. In comparison to reduction responses, the first oxidation response has comparable current height while the second oxidation response has relatively larger current heights, perhaps the first response involves the metal centre and the second response is due to ligand oxidation.

Our previously reported cyclometallated complexes of *trans*-$\{Ru(PPh_3)_2Cl\}^{2+}$ with aroylhydrazones of benzaldehyde display only a metal centred oxidation couple within 0.35 to 0.58 V [26], while analogous complexes with aroylhydrazones of acetophenone display both reduction (–0.66 to –0.70 V) and oxidation (0.75 to 0.80 V) of the metal centre [27]. In these complexes, the tridentate ligand is the phenyl *ortho*-C, the azomethine-N and the amidate-O donor, while pnbhR^{2-} uses the *ortho*-C of 1-pyrenyl together with the azomethine-N and the amidate-O to bind the metal centre in **1**–**5**. Thus it appears that the change in the aromatic part of the *ortho*-metallated fragment is primarily responsible for the observed differences in the electron transfer behaviour of these three very similar series of complexes. Perhaps the aromatic part plays a major role in tuning the distortion of the coordination geometry from octahedral symmetry and hence the electronic energy levels of the metal centre [27].

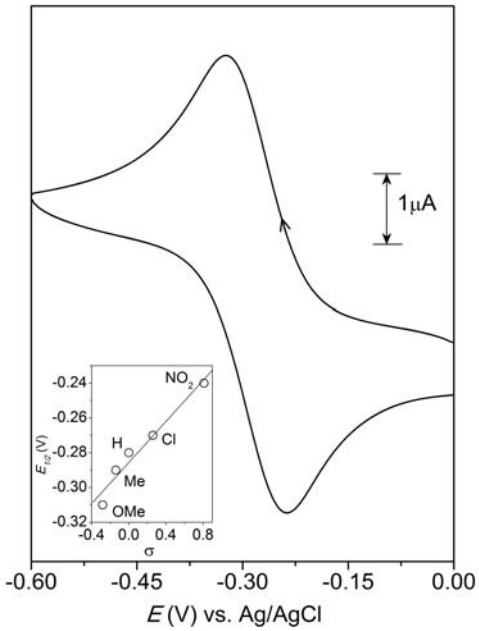

Figure 3.6. Cyclic voltammogram of *trans*-[Ru(pnbh*Cl*)(PPh_3)$_2$Cl] (**4**) in dimethylformamide (0.1 M TBAP) 298 K. Inset: Linear correlation between the $E_{1/2}$ and the Hammett substituent constant (σ).

Table 3.9. Cyclic voltammetric[a] data of *trans*-[Ru(pnbh*R*)(PPh_3)$_2$Cl]

Complex	$E_{1/2}$(V) (ΔE_p (mV))[b]	
	Reduction	Oxidation
trans-[Ru(pnbh*H*)(PPh_3)$_2$Cl]	–0.28 (90)	1.14[c], 1.59[c]
trans-[Ru(pnbh*Me*)(PPh_3)$_2$Cl]	–0.29 (100)	1.12[c], 1.48[c]
trans-[Ru(pnbh*OMe*)(PPh_3)$_2$Cl]	–0.31 (90)	1.10[c], 1.37[c]
trans-[Ru(pnbh*Cl*)(PPh_3)$_2$Cl]	–0.27 (90)	1.15[c], 1.77[c]
trans-[Ru(pnbh*NO$_2$*)(PPh_3)$_2$Cl]	–0.24 (130)	1.20[c], 1.83[c]

[a] In dimethylformamide.

[b] $E_{1/2} = (E_{pa} + E_{pc})/2$ and $\Delta E_p = E_{pa} - E_{pc}$, where E_{pa} and E_{pc} are anodic and cathodic peak potentials, respectively.

[c] E_{pa} values.

3.4. Conclusion

A series of cycloruthenated complexes, *trans*-[Ru(pnbh*R*)(PPh_3)$_2$Cl] (H_2pnbh*R* = 1-pyrenaldehyde 4-*R*-benzoylhydrazone (*R* = H, Me, OMe, Cl and NO_2) is reported. The magnetic moments and the EPR spectra are consistent for trivalent state of the metal ion in these complexes. X-ray structure of *trans*-[Ru(pnbh*Me*)(PPh_3)$_2$Cl] reveals an unsymmetrical pincer like coordination mode of pnbhMe^{2-} through the 1-pyrenyl *ortho*-C, the azomethine-N and the amidate-O. Very similar spectroscopic and electron transfer properties suggest the same coordination mode of pnbhR^{2-} in all the complexes. Thus regioselective *ortho*-metallation over *peri*-metallation of the 1-pyrenyl fragment of pnbhR^{2-} and hence formation of 5,5- instead of 6,5-fused chelate rings at the trivalent ruthenium is preferred in the present series of cycloruthenates.

3.5. References

[1] P.M. Maitlis, *Chem. Soc. Rev.* 10 (1981) 1.

[2] G. Wilkinson, F.G.A. Stone, E.W. Abel, (Eds.), Comprehensive Organometallic Chemistry, vol. 4, Pergamon, Oxford, 1982, pp. 651−820.

[3] G.R. Knox, Organometallic Compounds of Ruthenium and Osmium, Chapman and Hall, London, 1985, pp. 71−209.

[4] D.F. Shriver, M.I. Bruce (Eds.), Comprehensive Organometallic Chemistry II, vol. 7, Pergamon, Oxford, 1995, pp. 291−624.

[5] M.I. Bruce (Eds.), Comprehensive Organometallic Chemistry III, vol. 6, Elsevier, Amsterdam, 2007, pp. 353−646.

[6] V. Dragutan, I. Dragutan, L. Delaude, A. Demonceau, *Coord. Chem. Rev.* 251 (2007) 765.

[7] B. Therrien, *Coord. Chem. Rev.* 253 (2009) 493.

[8] A.J. Hewitt, J.H. Holloway, R.D. Peacock, J.B. Raynor, I.L. Wilson, *Dalton Trans.* (1976) 579.

[9] L.H. Pignolet, S.H. Wheeler, *Inorg. Chem.* 19 (1980) 935.

[10] M. Ke, S.J. Rettig, B.R. James, D. Dolphin, *J. Chem. Soc., Chem. Commun.* (1987) 1110.

[11] G.K. Lahiri, S. Bhattacharya, M. Mukherjee, A.K. Mukherjee, A. Chakravorty, *Inorg. Chem.* 26 (1987) 3359.

[12] P.G. Gassman, C.H. Winter, *J. Am. Chem. Soc.* 110 (1988) 6130.

[13] U. Koelle, J. Kossakowski*, J. Organomet. Chem.* 362 (1989) 383.

[14] M.M. Taqui Khan, D. Srinivas, R.I. Kureshy, N.H. Khan, *Inorg. Chem.* 29 (1990) 2320.

[15] J.W. Seyler, C.R. Leidner, *Inorg. Chem.* 29 (1990) 3636–3641.

[16] M. Ke, C. Sishta, B.R. James, D. Dolphin, J.W. Sparapany, J.A. Ibers, *Inorg. Chem.* 30 (1991) 4766.

[17] M. Beley, J.-P. Collin, R. Louis, B. Metz, J.-P. Sauvage, *J. Am. Chem. Soc.* 113 (1991) 8521.

[18] P. Ghosh, A. Pramanik, N. Bag, G.K. Lahiri, A. Chakravorty, *J. Organomet. Chem.* 454 (1993) 237.

[19] J.P. Collman, E. Rose, G.D. Venburg, *J. Chem. Soc., Chem. Commun.* (1994) 11.

[20] R. Hariram, B.K. Santra, G.K. Lahiri, *J. Organomet. Chem.* 540 (1997) 155.

[21] P. Munshi, R. Samanta, G.K. Lahiri, *J. Organomet. Chem.* 586 (1999) 176.

[22] S. Kannan, R. Ramesh, Y. Liu, *J. Organomet. Chem.* 692 (2007) 3380.

[23] R. Prabhakaran, R. Huang, R. Karvembu, C. Jayabalakrishnan, K. Natarajan, *Inorg. Chim. Acta* 360 (2007) 691.

[24] S.H. Wadman, R.W.A. Havenith, M. Lutz, A.L. Spek, G.P.M. van Klink, G. van Koten, *J. Am. Chem. Soc.* 132 (2010) 2849.

[25] K. Ghosh, S. Kumar, R. Kumar, U.P. Singh, *Eur. J. Inorg. Chem.* (2012) 929.

[26] R. Raveendran, S. Pal, *J. Organomet. Chem.* 692 (2007) 824.

[27] R. Raveendran, S. Pal, *J. Organomet. Chem.* 694 (2009) 1482.

[28] S. Das, S. Pal, *J. Organomet. Chem.* 689 (2004) 352.

[29] S. Das, S. Pal, *J. Organomet. Chem.* 691 (2006) 2575.

[30] A.R.B. Rao, S. Pal, *J. Organomet. Chem.* 696 (2011) 2660.

[31] A.R.B. Rao, S. Pal, *J. Organomet. Chem.* 701 (2012) 62.

[32] A.R.B. Rao, S. Pal, *J. Organomet. Chem.* 731 (2013), 67.

[33] N. Selander, K.J. Szabó, *Chem. Rev.* 111 (2011) 2048.

[34] M.M. Tamizh, K. Mereiter, K. Kirchner, R. Karvembu, *J. Organomet. Chem.* 700 (2012) 194.

[35] A. Abellán-López, M.-T. Chicote, D. Bautista, J. Vicente, *Organometallics* 31 (2012) 7434.

[36] T.A. Stephenson, G. Wilkinson, *J. Inorg. Nucl. Chem.* 28 (1966) 945.

[37] D.D. Perrin, W.L.F. Armarego, D.P. Perrin, Purification of Laboratory Chemicals, 2nd ed., Pergamon, Oxford, 1983.

[38] G.A. Bain, J.F. Berry, *J. Chem. Edu.* 85 (2008) 532.

[39] CrysAlisPro Version 1.171.33.55, Oxford Difraction Ltd., Abingdon, Oxford-shire UK, 2007.

[40] G.M. Sheldrick, SHELX-97, Structure Determination Software, University of Gottingen, Gottengen, Germany, 1997.

[41] L.J. Farrugia, WinGX, *J. Appl. Crystallogr.* 32 (1999) 837.

[42] A.L. Spek, Platon, A Multipurpose Crystallographic Tool, Utrecht University, Utrecht, The Netherlands, 2002.

[43] C.F. Macrae, I.J. Bruno, J.A. Chisholm, P.R. Edgington, P. McCabe, E. Pidcock, L. Rodriguez-Monge, R. Taylor, J. van de Streek, P.A. Wood, Mercury CSD 2.0, *J. Appl.* Crystallogr. 41 (2008) 466.

[44] J. March, in: Advanced Organic Chemistry, 4th ed., Wiley, New York, 1992, p. 280.

Chapter 4

Ortho-metallation of 1-naphthalenyl in 1-naphthaldehyde 4-*R*-benzoylhydrazones: Cycloruthenates(III) with CNO-pincer like ligands

In methanol, reactions of $[Ru(PPh_3)_3Cl_2]$, 1-naphthaldehyde 4-*R*-benzoylhydrazones (H_2nabh*R*, where *R* = H, Me, OMe, Cl and NO_2) and NaOAc in 1:1:2 mole ratio provide *ortho*-metallated ruthenium(III) complexes of general formula *trans*-[Ru(nabh*R*)$(PPh_3)_2$Cl] (**1**–**5**) in 50–58% yields. Elemental analysis, magnetic susceptibility, spectroscopic (IR, UV-Vis and EPR) and cyclic voltammetric measurements were used to characterize the complexes. Single crystal X-ray structures of **1** (*R* = H), **2** (*R* = Me) and **5** (*R* =NO_2) show pincer like coordination mode of nabhR^{2-}. The 1-naphthalenyl *ortho*-C, the azomethine-N and the amidate-O donor nabhR^{2-}, two mutually *trans* PPh_3 and the chloride assemble a distorted octahedral *trans*-$CNOClP_2$ coordination sphere around the trivalent metal centre. In the electronic spectra, dichloromethane solutions of **1**–**5** display multiple strong bands within 506−272 nm due to ligand to metal charge transfer and intraligand transitions. The room temperature (298 K) magnetic moments (μ_{eff}) of **1**–**5** are within 1.92−1.99 μ_B and they display rhombic EPR spectra in frozen (130 K) dichloromethane-toluene (1:1). Cyclic voltammetry with dimethylformamide solutions of the complexes reveals ligand substituent sensitive Ru(III) → Ru(II) reduction and Ru(III) → Ru(IV) oxidation in the potential ranges −0.27 to −0.36 V and 0.94 to 1.13 V (vs. Ag/AgCl), respectively.

4.1. Introduction

In the preceding chapter, we have described a series of cycloruthenated complexes of general formula *trans*-[Ru(pnbh*R*)(PPh_3)$_2$Cl] with 1-pyrenaldehyde 4-*R*-benzoylhydrazones (H_2pnbh*R*) [1]. In these complexes, regioselective *ortho*-ruthenation instead of *peri*-ruthenation of 1-pyrenyl moiety of (pnbh*R*)$^{2-}$ is favored. As a result, CNO-donor (pnbh*R*)$^{2-}$ forms 5,5- rather than 6,5-fused chelate rings at the ruthenium(III) centre. The work presented in this chapter originates from our investigation to find out whether the ruthenation of the bicyclic aromatic fragment of 1-naphthaldehyde 4-*R*-benzoylhydrazone (H_2nabh*R*) occurs at *peri* position as observed in its palladium(II) complex [2] or at *ortho* position as found for 1-pyrenyl in the ruthenium(III) complexes of (pnbh*R*)$^{2-}$ [1]. Herein we report the synthesis, physical properties and structures of a series of ruthenium(III) cyclometallates of the general formula *trans*-[Ru(nabh*R*)(PPh_3)$_2$Cl] where the 1-naphthalenyl fragment of (nabh*R*)$^{2-}$ is *ortho*-metallated (Scheme 1).

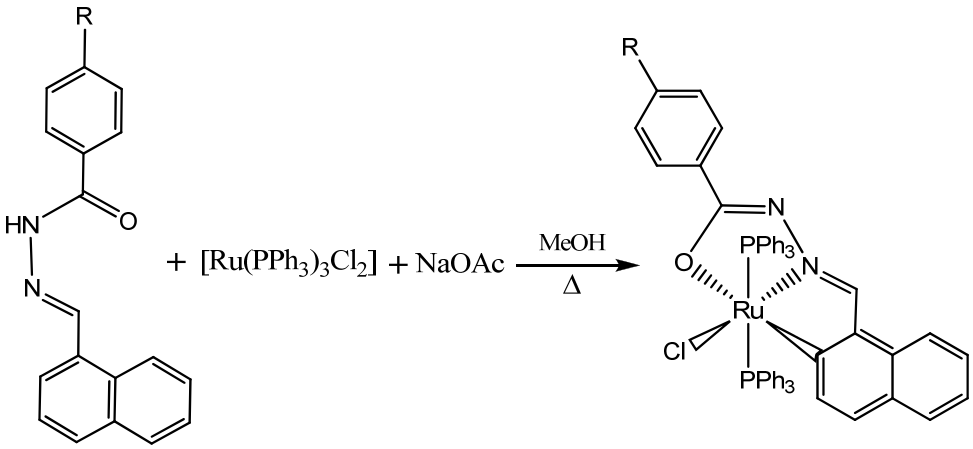

Scheme 1

4.2. Experimental section

4.2.1. Materials

The Schiff bases (H_2nabh*R*) were prepared from ethanol medium in 80–90% yields by condensing one mole equivalent of 1-naphthaldehyde with one mole equivalent of the corresponding 4-*R*-benzoylhydrazines (*R* = H, Me, OMe, Cl and NO_2) in presence of a few drops of acetic acid [2]. [$Ru(PPh_3)_3Cl_2$] was prepared using a literature procedure [3]. All other chemicals and solvents were of analytical grade available commercially and were used without further purification.

4.2.2. Physical measurements

A Thermo Finnigan Flash EA1112 series elemental analyzer was used for the microanalyses (C, H, N). Purity verification of the Schiff bases was performed with the help of a Shimadzu LCMS 2010 liquid chromatograph mass spectrometer. Room temperature (298 K) magnetic susceptibilities were measured using a Sherwood scientific balance. Diamagnetic corrections calculated from Pascal's constants [4] were used to obtain the molar paramagnetic susceptibilities. The infrared spectra of all the compounds were recorded in KBr pellets on a Jasco-5300 FT-IR spectrophotometer. A Cary 100 Conc UV/vis spectrophotometer was used to record the electronic spectra. X-band EPR spectra were recorded on a Jeol JES-FA200 spectrometer. Cyclic voltammetric measurements were performed with the help of a CH-Instruments model 620A electrochemical analyzer using dimethylformamide solutions of the complexes containing tetrabutylammonium perchlorate (TBAP) as the supporting electrolyte. A platinum disk working electrode, a platinum wire auxiliary electrode and an Ag/AgCl reference electrode were used in the three electrode measurements at

298 K under dinitrogen atmosphere. Under identical condition the $E_{1/2}$ value for the Fc^{+}/Fc couple was 0.48 V.

4.2.3. Synthesis of trans-[Ru(nabhH)(PPh_3)$_2$Cl] (1)

To a methanol solution (30 ml) of H_2nabh*H* (57 mg, 0.21 mmol) and NaOAc (35 mg, 0.43 mmol) solid [Ru(PPh_3)$_3$$Cl_2$] (200 mg, 0.21 mmol) was added. The mixture was boiled under reflux for 1 h and then concentrated to ~8 ml on a steam bath. On cooling to room temperature the complex separated as a red crystalline solid. It was collected by filtration, washed with little cold methanol followed by *n*-hexane and finally dried in air. Yield was 105 mg (54%).

Complexes **2**–**5** with the same general formula *trans*-[Ru(nabh*R*)(PPh_3)$_2$Cl] (**2** (*R* = Me), **3** (*R* = OMe), **4** (*R* = Cl) and **5** (*R* = NO_2)) were synthesized in 50–58% yields using [Ru(PPh_3)$_3$$Cl_2$], corresponding H_2nabh*R* and NaOAc (in 1:1:2 mole ratio) by following procedures very similar to that described above for **1** (*R* = H).

4.2.4. X-ray crystallography

X-ray quality single crystals of [Ru(nabh*H*)(PPh_3)$_2$Cl] (**1**), [Ru(nabh*Me*)(PPh_3)$_2$Cl] (**2**) and [Ru(nabh*NO*$_2$)(PPh_3)$_2$Cl] (**5**) were grown by slow evaporation of the corresponding dichloromethane-acetonitrile (1:1) solutions. **1** crystalizes as it is, while the other two complexes crystallize as **2**·0.5CH_3CN and **5**·1.5CH_3CN. An Oxford Diffraction Xcalibur Gemini single crystal X-ray diffractometer equiped with graphite monochromated Mo Kα radiation (λ = 0.71073 Å) was used for determination of the unit cell parameters and intensity data collection at 298 K for all the three complexes. The CrysAlisPro software [5] was used for data collection, reduction and absorption correction. In each case, the structure was solved by direct method and refined on F^2 by full-matrix least-

Table 4.1. Selected crystal data and structure refinement summary

Complex	**1**	**2**·0.5CH_3CN	**5**·1.5CH_3CN
Chemical formula	$C_{54}H_{42}N_2OClP_2Ru$	$C_{56}H_{45.5}N_{2.5}OClP_2Ru$	$C_{57}H_{45.5}N_{4.5}O_3ClP_2Ru$
Formula weight	933.36	967.91	1039.94
Crystal system	Orthorhombic	Monoclinic	Orthorhombic
Space group	*P*ca2_1	*P*2_1/n	*P*bca
a (Å)	18.7511(9)	15.8404(6)	18.9835(9)
b (Å)	16.9761(12)	17.7872(7)	14.9426(6)
c (Å)	14.9408(7)	17.2382(6)	35.7465(18)
α (°)	90	90	90
β (°)	90	95.373(4)	90
γ (°)	90	90	90
V (Å^3)	4756.0(5)	4835.6(3)	10140.0(8)
Z	4	4	8
ρ (g cm^{-3})	1.304	1.330	1.362
μ (mm^{-1})	0.493	0.487	0.474
Reflections collected	12635	20079	24459
Reflections unique	7518	8499	8915
Reflections [$I \geq 2\sigma(I)$]	5803	5221	5767
Parameters	550	573	616
Flack parameter	0.03(7)	–	–
*R*1, *wR*2 [$I \geq 2\sigma(I)$]	0.0736, 0.1949	0.0684, 0.1678	0.0675, 0.1678
*R*1, *wR*2 [all data]	0.0996, 0.2155	0.1191, 0.1999	0.1077, 0.1923
GOF on F^2	1.083	1.033	1.061
Max. / Min. peaks (e Å^{-3})	1.287 / –0.814	0.926 / –0.351	0.978 / –0.582

squares procedures. All non-hydrogen atoms with full occupancy were refined anisotropically. In **2**·0.5CH_3CN and **5**·1.5CH_3CN, the non-hydrogen atoms of the

partial occupancy solvent molecules were refined isotropically with geometrical restraints. Hydrogen atoms were included in the structure factor calculations by using a riding model. Structure solution and refinement were performed with the help of SHELX-97 programs [6] available in the WinGX package [7]. The Platon [8] and the Mercury [9] packages were used for molecular graphics. Selected crystal data and structures refinement summary are listed in Table 4.1.

4.3. Results and discussion

4.3.1. Synthesis and some properties

Complexes *trans*-[Ru(nabh*R*)(PPh_3)$_2$Cl] (**1**–**5**) were synthesized in moderate yields by reacting [Ru(PPh_3)$_3$$Cl_2$] with the corresponding H_2nabh*R* and NaOAc (1:1:2 mole ratio) in methanol (Scheme 1). They can also be synthesized in similar yields by using other bases such as NEt_3, NaOH and KOH instead of NaOAc. The general molecular formula of **1**–**5** are well supported by the elemental analyses data (Table 4.2). The effective magnetic moments (μ_{eff}) of **1**–**5** in powder phase at room temperature (298 K) are in the range 1.92–1.99 μ_B. These values are consistent with one electron paramagnetic character and hence trivalent low-spin state of ruthenium in **1**–**5**. Presumably oxygen in air acts as the oxidant during the synthesis of **1**–**5** from the bivalent ruthenium starting material [Ru(PPh_3)$_3$$Cl_2$]. The solubility behaviours of **1**–**5** are very similar to that of the analogous complexes of pnbhR^{2-} [1]. They are highly soluble in dichloromethane, chloroform, dimethylsulfoxide and dimethylformamide and give red solutions. In solution, all the complexes are electrically non-conducting.

Table 4.2. Elemental analysis and magnetic susceptibility data

Complex	Found (calc) (%)			μ_{eff} (μ_B)
	C	H	N	
trans-[Ru(nabh*H*)(PPh_3)$_2$Cl]	69.32 (69.47)	4.46 (4.54)	3.07 (3.00)	1.99
trans-[Ru(nabh*Me*)(PPh_3)$_2$Cl]	69.56 (69.71)	4.58 (4.58)	3.06 (2.96)	1.95
trans-[Ru(nabh*OMe*)(PPh_3)$_2$Cl]	68.41 (68.55)	4.67 (4.61)	2.85 (2.91)	1.97
trans-[Ru(nabh*Cl*)(PPh_3)$_2$Cl]	67.56 (66.99)	4.31 (4.27)	2.79 (2.90)	1.92
trans-[Ru(nabh*NO$_2$*)(PPh_3)$_2$Cl]	66.75 (66.27)	4.06 (4.23)	4.32 (4.30)	1.94

4.3.2. Infrared spectral properties

In the infrared spectra of the Schiff bases (H_2nabh*R*), the amide N–H and the C=O stretches appear in the ranges 3172–3287 and 1632–1671 cm^{-1}, respectively [1,2]. Absence of these stretches in the spectra of **1**–**5** indicates deprotonation of the amide functionality in the ligand $(nabhR)^{2-}$. The C=N stretch of H_2nabh*R* is observed as a medium to strong band within 1583–1605 cm^{-1}. In **1**–**5** the C=N stretch appears at a lower frequency range (1560–1577 cm^{-1}) due its coordination to the metal centre [1,2]. The three strong bands observed at ~740, ~695 and ~515 cm^{-1} in the spectra of the complexes indicate the metal bound PPh_3 in all of them. A representative spectrum is shown in Figure 4.1.

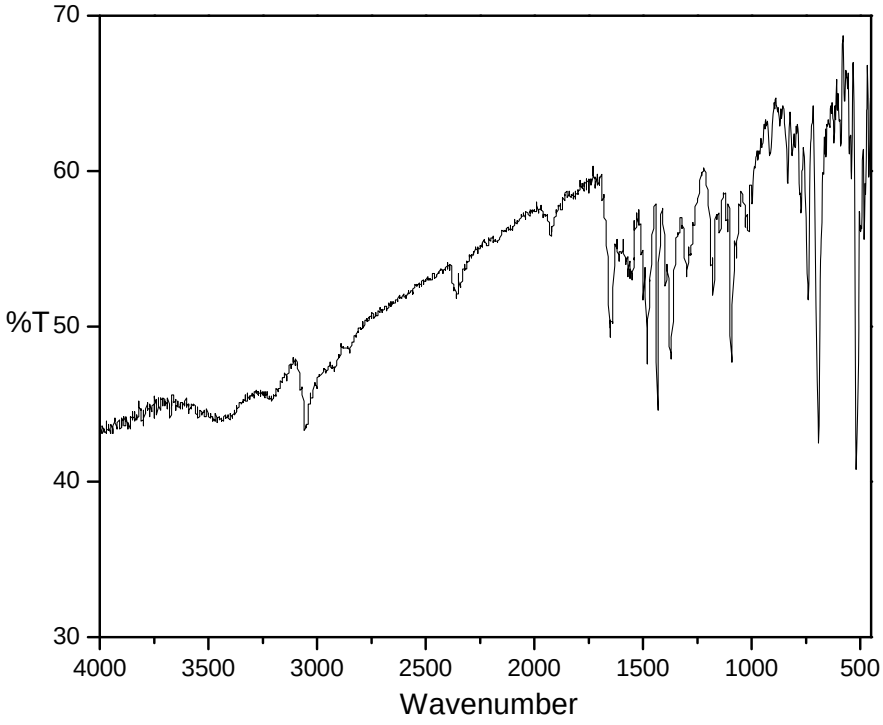

Figure 4.1. Infrared spectrum of *trans*-[Ru(nabh*Me*)(PPh_3)$_2$Cl]

4.3.3. Electronic spectral properties

Electronic spectra of the Schiff bases and the complexes were recorded in dichloromethane. The spectra of the Schiff bases are very similar and display a strong band at ~330 nm followed by a shoulder at ~265 nm [2]. The spectra of the complexes are also comparable but in contrast to the Schiff bases display several strong to very strong absorptions in the wavelength range 506–272 nm. A representative spectrum is illustrated in Figure 4.2 and the electronic spectral data of **1**–**5** are listed in Table 4.3. By comparing the spectra of the Schiff bases and the corresponding complexes, the absorptions of **1**–**5** above 350 nm are assigned to ligand to metal charge transfer transitions and the absorptions below 350 nm are attributed to predominantly ligand centred transitions [1,2].

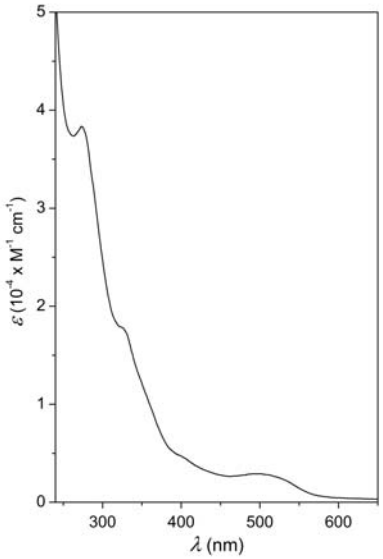

Figure 4.2. Electronic spectrum of *trans*-[Ru(nabh*Me*)(PPh_3)$_2$Cl] (**2**) in CH_2Cl_2.

Table 4.3. Electronic spectral data in dichloromethane solution

Complex	λ_{max} (nm) ($10^{-4} \times \varepsilon$ (M^{-1} cm^{-1}))
trans-[Ru(nabh*H*)(PPh_3)$_2$Cl]	506 (0.38), 400[c] (0.35), 325 (2.13), 277 (4.54)
trans-[Ru(nabh*Me*)(PPh_3)$_2$Cl]	503 (0.29), 403[c] (0.45), 327 (1.77), 273 (6.27)
trans-[Ru(nabh*OMe*)(PPh_3)$_2$Cl]	504 (0.32), 402[c] (0.39), 330 (1.50), 272 (4.35)
trans-[Ru(nabh*Cl*)(PPh_3)$_2$Cl]	506 (0.46), 404[c] (0.47), 326 (1.86), 273 (3.80)
trans-[Ru(nabh*NO_2*)(PPh_3)$_2$Cl]	490[c] (0.44), 332[c] (1.51), 273[c] (3.14)

[c]Shoulder.

4.3.4. EPR spectral properties

The EPR spectra of **1**–**5** in frozen (130 K) dichloromethane-toluene (1:1) are very similar. Each complex displays three distinct EPR signals. The spectrum of **4** is illustrated in Figure 4.3 and the g-values are listed in Table 4.4. This type of spectral profile indicates a rhombically distorted octahedral coordination geometry around one-electron paramagnetic ruthenium(III) centre in each of **1**–**5**.

In view of the ligand composition in the present series of complexes rhombic distortion from ideal octahedral geometry is not surprising. Rhombic distortion and similar EPR features are very common in analogous ruthenium(III) quaternary complexes with an asymmetric tridentate ligand and two different unidentate ligands [1,10,11,12–14]. X-ray molecular structures of **1**, **2** and **5** are in concurrence with the rhombic distortion indicated by the EPR measurements (*vide infra*).

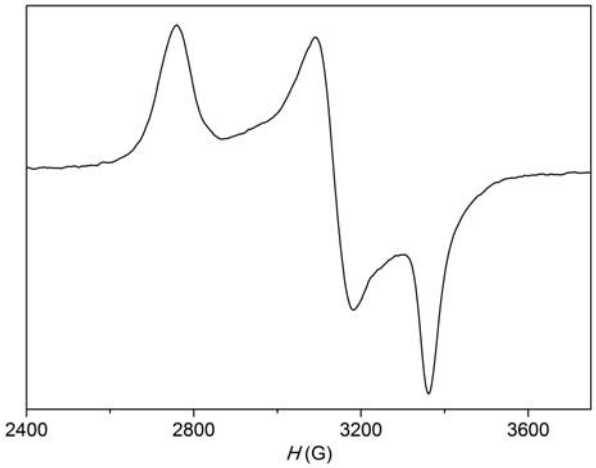

Figure 4.3. EPR spectrum of *trans*-[Ru(nabh*Cl*)(PPh_3)$_2$Cl] (**4**) in frozen (130 K) dichloromethane-toluene (1:1).

Table 4.4. EPR spectroscopic data[a] of *trans*-[Ru(nabh*R*)(PPh_3)$_2$Cl]

Complex	g_1	g_2	g_3
trans-[Ru(nabh*H*)(PPh_3)$_2$Cl]	2.37	2.09	1.95
trans-[Ru(nabh*Me*)(PPh_3)$_2$Cl]	2.41	2.07	1.95
trans-[Ru(nabh*OMe*)(PPh_3)$_2$Cl]	2.41	2.06	1.95
trans-[Ru(nabh*Cl*)(PPh_3)$_2$Cl]	2.37	2.09	1.95
trans-[Ru(nabh*Cl*)(PPh_3)$_2$Cl]	2.38	2.09	1.94

[a]In dichloromethane-toluene (1:1) at (130 K).

4.3.3. X-ray structures

Single crystal X-ray structures of **1** and solvated **2** and **5** have been determined. The molecular structure of **2** is illustrated in Figure 4.4 and that of both **1** and **5** are given in Figure 4.5. Bond parameters involving the metal centre for each of the three complex molecules are listed in Table 4.5. The gross molecular structures of the three complexes are very similar. In each complex molecule, the ruthenium atom is in distorted octahedral *trans*-$CNOClP_2$ coordination sphere. The C(12)–O(1) (1.266(7)–1.289(14) Å) and C(12)–N(2) (1.290(8)–1.310(15) Å) bond lengths in **1**, **2** and **5** are consistent with the deprotonated state of the amide functionality and hence the dibasic nature of their corresponding tridentate ligands $(nabh\mathit{R})^{2-}$ [1,2,10,11,15–18]. The meridionally spanning $(nabh\mathit{R})^{2-}$ acts as 1-naphthalenyl *ortho*-C, the imine-N and the amidate-O donor and forms 5,5-fused chelate rings at the ruthenium centre (Figures. 4.4 and 4.5). The $(nabh\mathit{R})^{2-}$ and the Cl-atom form a CNOCl square-plane around the metal centre and the P-atoms of the two PPh_3 molecules occupy the two axial positions. The chelate bite angles, O(1)–Ru–N(1) and C(1)–Ru–N(1), imposed by $(nabh\mathit{R})^{2-}$ are in the ranges 73.64(19)–75.1(3)º and 76.1(3)–77.4(2)º, respectively. These bite angles are very similar to those observed in Ru(III) complexes with CNO-pincer ligands [1,10–13]. Each of the 5,5-fused chelate rings is satisfactorily planar (mean deviation 0.01–0.03 Å). However, the rings are slightly folded by 3.7(2)–4.9(1)º along the Ru–N(1) bond. Other than the bite angles, the remaining *cis* bond angles span a much wider range of 83.75(10)–113.50(18)º. As expected due to steric constraint the *trans* bond angle (C(1)–Ru–O(1), 150.43(19)–150.7(2)º) formed by the two ends of $(nabh\mathit{R})^{2-}$ is much smaller than the remaining two *trans* bond angles (N(1)–Ru–Cl, 169.04(16)–176.6(3)º and P(1)–Ru–P(2), 174.11(10)–175.85(6)º). The Ru–C(aryl), the Ru–N(imine), the Ru–O(amidate), the Ru–Cl and the Ru–P bond lengths in **1**, **2** and **5** (Table 4.5)

are comparable with the corresponding bond lengths observed for ruthenium(III) complexes with similar ligands [1,10,11]

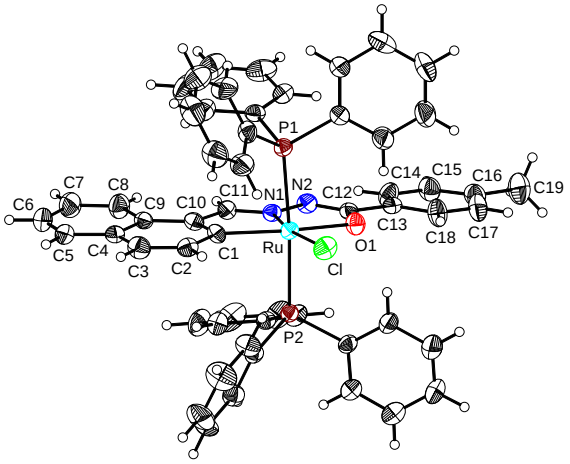

Figure 4.4. Molecular structure of *trans*-[Ru(nabh*Me*)(PPh_3)$_2$Cl] (**2**) with the atom numbering scheme. Thermal ellipsoids of all non-hydrogen atoms are drawn at the 40% probability level. C-atoms of PPh_3 are not labelled for clarity.

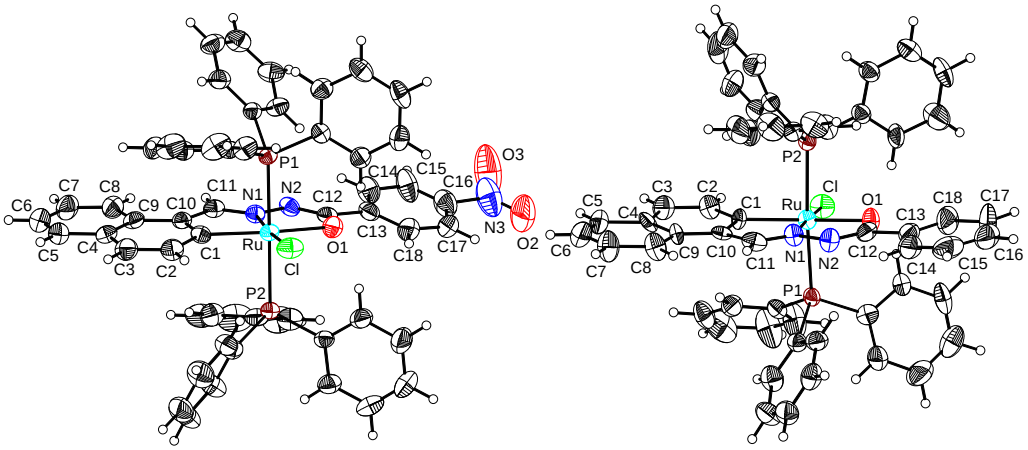

(a) **(b)**

Figure 4.5. Molecular structures of (a) *trans*-[Ru(nabh*H*)(PPh_3)$_2$Cl] (**1**) and (b) *trans*-[Ru(nabh*NO*$_2$)(PPh_3)$_2$Cl] (**5**) with the atom numbering schemes. Thermal ellipsoids of all non-hydrogen atoms are drawn at the 40% probability level. C-atoms of PPh_3 are not labelled for clarity.

Table 4.5. Selected bond lengths (Å) and bond angles (°) for **1**, **2**·0.5CH_3CN and **5**·1.5CH_3CN

Complex	**1**	**2**·0.5CH_3CN	**5**·1.5CH_3CN
Ru–C(1)	2.057(9)	2.040(6)	2.044(6)
Ru–N(1)	2.035(8)	2.018(5)	2.016(5)
Ru–O(1)	2.153(7)	2.138(4)	2.138(4)
Ru–Cl	2.361(3)	2.3711(18)	2.3574(16)
Ru–P(1)	2.404(2)	2.4091(17)	2.3938(15)
Ru–P(2)	2.397(2)	2.3935(16)	2.3958(15)
C(1)–Ru–N(1)	76.1(3)	77.4(2)	77.1(2)
C(1)–Ru–O(1)	150.4(3)	150.7(2)	150.43(19)
C(1)–Ru–Cl	103.6(2)	113.50(18)	105.98(16)
C(l)–Ru–P(1)	94.4(3)	88.01(17)	91.20(16)
C(1)–Ru–P(2)	89.1(3)	87.88(17)	88.27(16)
N(1)–Ru–O(1)	75.1(3)	73.64(19)	73.94(17)
N(1)–Ru–Cl	176.6(3)	169.04(16)	175.06(14)
N(1)–Ru–P(1)	92.9(3)	87.94(14)	91.97(14)
N(1)–Ru–P(2)	92.5(3)	90.63(14)	92.61(14)
O(1)–Ru–Cl	105.6(2)	95.57(13)	103.35(13)
O(1)–Ru–P(1)	93.5(2)	95.56(12)	95.50(12)
O(1)–Ru–P(2)	85.6(2)	87.77(12)	87.31(12)
Cl–Ru–P(1)	83.75(10)	91.33(6)	84.14(5)
Cl–Ru–P(2)	90.87(11)	90.82(6)	91.36(5)
P(1)–Ru–P(2)	174.11(10)	175.85(6)	175.15(5)

4.3.4. Redox properties

Electron transfer properties of **1**–**5** have been studied by cyclic voltammetry. In dimethylformamide, the complexes display a reduction response in the $E_{1/2}$ range of –0.27 to –0.36 V with ΔE_p within 90–100 mV and a quasi-reversible to irreversible oxidation response in the $E_{1/2}/E_{pa}$ range of 0.94 to 1.13 V

(vs. Ag/AgCl). The potential data are summarized in Table 4.6 and representative voltammograms are illustrated in Figure 4.6. The one-electron nature of these redox responses is ascertained by comparing the current heights with the current heights of known one-electron transfer processes under identical condition [1,10–12]. Taking into account the redox inactivity of the Schiff bases in the above redox potential range and the electron transfer behaviours of analogous ruthenium(III) complexes with tridentate acid hydrazones [1,10,11], we have ascribed the reduction and the oxidation responses of **1**–**5** to ruthenium(III) → ruthenium(II) and ruthenium(III) → ruthenium(IV) processes, respectively. In general, there is a cathodic shift of both reduction and oxidation potentials with the increasing electron donating ability of the substiuent *R* in the tridentate ligand $(\text{nabh}R)^{2-}$. Satisfactory linear relationships (Figure 4.7) are obtained for the reduction ($E_{1/2}$) as well as the oxidation (E_{pa}) potentials when the corresponding values are plotted against the Hammett substituent constants [19].

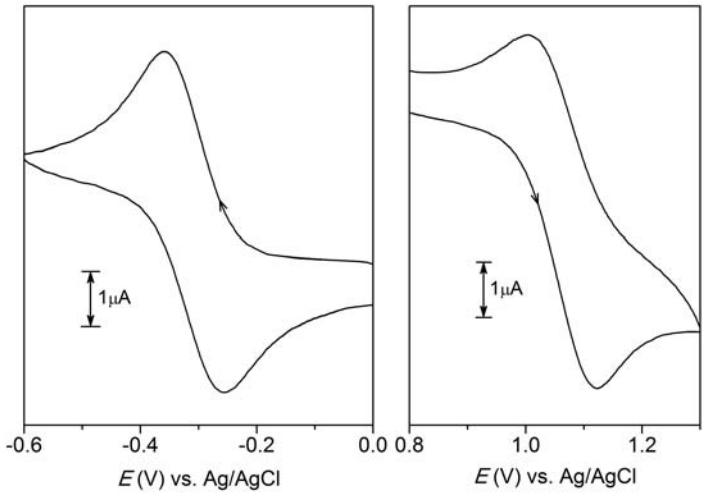

Figure 4.6. Cyclic voltammograms of *trans*-[Ru(nabh*H*)$(PPh_3)_2$Cl] (**1**) in dimethylformamide (0.1 M TBAP) at 298 K.

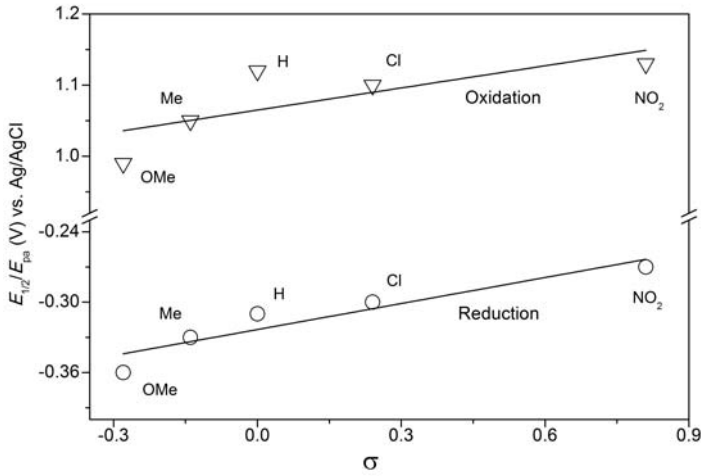

Figure 4.7. Linear correlations between the $E_{1/2}$ values of the reduction response (O) and E_{pa} values of the oxidation response (∇) for **1**–**5** and the Hammett substituent constants.

Table 4.6. Cyclic voltammetric[a] data of *trans*-[Ru(nabh*R*)$(PPh_3)_2$Cl]

Complex	$E_{1/2}$(V) (ΔE_p (mV))[b]	
	Reduction	Oxidation
trans-[Ru(nabh*H*)$(PPh_3)_2$Cl]	–0.31 (100)	1.06 (120)
trans-[Ru(nabh*Me*)$(PPh_3)_2$Cl]	–0.33 (100)	1.05[c]
trans-[Ru(nabh*OMe*)$(PPh_3)_2$Cl]	–0.36 (90)	0.94 (100)
trans-[Ru(nabh*Cl*)$(PPh_3)_2$Cl]	–0.30 (90)	1.10[c]
trans-[Ru(nabh*NO₂*)$(PPh_3)_2$Cl]	–0.27 (100)	1.13[c]

[a] In dimethylformamide.

[b] $E_{1/2} = (E_{pa} + E_{pc})/2$ and $\Delta E_p = E_{pa} - E_{pc}$, where E_{pa} and E_{pc} are anodic and cathodic peak potentials, respectively.

[c] E_{pa} value.

4.4. Conclusion

Synthesis and characterization of a series of cycloruthenates with 1-naphthaldehyde 4-*R*-benzoylhydrazones (H_2nabh*R*, *R* = H, Me, OMe, Cl and NO_2) are described. The magnetic moments and EPR spectra corroborate the trivalent low-spin state of the metal centre in each of these complexes of the formula *trans*-[Ru(nabh*R*)(PPh_3)$_2$Cl]. All the complexes are redox active and display a reduction and an oxidation both being metal centred and substituent sensitive. X-ray structures of three complexes where *R* = H, Me, and NO_2 show pincer like coordination mode of (nabh*R*)$^{2-}$ through the 1-naphthalenyl *ortho*-C, the imine-N and the amidate-O and formation of 5,5-fused chelate rings. Based on the similar physical properties of all the complexes, it is inferred that (nabh*R*)$^{2-}$ has the same coordination mode in the remaining two complexes where *R* = OMe and Cl. The regioselective *ortho*-ruthenation instead of *peri*-ruthenation of the 1-naphthalenyl moiety of (nabh*R*)$^{2-}$ is akin to our previous observation for the analogous cycloruthenates with 1-pyrenaldehyde 4-*R*-benzoylhydrazones [1]. In contrast, regioselective *peri*-palladation of both indole-3 and 1-naphthalenyl fragments of acid hydrazones of indole-3-aldehyde and 4-*R*-1-naphthaldehydes leading to the formation of 6,5-fused chelate rings has been observed for bivalent palladium [2,17]. A possible rationale that may account for this difference in regioselectivity is as follows. All these cyclopalladates and cycloruthenates were synthesized from bivalent metal ion containing starting materials ($[PdCl_4]^{2-}$ and [Ru(PPh_3)$_3$$Cl_2$], respectively), tridentate acid hydrazones and the base NaOAc. It is very likely that in presence of base, coordination of monobasic ligand (e.g. Hnabh*R*$^-$) to the bivalent metal centre through the imine-N and the amidate-O with the formation of the 5-membered N,O chelate ring precedes the C–H activation process [20]. In general, it has been found that small metal ions prefer 6-membered chelate ring, while large metal ions prefer 5-membered chelate ring

[21,22]. Palladium(II) is expected to be smaller than ruthenium(II). Perhaps for this size difference palladium(II) activates the *peri*-C–H and forms 6-membered metallacycle, while formation of 5-membered metallacycle by *ortho*-C–H activation occurs for ruthenium(II). Oxidation of the metal centre to the trivalent state by oxygen in air is the last step for the formation of the cycloruthenates. Currently we are engaged in the synthesis of cyclometallates of various platinum metal ions with the present and other acid hydrazones of various polycylic aromatic aldehydes for a better perception of the regioselective C–H activation process in this class of ligands.

4.5. References

[1] K. Nagaraju, S. Pal, *J. Organomet. Chem.* 737 (2013) 7.

[2] A.R.B. Rao, S. Pal, *J. Organomet. Chem.* 731 (2013) 67.

[3] T.A. Stephenson, G. Wilkinson, *J. Inorg. Nucl. Chem.* 28 (1966) 945.

[4] G.A. Bain, J.F. Berry, *J. Chem. Educ.* 85 (2008) 532.

[5] CrysAlisPro Version 1.171.33.55, Oxford Difraction Ltd., Abingdon, Oxford-shire UK, 2007.

[6] G.M. Sheldrick, SHELX-97, Structure Determination Software, University of Gottingen, Gottengen, Germany, 1997.

[7] L.J. Farrugia, WinGX, *J. Appl. Crystallogr.* 32 (1999) 837.

[8] A.L. Spek, Platon, A Multipurpose Crystallographic Tool, Utrecht University, Utrecht, The Netherlands, 2002.

[9] C.F. Macrae, I.J. Bruno, J.A. Chisholm, P.R. Edgington, P. McCabe, E. Pidcock, L. Rodriguez-Monge, R. Taylor, J. van de Streek, P.A. Wood, Mercury CSD 2.0, *J. Appl.* Crystallogr. 41 (2008) 466.

[10] R. Raveendran, S. Pal, *J. Organomet. Chem.* 692 (2007) 824.

[11] R. Raveendran, S. Pal, *J. Organomet. Chem.* 694 (2009) 1482.

[12] G.K. Lahiri, S. Bhattacharya, M. Mukherjee, A.K. Mukherjee, A. Chakravorty, *Inorg. Chem.* 26 (1987) 3359.

[13] S. Kannan, R. Ramesh, Y. Liu, *J. Organomet. Chem.* 692 (2007) 3380.

[14] R. Prabhakaran, R. Huang, R. Karvembu, C. Jayabalakrishnan, K. Natarajan, *Inorg. Chim. Acta* 360 (2007) 691.

[15] S. Das, S. Pal, *J. Organomet. Chem.* 689 (2004) 352.

[16] S. Das, S. Pal, Synthesis, *J. Organomet. Chem.* 691 (2006) 2575.

[17] A.R.B. Rao, S. Pal, *J. Organomet. Chem.* 696 (2011) 2660.

[18] A.R.B. Rao, S. Pal, *J. Organomet. Chem.* 701 (2012) 62.

[19] J. March, in: Advanced Organic Chemistry, 4th ed., Wiley, New York, 1992, p. 280.

[20] D.N. Neogi, A.N. Biswas, P. Das, R. Bhawmick, P. Bandyopadhyay, *J. Organomet. Chem.* 724 (2013) 147.

[21] R.D. Hancock, *Pure Appl. Chem.* 58 (1986) 1445.

[22] R.D. Hancock, *Chem. Soc. Rev.* 42 (2013) 1500.

Chapter 5

Complexes of *cis*-$\{Ru(PPh_3)_2\}^{2+}$ with thioamidate-N,S donor thiobenzhydrazones of polycyclic aromatic aldehydes

Reactions of $[Ru(PPh_3)_3Cl_2]$, H_2L^n (thiobenzhydrazones, n = 1–4) and NaOAc in 1:2:2 mole ratio in methanol produces ruthenium(II) complexes of formula *cis*-$[Ru(PPh_3)_2(HL^n)_2]$ (**1**–**4**) in ~80% yields. Microanalysis (C,H,N), magnetic susceptibility, solution conductivity, spectroscopic (IR, UV-Vis and NMR) and cyclic voltammetric measurements have been used for the characterization of **1**–**4**. The complexes are non-electrolytic and diamagnetic. In the electronic spectra of the complexes, multiple absorptions within 505–245 nm due to metal-to-ligand and ligand centred transitions have been observed. Molecular structures of **3** and **4** have been determined by X-ray crystallography. In each of **3** and **4**, two thioamidate-N,S coordinating $(HL^n)^-$ and two mutually *cis* oriented PPh_3 molecules assemble a $N_2S_2P_2$ coordination sphere around the metal centre. Cyclic voltammograms of **1**–**4** show an oxidation response within $E_{1/2}$ = 0.76–0.86 V (ΔE_p = 90–100 mV) vs. Ag/AgCl.

5.1. Introduction

Cyclometallation of the pendant aryl moiety in the acid hydrazones of various mono and polycyclic aromatic aldehydes is a convenient route to synthesize cyclometallates. The aryl group in the Ar–C(*R*)=N– (*R* = H or Me) fragment of the acid hydrazones of monocyclic aromatic aldehydes provides only the *ortho*-C for metallation [1–4]. On the other hand, in case of the acid

hydrazones of polycyclic aromatic aldehydes there is a choice between the *ortho* and the *peri* position of the aryl group for metallation depending upon the position of the –C(*R*)=N– on it [5,7–9]. In the resulting complexes, the acid hydrazones act as CNO pincer like ligands [10–12] and form 5,5- or 6,5-membered fused chelate rings for *ortho*- or *peri*-metallation, respectively. In general, with the acid hydrazones of polycyclic aromatic aldehydes, we have found that palladation occurs at the *peri* position [5,7], while, ruthenation occurs at the *ortho*-position [8,9] of the pendant aryl moiety. In the present work, we have studied the ruthenium chemistry of thiobenzhydrazones of some polycyclic aromatic aldehydes (H_2L^n, 2 H represent the aryl C–H and the thioamide N–H protons) to explore whether regioselective *ortho*-ruthenation and formation of 5,5-membered pincer complexes as observed for analogous polycyclic aromatic aldehyde benzhydrazones occur or not. Interestingly, there is no metallation of the polycyclic aryl moiety of the thiobenzhydrazones. Instead, a series of complexes with the formula *cis*-$[Ru(PPh_3)_2(HL^n)_2]$, where $(HL^n)^-$ acts as four-membered chelate ring forming thioamidate-N,S donor, has been isolated (Scheme 1). Herein, we describe the synthesis, characterization and physical properties of these complexes with the molecular structures of two representative complexes determined by X-ray crystallography.

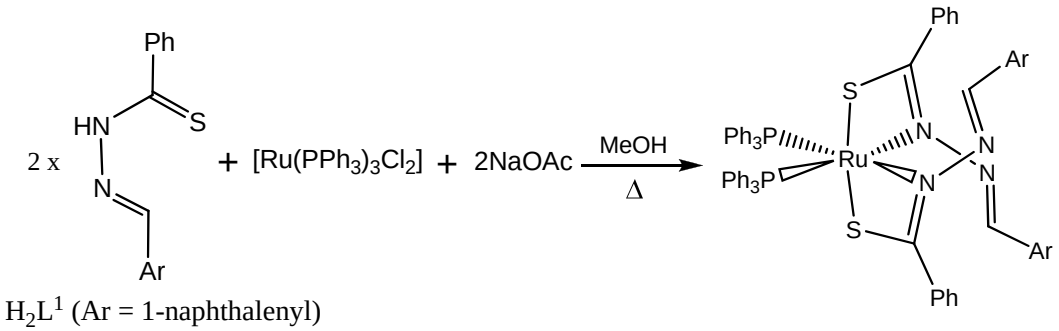

H_2L^1 (Ar = 1-naphthalenyl)
H_2L^2 (Ar = 9-anthracenyl)
H_2L^3 (Ar = 9-phenanthryl)
H_2L^4 (Ar = 1-pyrenyl)

cis-$[Ru(HL^n)_2(PPh_3)_2]$
(n = 1-4)

Scheme 1

5.2. Experimental Section

5.2.1. Materials

Thiobenzhydrazones of polycyclic aromatic aldehydes ($H_2L^{1–4}$ (Scheme 1)) were synthesised by following a procedure similar to that reported for analogous compounds [13,14]. $[Ru(PPh_3)_3Cl_2]$ was prepared according to the literature method [15]. All other chemicals were of analytical grade available commercially and were used as supplied without further purification. Purification of the solvents used was performed by following standard methods [16].

5.2.2. Physical measurements

Microanalysis (C, H, N) data were obtained with a Thermo Finnigan Flash EA1112 series elemental analyzer. Magnetic measurements were performed with the help of a Sherwood scientific balance. A Shimadzu LCMS 2010 liquid chromatograph mass spectrometer was used for the purity verification of the Schiff bases. A Bruker Maxis HRMS (ESI-TOF analyzer) spectrometer was used to record the mass spectra of the complexes. The infrared spectra were collected by using KBr pellets on a Jasco-5300 FT-IR spectrophotometer. The electronic

spectra were recorded on a Cary 100 Conc UV/Vis spectrophotometer. The fluorescence spectra were recorded on a Spex FluoroMax-3 spectrofluorimeter. The NMR spectra of the Schiff bases (in $(CD_3)_2SO$) and the complexes (in $CDCl_3$) were collected with the help of a Bruker 400 MHz NMR spectrometer. Cyclic voltammograms of the complexes in dimethylformamide containing the supporting electrolyte tetra-*n*-butylammonium perchlorate (TBAP) were recorded with a CH-Instruments model 620A electrochemical analyser. The measurements were carried out with platinum disk working electrode, a platinum wire auxiliary electrode and an Ag/AgCl reference electrode at 298 K under nitrogen atmosphere. The Fc^+/Fc couple was observed at $E_{1/2}$ = 0.65 V under identical condition.

5.2.3. Synthesis of *cis*-$[Ru(L^1)_2(PPh_3)_2]$ (1)

Solid $[Ru(PPh_3)_3Cl_2]$ (200 mg, 0.21 mmol) was added to a methanol solution (30 ml) of H_2L^1 (153 mg, 0.42 mmol) and NaOAc (35 mg, 0.42 mmol). The mixture was boiled under reflux for 1 h and then cooled to room temperature. The red solid deposited was collected by filtration and dried in air. This material was dissolved in minimum amount of dichloromethane and transferred to a silica gel column packed with dichloromethane. The yellow band moved with the first eluent 1:4 mixture of dichloromethane/*n*-hexane was discarded. The following red band containing the complex **1** was eluted with a 2:3 mixture of dichloromethane/*n*-hexane. The red solution thus obtained was evaporated to dryness and the complex was collected as a dark red solid. The yield was 220 mg (78%).

The remaining three complexes **2**–**4** with the general formula *cis*-$[Ru(L^n)_2(PPh_3)_2]$ (n = 2–4) were synthesized in 77–81% yields using $[Ru(PPh_3)_3Cl_2]$, NaOAc and the corresponding Schiff bases in 1:2:2 mole ratio by following procedures very similar to that used for **1**.

5.2.4. X-ray crystallography

X-ray quality single crystals of **3** and **4** were obtained by slow evaporation of the respective dichloromethane-acetonitrile (1:1) solutions. **3** crystallizes as it is in the space group $P\bar{1}$, while **4** crystallizes with a dichloromethane molecule in the space group $P2_1/c$. Determination of the unit cell parameters and intensity data collection at 298 K for **3** were performed on a Bruker-Nonius SMART APEX CCD single crystal diffractometer using graphite monochromated Mo $K\alpha$ radiation (λ = 0.71073 Å). The SMART and the SAINT-Plus programs [17] were used for data acquisition and data extraction, respectively. The SADABS program [18] was used for absorption correction. Unit cell parameters and the intensity data at 298 K for **4**·CH_2Cl_2 were obtained using graphite monochromated Mo Kα radiation (λ = 0.71073 Å) with the help of an Oxford Diffraction Xcalibur Gemini single crystal X-ray diffractometer. The CrysAlisPro software [19] was used for data collection, reduction and absorption correction. The structures of both complexes were solved by direct method and refined on F^2 by full-matrix least-squares procedures. In case of **3**, 9-phenanthryl moiety of one of the two $(HL^3)^-$ is refined with geometrical and thermal restraints due to disorder. On the other hand, in case of **4**, *ortho*- and *meta*-C atoms of the phenyl ring in one of the two $(HL^4)^-$ were located at eight positions about an approximate two-fold axis passing through remaining two C-atoms. These disordered C atoms were refined isotropically with half occupancy and geometric restraints. The location of CH_2Cl_2 molecule in **4**·CH_2Cl_2 indicates its possible involvement in a very weak C–H···S interaction (C···S, 3.71(2) Å; <C–H···S, 170º) with the complex molecule [20]. In both structures, all non-hydrogen atoms with full occupancy were refined anisotropically. The hydrogen atoms were included at ideal positions for structure factor calculation by using a riding model. Structure solution and refinement were done using the SHELX-97 programs [21] available in the

WinGX package [22]. The Platon [23] and Mercury [24] software packages were used for molecular graphics. Selected crystal and refinement data are listed in Table 5.1.

Table 5.1 Selected crystal data and structure refinement summary

Complex	**3**	**4**·CH_2Cl_2
Chemical formula	$C_{80}H_{60}N_4P_2S_2Ru$	$C_{85}H_{62}N_4P_2S_2Cl_2Ru$
Formula weight	1304.45	1437.42
Crystal system	Triclinic	Monoclinic
Space group	$P\bar{1}$	$P2_1/c$
a (Å)	13.6102(18)	14.0029(12)
b (Å)	13.8872(18)	17.7848(14)
c (Å)	17.727(2)	27.8436(19)
α (°)	90.939(2)	90
β (°)	106.070(2)	96.712(6)
γ (°)	94.427(2)	90
V (Å^3)	3207.5(7)	6886.6(9)
Z	2	4
ρ (g cm^{-3})	1.351	1.386
μ (mm^{-1})	0.409	0.463
Reflections collected	26861	27143
Reflections unique	11238	12106
Reflections [$I \geq 2\sigma(I)$]	8397	3192
Parameters	802	861
$R1$, $wR2$ [$I \geq 2\sigma(I)$]	0.0695, 0.1796	0.0946, 0.1202
$R1$, $wR2$ [all data]	0.0962, 0.1949	0.3174, 0.2001
GOF on F^2	1.036	0.824
Max. / Min. peaks (e Å^{-3})	1.868 / –0.810	0.510 / –0.373

5.3. Results and discussion

5.3.1. Synthesis and some properties

The Schiff bases $H_2L^{1–4}$ were prepared in 92–95% yields by condensation reactions of equimolar amounts of thiobenzhydrazide and the corresponding polycyclic aromatic aldehydes in ethanol. All the Schiff bases were characterized by microanalysis and various spectroscopic (infrared, electronic, mass and ^{1}H NMR) measurements. These characterization data are listed in Tables 5.2, 5.3 and 5.5. In our attempts to prepare ruthenium(III) cyclometallates with CNS pincer like ligands, $[Ru(PPh_3)_3Cl_2]$, H_2L^n and NaOAc (1:1:2 mole ratio) were reacted in methanol. Under similar reaction conditions, the analogous benzhydrazones are known to provide cycloruthenates [8,9]. However, instead of the cycloruthenates, complexes with the general formula $[Ru(PPh_3)_2(HL^n)_2]$ (**1**–**4**), where $(HL^n)^-$ acts as thioamidate-N,S donor 4-membered chelate ring forming ligand, have been formed. Based on the metal to ligand ratio in these complexes the reactions were performed again using $[Ru(PPh_3)_3Cl_2]$, H_2L^n and NaOAc in 1:2:2 mole ratio (Scheme 1) and the complexes have been isolated in much improved yields (77–81%) compared to the previous reactions. The microanalysis data for **1**–**4** are in very good agreement with their molecular formulae (Table 5.4). The diamagnetic nature of **1**–**4** is consistent with the bivalent low-spin state of ruthenium in them. All the complexes are readily soluble in dichloromethane, chloroform, dimethylformamide and dimethylsulfoxide and provide red solutions. In solution, they are electrically non-conducting.

Table 5.2. Elemental analysis, and LCMS[a] data for the Schiff base (H_2L^n)

H_2L^n	Found (calc) (%)			*m/z*
	C	H	N	$(M+1)^+$
H_2L^1	74.32 (74.45)	4.91 (4.86)	9.56 (9.65)	291
H_2L^2	77.48 (77.62)	4.65 (4.74)	8.32 (8.23)	341
H_2L^3	76.85 (77.62)	4.81 (4.74)	8.18 (8.23)	341
H_2L^4	78.49 (79.09)	4.86 (4.42)	7.75 (7.69)	367

[a] In dichloromethane.

Table 5.3. Electronic spectroscopic[a] data for the Schiff bases (H_2L^n)

H_2L^n	Absorption λ_{max} (nm) ($10^{-4} \times \varepsilon$ (M^{-1} cm^{-1}))	Emission λ_{max} (nm)
H_2L^1	316 (0.77), 290 (0.79), 242 (0.88)	410
H_2L^2	435[b] (0.28), 395 (0.72), 374 (0.75), 355 (0.63), 335 (0.62), 257 (1.37)	515
H_2L^3	328[b] (0.38), 298 (0.96), 289[b] (0.96), 255 (1.26),	415
H_2L^4	405[b] (0.99), 370 (1.62), 354[b] (1.57), 280 (1.76), 270[b] (1.38), 235 (1.53)	460

[a] In dichloromethane (concentration range 0.60–0.76 x 10^{-4} M). The λ_{exc} values are 315, 375, 328 and 275 nm for H_2L^{1-4}, respectively.

[b] Shoulder.

Table 5.4. Elemental analysis, and ESI-MS[a], data of *cis*-[Ru(L^{1-4})$_2$(PPh_3)$_2$]

Complex	Found (calc) (%)			*m/z*
	C	H	N	$(M+1)^+$
1	71.56 (71.80)	4.81 (4.69)	4.71 (4.65)	1205
2	73.26 (73..65)	4.89 (4.64)	5.12 (4.30)	1305
3	73.35 (73.65)	4.91 (4.64)	5.07 (4.30)	1305
4	73.65 (74.59)	5.05 (4.65)	4.96 (4.14)	1353

[a] In dichloromethane.

5.3.2. Infrared Spectral properties

Infrared spectra of $H_2L^{1–4}$ display two sharp and moderately strong bands in the range 3184–3293 and 953–975 cm^{-1} due to the thioamide N–H and C=S, respectively [25]. Absence of both these bands in the spectra of **1**–**4** indicates deprotonation of the thioamide fragment on complexation. A medium intensity band within 1575–1595 cm^{-1} observed for H_2L^n is most likely due to its azomethine fragment. The spectra of **1**–**4** display a similar band at a slightly lower frequency range of 1567–1589 cm^{-1}. In the complexes, the azomethine-N does not coordinate the metal centre, while the adjacent thioamidate acts as four-membered chelate ring forming N,S-donor (*vide infra*). Perhaps the band observed for the complexes is due to the conjugated –HC=N–N=C(S^-)– moiety of $(HL^n)^-$. A representative spectrum is shown in figure 5.1.

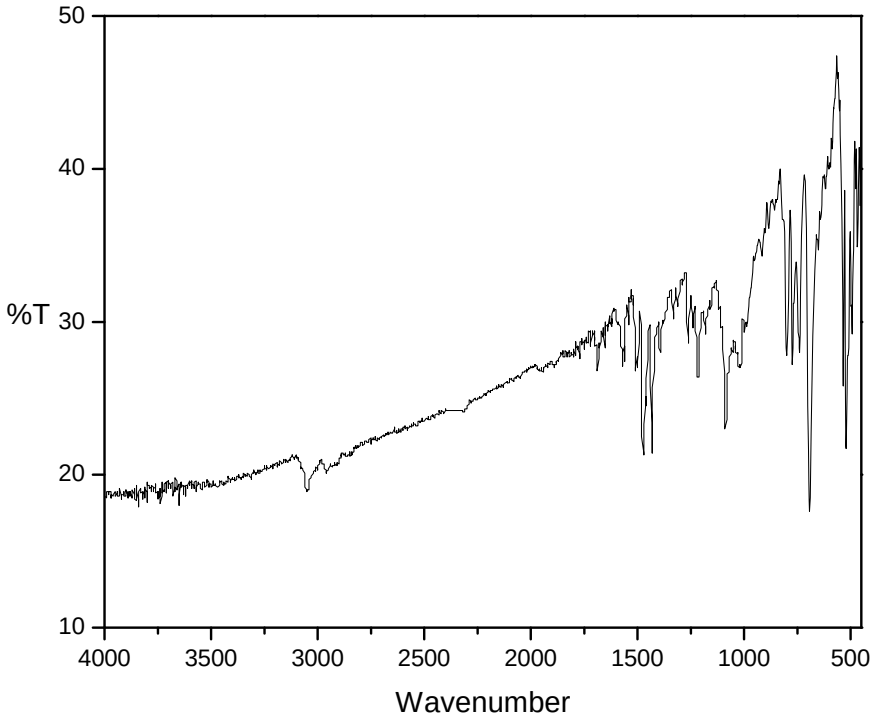

Figure 5.1 Infrared spectrum of *cis*-[Ru(L^1)$_2$(PPh_3)$_2$] (**1**)

5.3.3. NMR spectral properties

Proton NMR spectroscopic data of the Schiff bases and the corresponding complexes have been listed in Tables 5.5 and 5.6 and representative spectrums of Figure 5.2 and 5.3 respectively. The spectra of H_2L^n indicate the thioamide-iminothiol tautomerism. Both NH and SH protons appear as singlets in the ranges δ 13.33–13.45 ppm and δ 7.26–7.53 ppm, respectively. Neither of these two signals is observed in the spectra of **1**–**4**. Thus the Schiff base in each complex is in monoanionic thioamidate form ($(HL^n)^-$). The spectra of the complexes are quite complex and hence difficult to assign due to the overlapping of the $(HL^n)^-$ protons with the PPh_3 protons. Nevertheless, the spectra clearly indicate that each pair of $(HL^n)^-$ and PPh_3 in all four complexes is chemically equivalent. The coordination sphere around the metal centre as found in the X-ray structures of **3** and **4** (*vide*

infra) suggest that in solution the two $(HL^n)^-$ as well as the two *cis*-oriented PPh_3 molecules are very likely to be related to each other by a two-fold axis passing through the metal centre. The azomethine proton of H_2L^n appears as a singlet in the range δ 8.71–9.96 ppm. A similar singlet observed within δ 9.70–10.10 ppm for **1**–**4** is assigned to the azomethine proton of $(HL^n)^-$. The downfield shift of the azomethine proton in **1**–**4** is possibly due to the passage of its electron density towards the adjacent metal-bound bidentate thioamidate. The remaining few protons of the complexes that could be assigned do not show any particular trend in the chemical shifts when compared with the chemical shifts of the corresponding protons in the free Schiff bases (Tables 5.5 and 5.6). The ^{31}P NMR spectra of **1**–**4** display a singlet (Figure 5.4) within the narrow range of δ 49.19–49.51 ppm. This resonance also corroborates the chemically equivalent nature of the two *cis* oriented PPh_3 molecules as observed in the proton NMR spectra.

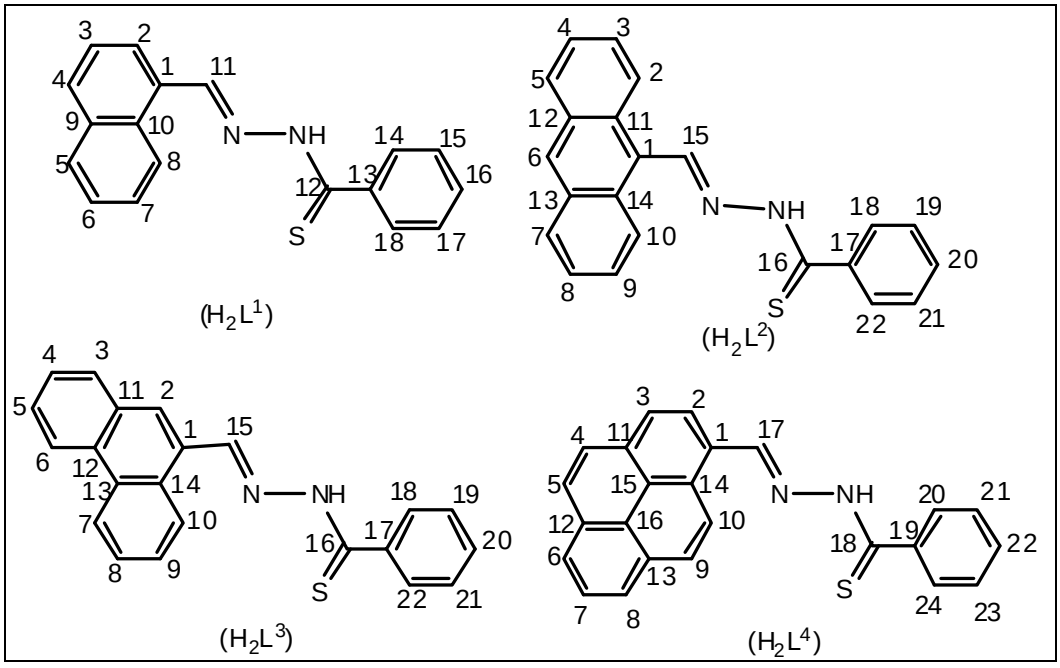

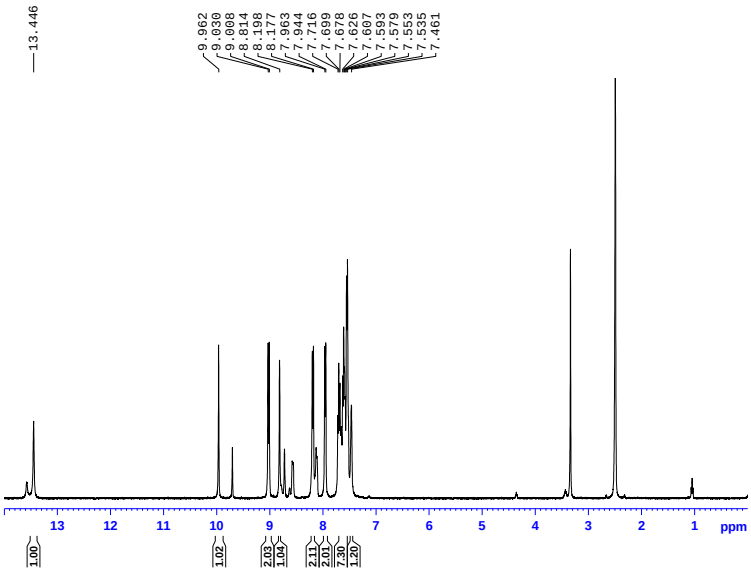

Figure 5.2. Proton NMR spectra of Schiff base H_2L^2

Table 5.5. ^1H NMR data for the Schiff bases (H_2L^n) in $(CD_3)_2SO$

H_2L^n	δ (ppm) (J (Hz))
H_2L^1	13.33 (s, 1H, NH); 8.71 (s, 1H, H^{11}); 8.19 (8) (d, 1H, H^2); 8.13 (8) (d, 1H, H^4); 8.09 (m, 1H, H^3); 7.91 (8) (d, 1H, H^5); 7.69 (8) (d, 2H, H^{14}, H^{18}); 7.62–7.54 (m, 4H, H^8, H^{15}, H^{16}, H^{17}); 7.39 (8) (q, 2H, H^6,H^7); 7.26 (s, SH).
H_2L^2	13.45 (s, 1H, NH); 9.96 (s, 1H, H^{15}); 9.02 (9) (d, 2H, H^2, H^{10}); 8.81 (s, 1H, H^6); 8.19 (8) (d, 2H, H^5, H^7); 7.95 (8) (d, 2H, H^{18}, H^{22}); 7.71–7.61 (m, 7H, H^3, H^4, H^8, H^9, H^{19}, H^{20}, H^{21}); 7.46 (s, SH).
H_2L^3	13.41 (s, 1H, NH); 8.91 (8) (d, 1H, H^7); 8.82 (8) (d, 1H, H^6); 8.79 (s, 1H, H^{15}); 8.17 (7) (d, 1H, H^2); 8.0 (8) (d, 2H, H^3, H^{10}); 7.70 (m, 4H, H^4, H^5, H^8 , H^9); 7.57 (7) (d, 2H, H^{18}, H^{22}); 7.38 (m, 3H, H^{19}, H^{20}, H^{21}); 7.28 (s, SH).
H_2L^4	13.41 (s, 1H, NH); 8.87 (s, 1H, H^{17}); 8.46 (9) (d, 1H, H^2); 8.39 (8) (d, 1H, H^3); 8.35 (m, 4H, H^4, H^5, H^9, H^{10}); 8.17 (d, 2H, H^6, H^8); 8.09 (8) (t, 1H, H^7); 7.60 (7) (d, 2H, H^{20}, H^{24}); 7.40 (m, 3H, H^{21}, H^{22}, H^{23}); 7.53 (s, SH).

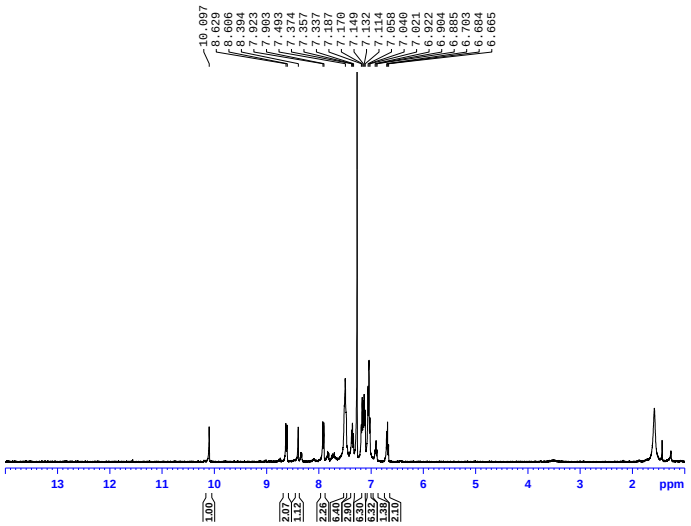

Figure 5.3. Proton NMR spectra of *cis*-[Ru(PPh$_3$)$_2$(HL^2)$_2$] (**2**)

Table 5.6. ^{1}H NMR data of *cis*-[Ru(PPh$_3$)$_2$(HL$^{1–4}$)$_2$] (**1**–**4**) in CDCl$_3$

Complex	δ (ppm) (J (Hz))
1	9.68 (s, 1H, H^{11}); 8.59 (9) (d, 1H, H^2); 7.82–7.75 (m, 3H, Ar-*H*); 7.46 (br, 9H, Ar-*H*); 7.21–7.15 (m, 5H, Ar-*H*); 7.04–7.01 (m, 7H, Ar-*H*); 6.91 (8) (t, 2H, H^{15},H^{17}).
2	10.10 (s, 1H, H^{15}); 8.61 (9) (d, 2H, H^2, H^{10}); 8.40 (s, 1H, H^6); 7.91 (8) (d, 2H, H^5, H^7); 7.49 (br, 6H, Ar-*H*); 7.36 (t, 3H, triphenylphoshine *para*-*H*); 7.19–7.11 (m, 6H, Ar-*H*); 7.06–7.02 (m, 6H, Ar-*H*); 6.90 (8) (t, 1H, H^{20}); 6.68 (8) (t, 2H, H^{19}, H^{21}).
3	9.70 (s, 1H, H^{15}); 8.69 (8) (t, 2H, H^6, H^7); 8.62 (8) (d,1H, H^{10}); 8.0 (s,1H, H^2); 7.77 (8) (d, 1H, H^3); 7.63 (7) (t, 2H, H^4, H^5); 7.56–7.45 (m, 5H, Ar-*H*); 6.92 (7) (t, 3H, triphenylphosphine *para*-*H*); 7.06–7.02 (m, 7H, Ar-*H*); 6.92 (7) (t, 2H, H^{19}, H^{21}).
4	10.02 (s, 1H, H^{17}); 8.89 (9) (d, 1H, H^2); 8.32–8.87 (m, 4H, Ar-*H*); 8.16–8.08 (m, 4H, Ar-*H*); 8.04–7.99 (m, 2H, Ar-*H*); 7.57–7.51 (m, 7H, Ar-*H*); 7.18 (7) (t, 3H, triphenylphosphine *para*-*H*); 7.07–7.03 (m, 7H, Ar-*H*); 6.87 (8) (t, 2H, H^{21}, H^{23}).

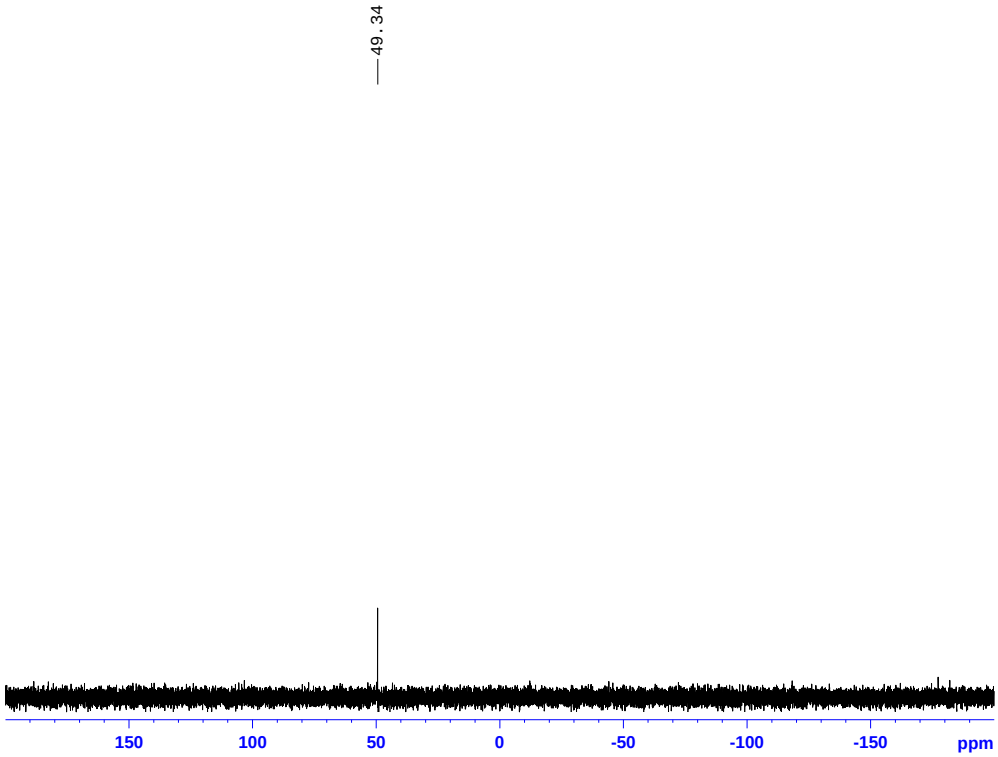

Figure 5.4. ^{31}PNMR spectra of *cis*-[Ru(PPh$_3$)$_2$(HL^4)$_2$] (**4**)

5.3.4. Electronic spectral properties

Electronic spectra of H_2L^{1-4} and the corresponding complexes (**1**–**4**) were recorded in dichloromethane. Representative spectra are illustrated in Figure 5.5. Other than two shoulders at 435 and 405 nm for H_2L^2 and H_2L^4, respectively, the remaining absorptions for all the Schiff bases are below 390 nm (Table 5.3). On the other hand, the spectra of **1**–**4** display three to four strong absorptions in the range 505–245 nm (Table 5.7). Thus for the complexes the lowest energy band is likely to be due to largely metal to ligand charge transfer, while the following two absorptions are attributed to ligand centred transitions.

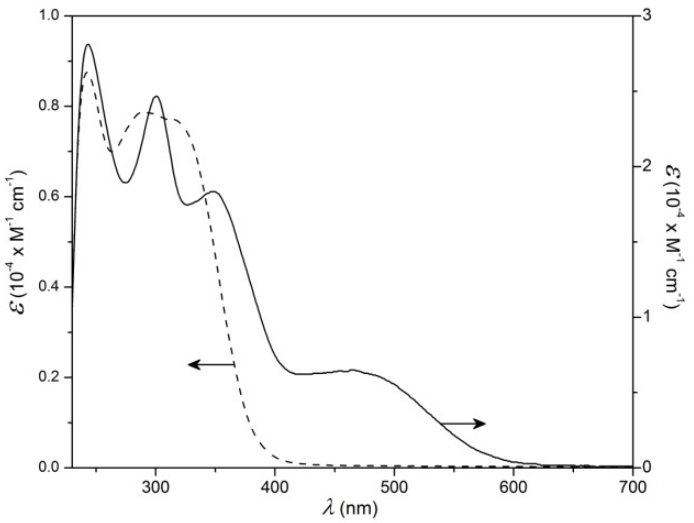

Figure 5.5. Electronic spectra of H_2L^1 (---) and *cis*-$[Ru(HL^1)_2(PPh_3)_2]$ (—) in CH_2Cl_2.

Table 5.7. Electronic absorption and emission spectroscopic[a] data of *cis*-$[Ru(L^{1\text{-}4})_2(PPh_3)_2]$

Complex	Absorption	Emission
	λ_{max} (nm) ($10^{-4} \times \varepsilon$ (M^{-1} cm^{-1}))	λ_{max} (nm)
1	465 (0.65), 348 (1.83), 301 (2.47), 244 (2.81)	372
2	497[d] (0.47), 415 (0.89), 259 (3.69)	416, 442, 468
3	466 (0.69), 347 (2.09), 254 (4.33)	367,[d] 381, 401[d]
4	505 (1.02), 391 (3.08), 295 (2.15), 245 (2.85)	395,[d] 424, 349[d]

[a] In dichloromethane

[d] Shoulder.

5.3.5. Emission spectral properties

All the Schiff bases and their corresponding complexes are emissive in nature. Emission properties have been studied by using their dichoromethane solutions. Representative emission spectra are illustrated in Figure 5.6. On

excitation at the wavelength of either the lowest energy absorption band or the most intense absorption band the Schiff bases display a broad emission in the wavelength range 410–515 nm (Table 5.3, Figure 5.6). The emission spectra of **1**–**4** have been collected with excitation at ~300 nm. The data have been summarized in Table 5.7. A broad emission band is observed for **1**, while **2**–**4** display a group of bands (Figure 5.6). This type of emission response is typical of the polycyclic aromatic fragment of $(HL^n)^-$ and indicates the involvement of its π–π^* state.

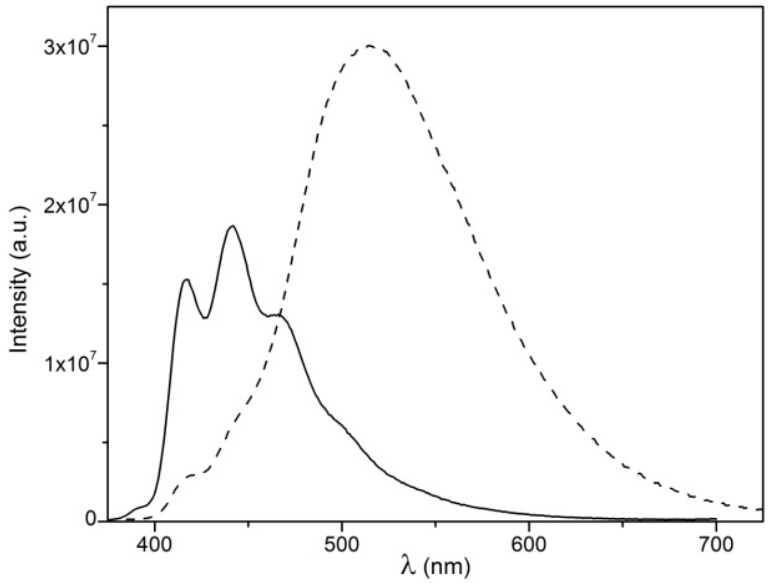

Figure 5.6. Emission spectra of H_2L^2 (0.59 x 10^{-4} M) (---) and *cis*-[$Ru(HL^2)_2(PPh_3)_2$] (0.14 x 10^{-4} M) (—) in CH_2Cl_2

5.3.6. X-ray molecular structures of cis-[$Ru(PPh_3)_2(HL^3)_2$] (3) and cis-[$Ru(PPh_3)_2(HL^4)_2$] (4)

The molecular structures of **3** and **4** are illustrated in Figure 5.7 and the bond lengths and angles in the coordination spheres of the metal centres are listed

in Table 5.8. In both complex molecules, the metal centre is in a distorted octahedral $N_2S_2P_2$ coordination environment. Both thiobenzhydrazonates act as thioamidate-N,S donor and form four-membered chelate rings. The deprotonated state of the thioamide fragments of $(HL^n)^-$ in **3** and **4** is indicated by the shorter C–N (1.289(12)–1.320(11) Å) and C–S (1.713(11)–1.723(6) Å) bond lengths than the corresponding bond lengths in free 2-hydroxy-thiobenzhydrazide [26] or thiosemicarbazones [27–29]. The mutually *cis* PPh_3 ligands are *trans* to the two thioamidate-N atoms. The bond parameters associated with the metal centre in both complexes are very similar (Table 5.8). The bite angles of the four-membered chelate rings formed by $(HL^n)^-$ are within 65.12(13)–66.4(3)º, while the remaining *cis* bond angles are in the range 79.9(3)–104.42(11)º. The *trans* bond angles span a smaller range of 158.41(6)–166.7(3)º compared to the *cis* bond angles. Overall, the bond angles and the bond lengths involving the metal centre in each of **3** and **4** are comparable with those observed for similar complexes of *cis*-$\{Ru(PPh_3)_2\}^{2+}$ with four membered chelate ring forming thioamidate-N,S donor thiosemicarbazonates [30–36]. The very similar physical properties of all four complexes indicate that **1** and **2** have the same gross molecular structure as that of **3** and **4**.

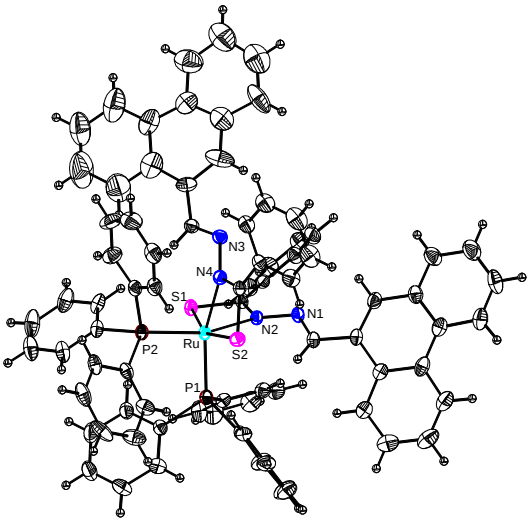

(**a**)

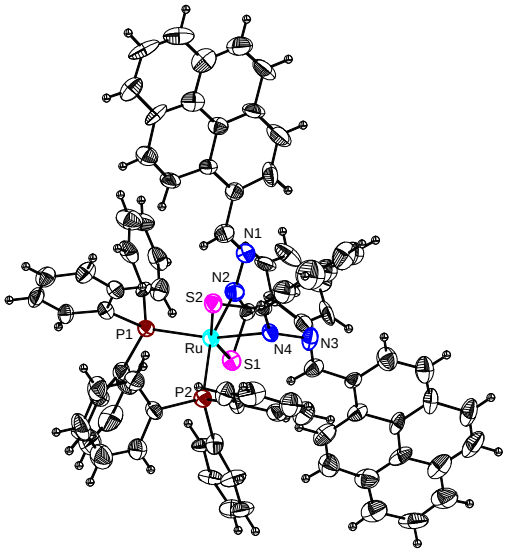

(**b**)

Figure 5.7. Molecular structure of (a) *cis*-[Ru(PPh$_3$)$_2$(HL^3)$_2$] (**3**) and (b) *cis*-[Ru(PPh$_3$)$_2$(HL^4)$_2$] (**4**). Thermal ellipsoids of all non-hydrogen atoms are drawn at the 30% probability level. For clarity only non-carbon atoms are labelled and only one orientation of the disordered phenyl ring of **4** is shown.

Table 5.8. Selected bond lengths (Å) and bond angles (^{o}) for **3** and **4**·CH_2Cl_2

Complex	**3**	**4**·CH_2Cl_2
Ru–N(2)	2.141(4)	2.164(10)
Ru–N(4)	2.149(5)	2.154(9)
Ru–P(1)	2.3216(16)	2.309(3)
Ru–P(2)	2.3331(15)	2.308(3)
Ru–S(1)	2.4133(14)	2.400(3)
Ru–S(2)	2.4190(15)	2.396(3)
N(2)–Ru–N(4)	80.29(17)	79.9(3)
N(2)–Ru–P(1)	90.12(13)	92.7(3)
N(2)–Ru–P(2)	164.12(13)	162.0(3)
N(2)–Ru–S(1)	65.86(12)	65.1(3)
N(2)–Ru–S(2)	96.57(12)	98.8(3)
N(4)–Ru–P(1)	164.21(13)	166.7(3)
N(4)–Ru–P(2)	90.93(13)	90.0(3)
N(4)–Ru–S(1)	98.22(13)	95.8(2)
N(4)–Ru–S(2)	65.12(13)	66.4(3)
P(1)–Ru–P(2)	101.12(6)	99.93(12)
P(1)–Ru–S(1)	89.12(5)	90.89(11)
P(1)–Ru–S(2)	103.99(5)	104.42(11)
P(2)–Ru–S(1)	102.78(5)	101.60(11)
P(2)–Ru–S(2)	91.60(5)	90.49(11)
S(1)–Ru–S(2)	158.41(6)	158.65(11)

5.3.7. Redox properties

Electron transfer properties of **1**–**4** in dimethylformamide have been investigated using cyclic voltammetry. The potential data are listed in Table 5.9 and a representative cyclic voltammogram is illustrated in Figure 5.8. All the complexes display an oxidation response in the potential range 0.76 to 0.86 V (vs. Ag/AgCl). Comparison of the current heights of the observed responses with the current heights of known one electron transfer processes under identical condition indicates its one-electron nature [3,4,9,10]. Generally similar *cis*-$\{Ru(PPh_3)_2\}^{2+}$ bis-thiosemicarbazonate complexes where the thiosemicarbazonates are four-membered chelate ring forming thioamidate-N,S donor display two successive oxidations in the potential ranges 0.2 to 0.6 V and 0.8 to 1.3 V [30,31,33]. However, like **1**–**4** only one oxidation response is observed in one case [36]. Theoretical calculations on some of these thiosemicarbazonate complexes have been performed and it has been shown that the HOMO consists of only ~35% ruthenium based orbitals [32,33,36]. EPR studies on one of these complexes [36] indicate that the oxidised species is at the borderline between an authentic ruthenium(III) and the ruthenium(II) stabilised ligand radical system. Considering the higher potential required for the oxidation of **1**–**4** compared to that needed for the first oxidation of analogous complexes of thiosemicarbazonates and the very similar coordination environment around the metal centre in both type of complexes perhaps a similar borderline situation exists in the oxidised species $\mathbf{1}^{+}$–$\mathbf{4}^{+}$.

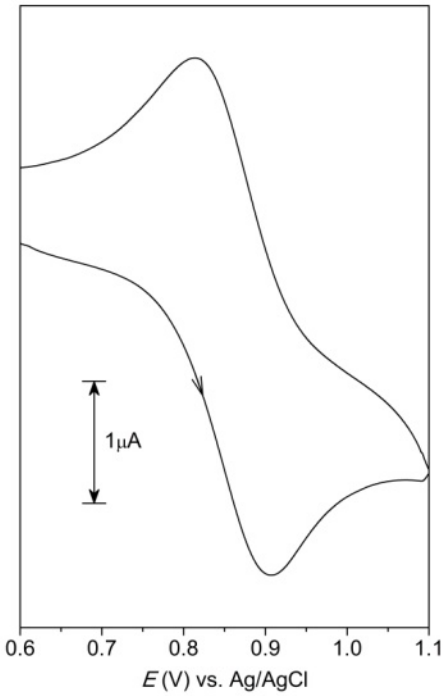

Figure 5.8. Cyclic voltammogram of *cis*-[$Ru(PPh_3)_2(HL^3)_2$] (**3**) in dimethylformamide (0.1 M TBAP) at 298 K.

Table 5.9. Cyclic voltammetric data[b,c]

Complex	$E_{1/2}$ (V)	(ΔE_p (mV))
1	0.83	100
2	0.84	90
3	0.86	90
4	0.76	100

[b] In dimethylformamide.

[c] $E_{1/2} = (E_{pa} + E_{pc})/2$ and $\Delta E_p = E_{pa} - E_{pc}$, where E_{pa} and E_{pc} are cathodic and anodic peak potentials, respectively.

5.4. Conclusion

In our attempts to explore the regioselective cyloruthenation of the fused aromatic ring fragment in thiobenzhydrazones of polycyclic aromatic aldehydes (H_2L^n) we have isolated a series of *cis*-$\{Ru(PPh_3)_2\}^{2+}$ bis-thiobenzhydrazonate complexes. The five-membered chelate ring forming imine-N and thioamidate-S coordination mode of $(HL^n)^-$ is expected to facilitate cyclometallation of its polycyclic aromatic fragment as observed in the complexes of analogous benzhydrazonates having the five-membered chelate ring forming imine-N and amidate-O coordination mode [8,9]. However, $(HL^n)^-$ acts as thioamidate-N,S donor and forms four-membered chelate ring at the metal centre. As a result, the polycyclic aromatic ring is oriented far away from the ruthenium atom and hence there is no regioselective cycloruthenation. In general, for thiosemicarbazonates it has been found that the large *R* in its *R*CH=N–N fragment leads to four-membered chelate ring formation, while small *R* leads to five-membered chelate ring formation [37]. It is very likely, that the bulky polycyclic aromatic ring of the present thiobenzhydrazonates plays the same role as observed for thiosemicarbazonates in deciding the chelate ring size and hence the non-occurrence of its cycloruthenation.

5.5. References

[1] S. Das, S. Pal, *J. Organomet. Chem.* 689 (2004) 352.

[2] S. Das, S. Pal, *J. Organomet. Chem.* 691 (2006) 2575.

[3] R. Raveendran, S. Pal, *J. Organomet. Chem.* 692 (2007) 824.

[4] R. Raveendran, S. Pal, *J. Organomet. Chem.* 694 (2009) 1482.

[5] A.R.B. Rao, S. Pal, *J. Organomet. Chem.* 696 (2011) 2660.

[6] A.R.B. Rao, S. Pal, *J. Organomet. Chem.* 701 (2012) 62.

[7] A.R.B. Rao, S. Pal, *J. Organomet. Chem.* 731 (2013) 67.

[8] K. Nagaraju, S. Pal, *J. Organomet. Chem.* 737 (2013) 7.

[9] K. Nagaraju, S. Pal, *J. Organomet. Chem.* 745–746 (2013) 404.

[10] N. Selander, K.J. Szabó, *Chem. Rev.* 111 (2011) 2048.

[11] D. Gelman, S. Musa, *ACS Catal.* 2 (2012) 2456.

[12] G. van Koten, D. Milstein (Eds.), Organometallic Pincer Chemistry: Topics in Organometallic Chemistry, vol. 40, Springer, Heidelberg, 2013, pp. 1–352.

[13] N.K. Singh, D.K. Singh, J. Singh, *Indian J. Chem. Sect. A* 40 (2001) 1064.

[14] A. Sarkar, S. Pal, *Inorg. Chim. Acta* 361 (2008) 2296.

[15] T.A. Stephenson, G. Wilkinson, *J. Inorg. Nucl. Chem.* 28 (1966) 945.

[16] D.D. Perrin, W.L.F. Armarego, D.P. Perrin, Purification of Laboratory Chemicals, 2nd ed., Pergamon, Oxford, 1983.

[17] SMART version 5.630 and SAINT-plus version 6.45, Bruker-Nonius Analytical X-ray Systems Inc., Madison, WI, USA, 2003.

[18] G.M. Sheldrick, SADABS, Program for Area Detector Absorption Correction, University of Göttingen, Göttingen, Germany, 1997.

[19] CrysAlisPro version 1.171.33.55, Oxford Diffraction Ltd., Abingdon, Oxfordshire, UK, 2007.

[20] R. Dubey, A.K. Tewari, K. Ravikumar, B. Sridhar, *Bull. Korean Chem. Soc.* 31 (2010) 1326.

[21] G.M. Sheldrick, XHELX-97, Structure Determination Software, University of Göttingen, Göttingen, Germany, 1997.

[22] L.J. Farrugia, WinGX, *J. Appl. Crystallogr.* 32 (1999) 837.

[23] A.L. Spek, Platon, A Multipurpose Crystallographic Tool, Utrecht University, Utrecht, The Netherlands, 2002.

[24] C.F. Macrae, I.J. Bruno, J.A. Chisholm, P.R. Edgington, P. McCabe, E. Pidcock, L. Rodriguez-Monge, R. Taylor, J. van de Streek, P.A. Wood, J. Appl. Cryst. 41 (2008) 466.

[25] D. Nin-Vien, N.B. Clothup, W.G. Fateley, J.G. Grasselli, The Handbook of Infrared and Raman Characteristic Frequencies of Organic Molecules, Academic Press, London, 1991, pp. 236–238.

[26] G.J. Palenik, D.F. Rendle, W.S. Carter, *Acta Cryst., Sect. B* 30 (1974) 2390.

[27] W. Mikenda, F. Pertlik, E. Steinwender, *Monatshefte für Chemie* 124 (1993) 867.

[28] P.N. Bourosh, M.D. Revenko, M. Gdaniec, E.F. Stratulat, Y.A. Simonov, *J. Struct. Chem.* 50 (2009) 510.

[29] D. Chattopadhyay, S.K. Mazumdar, T. Banerjee, S. Ghosh, T.C.W. Mak, *Acta Cryatallogr., Sect. C* 44 (1988) 1025.

[30] F. Basuli, S.-M. Peng, S. Bhattacharya, *Inorg. Chem.* 36 (1997) 5645.

[31] F. Basuli, M. Ruf, C.G. Pierpont, S. Bhattacharya, *Inorg. Chem.* 37 (1998) 6113.

[32] D. Mishra, S.N., M.G.B. Drew, S.K. Chattopadhyay, *Polyhedron* 24 (2005) 1861.

[33] D. Mishra, S. Naskar, M.G.B. Drew, S.K. Chattopadhyay, *Inorg. Chim. Acta* 359 (2006) 585.

[34] T.S. Lobana, G. Bawa, R.J. Butcher, B.-J. Liaw, C.W. Liu, *Polyhedron* 25 (2006) 2897.

[35] T.S. Lobana, G. Bawa, R.J. Butcher, C.W. Liu, *Z. Anorg. Allg. Chem.* 635 (2009) 355.

[36] S. Naskar, S. Naskar, M.G.B. Drew, S.I. Gorelsky, B. Lassalle-Kaiser, A. Aukauloo, D. Mishra, S.K. Chattopadhyay, *Polyhedron* 28 (2009) 4101.

[37] I. Pal, F. Basuli, S. Bhattacharya, *Indian Acad. Sci. (Chem. Sci.)* 114 (2002) 255.

Appendix

Tables for atomic coordinates (x 10^4) and equivalent isotropic displacement parameters ($Å^2$x 10^3). U(eq) is defined as one third of the trace of the orthogonalized U^{ij} tensor.

Table A.1 for $[Ru(L^1)_2]ClO_4$ (1) (Chapter 2)

Atom	x	y	z	U(eq)
Ru	8200(1)	5699(1)	2158(1)	32(1)
O(1)	8813(3)	4871(2)	3400(2)	40(1)
O(2)	10174(2)	6395(2)	1435(2)	38(1)
N(1)	8702(3)	4352(2)	1344(2)	31(1)
N(2)	8280(3)	4507(2)	410(2)	40(1)
N(3)	7487(3)	6331(3)	835(2)	38(1)
N(4)	7572(3)	7041(2)	2965(2)	35(1)
N(5)	6096(3)	6995(3)	3507(3)	51(1)
N(6)	6076(3)	5229(3)	2938(2)	39(1)
C(1)	9463(3)	3834(3)	3430(3)	36(1)
C(2)	9894(4)	3414(3)	4355(3)	44(1)
C(3)	10588(4)	2350(4)	4479(3)	50(1)
C(4)	10852(4)	1655(4)	3691(3)	53(1)
C(5)	10408(4)	2026(3)	2781(3)	46(1)
C(6)	9715(3)	3112(3)	2616(3)	37(1)
C(7)	9309(4)	3381(3)	1635(3)	39(1)
C(8)	7647(3)	5562(3)	151(3)	39(1)
C(9)	7159(4)	5809(4)	-774(3)	50(1)
C(10)	6531(4)	6872(4)	-977(3)	58(1)
C(11)	6386(5)	7677(4)	-282(3)	58(1)
C(12)	6865(4)	7388(4)	607(3)	49(1)
C(13)	10726(4)	7279(3)	1761(3)	37(1)
C(14)	12221(4)	7508(4)	1329(3)	50(1)
C(15)	12884(4)	8416(4)	1574(4)	58(1)

C(16)	12079(4)	9133(4)	2268(3)	53(1)
C(17)	10612(4)	8933(3)	2697(3)	44(1)
C(18)	9897(4)	8003(3)	2474(3)	36(1)
C(19)	8355(4)	7903(3)	2997(3)	37(1)
C(20)	5358(4)	6007(3)	3543(3)	48(1)
C(21)	3931(4)	5810(4)	4185(4)	64(1)
C(22)	3261(5)	4790(5)	4192(4)	72(1)
C(23)	3991(5)	3992(4)	3546(4)	65(1)
C(24)	5383(4)	4231(4)	2943(3)	50(1)
Cl	6130(1)	887(1)	2162(1)	62(1)
O(3)	5824(6)	-20(6)	1741(7)	190(4)
O(4)	7239(7)	609(5)	2677(5)	146(2)
O(5)	4840(5)	1267(4)	2870(4)	106(1)
O(6)	6666(5)	1862(4)	1365(4)	116(2)
O(7)	5396(5)	1594(5)	5015(4)	104(1)
C(25)	6641(7)	1064(6)	5156(6)	97(2)
O(8)	9945(14)	1006(11)	415(11)	144(4)
C(26)	10000	0	0	146(6)

Table A.2 for $[Ru(L^n)_2]ClO_4$ (2) (Chapter 2)

Atom	x	y	z	U(eq)
Ru	2303(1)	6882(1)	1803(1)	36(1)
Cl(1)	5049(2)	9496(2)	3497(1)	57(1)
Cl(2)	-50(2)	4272(2)	3637(1)	73(1)
O(1)	2025(4)	7639(3)	2339(3)	41(2)
O(2)	2688(5)	6113(4)	2317(2)	43(2)
N(1)	3853(5)	7138(4)	1753(3)	39(2)
N(2)	4367(6)	6784(5)	1351(3)	55(3)
N(3)	2764(6)	6204(4)	1201(3)	40(2)
N(4)	767(5)	6619(4)	1838(3)	37(2)
N(5)	167(6)	6983(5)	1465(3)	47(2)

N(6)	1726(6)	7556(4)	1224(3)	41(2)
C(1)	2764(7)	8040(6)	2576(3)	35(2)
C(2)	2440(7)	8530(5)	2969(4)	50(3)
C(3)	3118(7)	8977(5)	3250(4)	51(3)
C(4)	4201(6)	8931(5)	3138(4)	39(2)
C(5)	4545(7)	8457(5)	2767(4)	44(3)
C(6)	3880(6)	7998(5)	2472(4)	36(3)
C(7)	4358(6)	7573(6)	2071(4)	43(3)
C(8)	3802(8)	6275(6)	1056(4)	48(3)
C(9)	4253(8)	5891(6)	638(4)	61(3)
C(10)	3646(10)	5395(6)	379(4)	65(4)
C(11)	2585(10)	5292(6)	522(4)	61(3)
C(12)	2200(9)	5706(6)	919(4)	49(3)
C(13)	2014(7)	5728(5)	2598(4)	34(3)
C(14)	2430(8)	5219(5)	2948(4)	48(3)
C(15)	1827(7)	4787(5)	3268(4)	53(3)
C(16)	728(7)	4845(5)	3228(4)	46(3)
C(17)	263(7)	5315(5)	2885(4)	50(3)
C(18)	885(7)	5768(5)	2556(4)	38(3)
C(19)	308(7)	6199(5)	2176(4)	41(3)
C(20)	665(7)	7465(6)	1135(4)	41(3)
C(21)	147(9)	7850(6)	736(4)	61(3)
C(22)	691(9)	8329(6)	427(5)	71(4)
C(23)	1773(9)	8424(6)	523(4)	60(3)
C(24)	2249(9)	8043(6)	921(4)	57(3)
Cl(3)	-1863(3)	6054(2)	639(2)	74(1)
O(3)	-1871(5)	6506(5)	1108(3)	89(3)
O(4)	-2887(9)	5774(7)	569(4)	173(6)
O(5)	-1668(8)	6478(6)	185(4)	127(4)
O(6)	-1128(11)	5529(7)	677(5)	211(7)
O(7)	6288(7)	7382(6)	1128(5)	115(4)

C(25)	6433(14)	7861(9)	686(6)	161(8)

Table A.3 for $[Ru(L^n)_4]ClO_4$ (4) (Chapter 2)

Atom	x	y	z	U(eq)
Ru(1)	617(1)	8138(1)	3766(1)	33(1)
O(1)	-660(3)	9291(3)	3666(1)	42(1)
O(2)	-515(3)	7106(2)	4119(1)	42(1)
N(1)	30(3)	7451(3)	2941(2)	36(1)
N(2)	721(4)	6568(3)	2799(2)	47(1)
N(3)	1923(3)	6937(3)	3732(2)	38(1)
N(4)	1266(3)	8863(3)	4579(2)	37(1)
N(5)	2299(4)	9568(3)	4572(2)	50(1)
N(6)	1996(3)	9192(3)	3541(2)	36(1)
C(1)	-1451(4)	9414(4)	3156(2)	37(1)
C(2)	-2188(5)	10341(4)	3141(2)	49(1)
C(3)	-3040(5)	10553(4)	2643(2)	51(1)
C(4)	-3218(4)	9859(4)	2130(2)	50(1)
C(5)	-2507(4)	8954(4)	2138(2)	47(1)
C(6)	-1610(4)	8699(4)	2635(2)	38(1)
C(7)	-881(4)	7752(4)	2548(2)	40(1)
C(8)	1748(5)	6344(3)	3203(2)	41(1)
C(9)	2579(5)	5525(4)	3074(3)	53(1)
C(10)	3581(5)	5340(4)	3495(3)	59(1)
C(11)	3760(5)	5942(5)	4050(3)	61(1)
C(12)	2928(5)	6723(4)	4149(2)	49(1)
C(13)	-4150(6)	10111(6)	1578(3)	73(2)
C(14)	-782(4)	7226(4)	4686(2)	39(1)
C(15)	-1698(5)	6492(4)	4846(2)	55(1)
C(16)	-2044(6)	6526(5)	5421(3)	61(1)
C(17)	-1495(5)	7294(4)	5864(2)	52(1)
C(18)	-604(5)	8013(4)	5711(2)	45(1)

C(19)	-214(4)	8008(4)	5137(2)	39(1)
C(20)	796(4)	8773(4)	5072(2)	41(1)
C(21)	2676(5)	9744(4)	4026(2)	43(1)
C(22)	3697(5)	10441(4)	3971(3)	57(1)
C(23)	4023(6)	10569(4)	3410(3)	61(1)
C(24)	3330(5)	10031(4)	2909(3)	57(1)
C(25)	2336(5)	9346(4)	2988(2)	43(1)
C(26)	-1828(6)	7288(5)	6497(3)	68(2)
Ru(2)	6264(1)	4982(1)	1508(1)	29(1)
O(3)	7553(3)	6038(2)	1283(1)	37(1)
O(4)	6751(3)	3786(2)	968(1)	37(1)
N(7)	4928(3)	5400(3)	837(2)	31(1)
N(8)	3791(3)	4821(3)	820(2)	41(1)
N(9)	4747(3)	4039(3)	1678(2)	34(1)
N(10)	7510(3)	4568(3)	2210(2)	33(1)
N(11)	7527(4)	5264(3)	2716(2)	46(1)
N(12)	5866(3)	6085(3)	2161(2)	33(1)
C(27)	7313(4)	6743(3)	844(2)	36(1)
C(28)	8308(4)	7461(4)	763(2)	48(1)
C(29)	8175(5)	8231(4)	335(2)	56(1)
C(30)	7034(5)	8331(4)	-42(2)	54(1)
C(31)	6048(5)	7620(4)	26(2)	47(1)
C(32)	6140(4)	6816(3)	455(2)	36(1)
C(33)	5022(4)	6136(3)	457(2)	36(1)
C(34)	3682(4)	4142(4)	1270(2)	40(1)
C(35)	2534(5)	3581(4)	1311(3)	56(1)
C(36)	2502(6)	2924(5)	1784(3)	67(2)
C(37)	3582(5)	2826(5)	2204(3)	60(1)
C(38)	4667(5)	3384(4)	2141(2)	45(1)
C(39)	6883(7)	9214(6)	-488(3)	92(2)
C(40)	7587(4)	3032(3)	1148(2)	34(1)

C(41)	7807(5)	2235(4)	712(2)	48(1)
C(42)	8634(5)	1412(4)	846(3)	54(1)
C(43)	9271(4)	1322(4)	1425(2)	47(1)
C(44)	9084(4)	2101(4)	1853(2)	42(1)
C(45)	8266(4)	2978(3)	1740(2)	34(1)
C(46)	8225(4)	3745(4)	2238(2)	39(1)
C(47)	6637(4)	6030(4)	2694(2)	37(1)
C(48)	6526(5)	6737(4)	3185(2)	50(1)
C(49)	5605(5)	7491(4)	3128(2)	54(1)
C(50)	4825(5)	7545(4)	2585(2)	54(1)
C(51)	4977(4)	6843(4)	2112(2)	41(1)
C(52)	10141(5)	384(4)	1578(3)	68(2)
Cl(1)	3495(2)	6890(1)	5965(1)	72(1)
O(5)	2303(9)	6651(10)	5812(8)	320(9)
O(6)	3571(8)	7878(5)	5682(3)	149(3)
O(7)	3886(16)	6041(11)	5708(5)	323(9)
O(8)	3958(14)	7002(6)	6522(3)	271(7)
Cl(2)	2092(1)	7873(1)	1140(1)	64(1)
O(9)	2085(8)	6736(5)	1077(4)	167(3)
O(10)	1269(4)	8321(5)	678(2)	90(2)
O(11)	1607(10)	8007(7)	1660(3)	194(4)
O(12)	3238(7)	8224(10)	1134(6)	331(10)
O(13)	156(4)	5481(3)	1661(2)	59(1)
O(14)	3033(6)	10931(6)	5615(3)	122(2)
O(15)	1679(6)	5248(5)	-53(3)	114(2)
O(16)	9376(4)	4862(3)	3679(2)	64(1)

Table A.4 for $[Ru(L^n)_5]ClO_4$ (5) (Chapter 2)

Atom	x	y	z	U(eq)
Ru	846(1)	2666(1)	4392(1)	49(1)
O(1)	-169(6)	3193(5)	5655(6)	46(2)
O(2)	-553(6)	1358(5)	3463(6)	52(2)
O(3)	-1100(8)	1659(7)	9149(7)	84(3)
O(4)	-4052(7)	1431(7)	444(7)	70(2)
N(1)	1347(7)	1524(6)	4972(7)	41(2)
N(2)	2147(8)	896(7)	4311(8)	54(2)
N(3)	2007(8)	2052(6)	3259(7)	44(2)
N(4)	419(7)	3829(7)	3801(7)	41(2)
N(5)	1257(8)	4989(6)	4260(7)	51(2)
N(6)	2269(7)	4115(6)	5204(7)	41(2)
C(1)	-419(9)	2710(8)	6444(9)	45(3)
C(2)	-1211(11)	3104(8)	7190(10)	58(3)
C(3)	-1405(11)	2754(11)	8073(11)	74(4)
C(4)	-818(11)	1945(9)	8213(10)	58(3)
C(5)	-74(11)	1476(9)	7468(10)	56(3)
C(6)	159(9)	1832(8)	6550(9)	44(3)
C(7)	971(10)	1256(9)	5816(10)	53(3)
C(8)	2485(10)	1170(9)	3424(10)	50(3)
C(9)	3267(12)	611(10)	2737(12)	73(4)
C(10)	3562(12)	903(11)	1855(12)	74(4)
C(11)	3092(12)	1821(11)	1652(10)	76(4)
C(12)	2362(10)	2362(9)	2387(9)	55(3)
C(13)	-450(12)	867(10)	9384(11)	81(4)
C(14)	-1355(9)	1503(9)	2798(9)	45(3)
C(15)	-2296(10)	457(9)	2181(10)	56(3)
C(16)	-3174(10)	483(9)	1440(10)	57(3)
C(17)	-3154(11)	1508(11)	1223(11)	64(3)
C(18)	-2224(10)	2541(10)	1780(9)	53(3)

C(19)	-1324(10)	2569(8)	2569(9)	44(3)
C(20)	-468(10)	3666(8)	3098(9)	47(3)
C(21)	2231(10)	5097(9)	4949(9)	47(3)
C(22)	3089(11)	6135(9)	5381(10)	58(3)
C(23)	4052(12)	6235(11)	6081(12)	75(4)
C(24)	4202(11)	5252(11)	6316(11)	79(4)
C(25)	3251(11)	4240(9)	5876(10)	60(3)
C(26)	-3989(11)	2481(12)	189(11)	83(4)
Cl	4852(5)	2144(5)	6875(6)	128(2)
O(5)	3621(12)	2170(10)	7035(13)	162(6)
O(6)	5211(14)	1331(16)	7094(17)	229(9)
O(7)	5644(15)	3210(20)	7550(30)	321(16)
O(8)	5000(20)	2100(20)	5846(19)	244(11)
O(9)	2970(12)	-772(8)	5011(11)	141(5)
O(10)	1230(30)	4137(13)	10556(15)	400(20)
C(27)	2360(20)	3990(40)	10630(50)	480(50)

Table A.5 for *trans*-[Ru(pnbh*Me*)(PPh_3)$_2$Cl] (2) (Chapter 3)

Atom	x	y	z	U(eq)
Ru	1815(1)	2149(1)	8303(1)	32(1)
Cl	914(1)	2155(1)	7387(1)	44(1)
P(1)	3156(1)	1845(1)	7822(1)	39(1)
P(2)	503(1)	2498(1)	8798(1)	35(1)
O	2307(2)	3492(1)	8350(1)	42(1)
N(1)	2506(2)	2256(2)	9116(1)	37(1)
N(2)	2863(2)	3077(2)	9299(1)	43(1)
C(1)	1835(2)	853(2)	8610(1)	37(1)
C(2)	1547(2)	91(2)	8301(1)	42(1)
C(3)	1603(2)	-770(2)	8560(1)	43(1)
C(4)	1300(3)	-1563(3)	8240(2)	57(1)
C(5)	1353(3)	-2374(3)	8496(2)	62(1)

C(6)	1701(2)	-2493(3)	9108(2)	52(1)
C(7)	1761(3)	-3339(3)	9386(2)	66(1)
C(8)	2102(3)	-3422(3)	9971(2)	69(1)
C(9)	2382(3)	-2678(3)	10302(2)	66(1)
C(10)	2330(2)	-1819(3)	10050(2)	49(1)
C(11)	2604(3)	-1035(3)	10371(2)	59(1)
C(12)	2569(2)	-213(3)	10117(2)	53(1)
C(13)	2255(2)	-89(2)	9495(1)	40(1)
C(14)	1956(2)	-861(2)	9167(2)	41(1)
C(15)	2005(2)	-1726(2)	9439(2)	45(1)
C(16)	2211(2)	755(2)	9214(1)	37(1)
C(17)	2581(2)	1564(2)	9464(1)	40(1)
C(18)	2740(2)	3661(2)	8858(2)	40(1)
C(19)	3169(2)	4555(2)	8943(2)	44(1)
C(20)	3087(3)	5168(3)	8479(2)	63(1)
C(21)	3504(3)	6003(3)	8539(2)	80(1)
C(22)	4004(3)	6222(3)	9053(2)	73(1)
C(23)	4091(3)	5599(3)	9515(2)	71(1)
C(24)	3674(3)	4779(3)	9464(2)	63(1)
C(25)	4466(4)	7136(3)	9115(2)	118(2)
C(26)	3278(2)	915(2)	7295(1)	43(1)
C(27)	4119(2)	593(3)	7189(2)	63(1)
C(28)	4215(3)	-45(3)	6755(2)	77(1)
C(29)	3485(3)	-385(3)	6433(2)	89(2)
C(30)	2653(3)	-83(3)	6539(2)	84(2)
C(31)	2553(3)	566(3)	6969(2)	61(1)
C(32)	3523(2)	2790(2)	7375(2)	48(1)
C(33)	4416(3)	3000(3)	7324(2)	77(1)
C(34)	4631(4)	3717(4)	6951(2)	92(2)
C(35)	3970(4)	4199(4)	6641(2)	96(2)
C(36)	3113(4)	3985(3)	6680(2)	88(2)

C(37)	2893(3)	3293(3)	7055(2)	66(1)
C(38)	4040(2)	1641(3)	8414(2)	54(1)
C(39)	4105(3)	783(3)	8662(2)	69(1)
C(40)	4663(3)	641(4)	9184(2)	95(2)
C(41)	5141(4)	1336(6)	9446(2)	111(2)
C(42)	5082(3)	2169(5)	9207(2)	104(2)
C(43)	4529(3)	2335(4)	8698(2)	73(1)
C(44)	234(2)	3696(2)	8790(1)	36(1)
C(45)	-172(2)	4108(2)	9254(1)	44(1)
C(46)	-393(2)	5008(3)	9218(2)	54(1)
C(47)	-225(2)	5498(3)	8724(2)	54(1)
C(48)	164(2)	5098(2)	8252(2)	52(1)
C(49)	400(2)	4207(2)	8286(1)	44(1)
C(50)	-531(2)	1984(2)	8469(1)	40(1)
C(51)	-559(3)	1068(3)	8358(2)	56(1)
C(52)	-1339(3)	671(3)	8115(2)	68(1)
C(53)	-2081(3)	1173(4)	7976(2)	73(1)
C(54)	-2056(3)	2079(3)	8068(2)	71(1)
C(55)	-1285(2)	2489(3)	8319(2)	54(1)
C(56)	540(2)	2191(2)	9600(1)	39(1)
C(57)	1097(2)	2676(3)	10009(2)	49(1)
C(58)	1186(3)	2427(3)	10609(2)	62(1)
C(59)	740(3)	1696(3)	10802(2)	72(1)
C(60)	200(3)	1211(3)	10404(2)	67(1)
C(61)	91(2)	1453(3)	9802(2)	52(1)

Table A.6 for *trans*-[Ru(nabh*Me*)(PPh_3)$_2$Cl] (2) (Chapter 4)

Atom	x	y	z	U(eq)
Ru	2548(1)	2180(1)	4876(1)	31(1)
Cl	1269(1)	2846(1)	4542(1)	50(1)
P(1)	2554(1)	2550(1)	6220(1)	34(1)

P(2)	2640(1)	1856(1)	3539(1)	31(1)
O(1)	1957(3)	1114(2)	5015(3)	42(1)
N(1)	3489(3)	1451(3)	5211(3)	32(1)
N(2)	3306(4)	714(3)	5388(3)	38(1)
C(1)	3609(4)	2819(3)	4818(3)	32(2)
C(2)	3640(4)	3569(4)	4566(4)	41(2)
C(3)	4392(5)	3937(4)	4560(4)	49(2)
C(4)	5184(4)	3585(4)	4805(3)	39(2)
C(5)	5964(5)	3965(4)	4803(4)	52(2)
C(6)	6705(5)	3620(5)	5067(4)	61(2)
C(7)	6696(5)	2883(5)	5338(5)	62(2)
C(8)	5956(5)	2483(5)	5321(4)	54(2)
C(9)	5164(4)	2827(4)	5061(3)	34(2)
C(10)	4370(4)	2462(4)	5046(3)	36(2)
C(11)	4270(4)	1684(4)	5262(3)	34(2)
C(12)	2494(4)	606(4)	5254(3)	32(2)
C(13)	2154(4)	-162(4)	5369(3)	37(2)
C(14)	2693(5)	-758(4)	5579(4)	49(2)
C(15)	2359(5)	-1461(4)	5688(4)	53(2)
C(16)	1497(5)	-1602(4)	5579(4)	52(2)
C(17)	974(5)	-1009(4)	5346(5)	59(2)
C(18)	1291(5)	-299(4)	5239(4)	53(2)
C(19)	1150(6)	-2380(4)	5711(5)	81(3)
C(20)	1677(4)	2201(4)	6741(4)	36(2)
C(21)	1668(5)	2325(4)	7526(4)	54(2)
C(22)	1041(6)	2026(5)	7930(5)	66(2)
C(23)	405(6)	1594(5)	7531(5)	70(2)
C(24)	405(5)	1486(5)	6772(5)	74(3)
C(25)	1036(5)	1779(4)	6375(4)	57(2)
C(26)	3480(4)	2186(4)	6809(4)	37(2)
C(27)	4257(5)	2576(4)	6859(4)	50(2)

C(28)	4960(5)	2260(6)	7260(5)	66(2)
C(29)	4924(5)	1566(6)	7611(5)	71(3)
C(30)	4162(6)	1183(5)	7555(4)	64(2)
C(31)	3439(5)	1479(4)	7153(4)	45(2)
C(32)	2586(4)	3569(4)	6434(4)	42(2)
C(33)	2937(5)	3849(4)	7140(4)	60(2)
C(34)	2964(6)	4601(5)	7281(5)	75(3)
C(35)	2645(6)	5097(5)	6722(6)	77(3)
C(36)	2291(6)	4834(5)	6021(5)	70(3)
C(37)	2269(5)	4067(4)	5875(4)	55(2)
C(38)	2753(4)	2616(4)	2847(4)	36(2)
C(39)	2391(5)	3301(4)	2957(4)	51(2)
C(40)	2468(6)	3889(5)	2432(5)	77(3)
C(41)	2913(6)	3773(5)	1781(5)	75(3)
C(42)	3266(5)	3099(5)	1652(4)	59(2)
C(43)	3200(4)	2503(4)	2185(4)	48(2)
C(44)	1766(4)	1303(4)	3044(4)	38(2)
C(45)	1826(5)	1014(5)	2310(4)	64(2)
C(46)	1183(6)	622(5)	1927(5)	82(3)
C(47)	442(5)	490(5)	2280(5)	65(2)
C(48)	379(5)	772(5)	2991(5)	67(2)
C(49)	1033(4)	1182(4)	3378(4)	48(2)
C(50)	3562(4)	1267(4)	3460(3)	35(2)
C(51)	3503(5)	489(4)	3569(4)	47(2)
C(52)	4212(5)	32(5)	3612(5)	62(2)
C(53)	4991(6)	333(5)	3570(5)	71(3)
C(54)	5074(5)	1109(5)	3457(5)	65(2)
C(55)	4352(4)	1565(4)	3409(4)	44(2)
N(3)	4958(11)	1271(10)	1153(11)	123(7)
C(56)	4330(12)	920(11)	1076(13)	131(9)
C(57)	3699(11)	326(10)	1157(11)	96(6)

Table A.7 for *trans*-[Ru(nabh*H*)(PPh_3)$_2$Cl] (1) (Chapter 4)

Atom	x	y	z	U(eq)
Ru	587(1)	2380(1)	4992(1)	38(1)
Cl	100(2)	2378(2)	6449(2)	59(1)
P(1)	645(1)	978(1)	5210(2)	38(1)
P(2)	434(1)	3778(1)	4887(2)	38(1)
O(1)	-312(4)	2306(5)	4099(5)	49(2)
N(1)	1020(5)	2312(5)	3745(5)	42(2)
N(2)	556(5)	2222(5)	2998(5)	46(2)
C(1)	1659(5)	2554(5)	5206(5)	33(2)
C(2)	1994(7)	2744(7)	6002(8)	51(3)
C(3)	2726(7)	2854(8)	6072(9)	66(4)
C(4)	3115(6)	2743(7)	5329(7)	46(3)
C(5)	3899(7)	2875(8)	5386(10)	66(3)
C(6)	4324(9)	2805(9)	4640(12)	84(5)
C(7)	4030(7)	2628(9)	3814(10)	77(4)
C(8)	3280(7)	2499(8)	3733(8)	62(3)
C(9)	2806(6)	2564(6)	4473(9)	46(3)
C(10)	2076(6)	2459(5)	4446(7)	35(2)
C(11)	1688(7)	2324(6)	3622(7)	49(3)
C(12)	-104(7)	2225(6)	3282(8)	47(3)
C(13)	-683(6)	2175(6)	2585(7)	54(3)
C(14)	-543(7)	2045(8)	1712(8)	74(4)
C(15)	-1063(9)	2006(9)	1086(10)	90(5)
C(16)	-1751(9)	2064(8)	1322(10)	84(5)
C(17)	-1922(7)	2212(12)	2185(12)	102(6)
C(18)	-1370(7)	2259(9)	2840(10)	86(5)
C(19)	1097(6)	330(5)	4389(7)	43(2)
C(20)	1546(6)	-267(7)	4621(8)	65(3)
C(21)	1775(7)	-792(8)	3995(8)	73(4)
C(22)	1596(7)	-710(8)	3115(8)	67(4)

C(23)	1160(7)	-110(7)	2869(8)	64(3)
C(24)	902(7)	418(7)	3507(8)	56(3)
C(25)	1079(6)	720(6)	6288(7)	46(3)
C(26)	719(8)	374(11)	6979(10)	90(5)
C(27)	1038(9)	208(12)	7752(11)	105(6)
C(28)	1786(11)	360(12)	7855(11)	107(6)
C(29)	2137(7)	707(9)	7174(8)	70(4)
C(30)	1784(7)	891(7)	6385(8)	57(3)
C(31)	-224(6)	506(6)	5244(7)	48(3)
C(32)	-857(6)	926(7)	5347(8)	59(3)
C(33)	-1498(6)	555(10)	5397(9)	75(4)
C(34)	-1541(9)	-217(11)	5328(9)	82(5)
C(35)	-944(9)	-671(10)	5240(14)	110(7)
C(36)	-286(6)	-280(7)	5175(9)	67(4)
C(37)	829(6)	4456(6)	5695(7)	46(3)
C(38)	905(8)	4217(8)	6594(8)	65(4)
C(39)	1183(8)	4696(10)	7199(11)	82(4)
C(40)	1375(8)	5393(13)	6987(13)	101(7)
C(41)	1330(7)	5696(9)	6110(12)	83(4)
C(42)	1047(6)	5188(7)	5472(9)	64(3)
C(43)	794(6)	4123(6)	3851(7)	43(2)
C(44)	1516(7)	4237(8)	3755(9)	64(3)
C(45)	1806(8)	4433(9)	2942(11)	81(4)
C(46)	1388(9)	4493(9)	2172(10)	80(4)
C(47)	663(9)	4394(8)	2260(9)	74(4)
C(48)	353(7)	4211(7)	3082(7)	56(3)
C(49)	-499(5)	4105(5)	4902(9)	45(2)
C(50)	-686(6)	4852(7)	4677(7)	53(3)
C(51)	-1380(7)	5114(8)	4679(8)	66(4)
C(52)	-1911(6)	4603(8)	4906(10)	72(3)
C(53)	-1742(7)	3815(8)	5107(13)	97(5)

C(54)	-1042(5)	3589(7)	5103(10)	64(3)

Table A.8 for *trans*-[Ru(nabhNO_2)(PPh_3)$_2$Cl] (5) (Chapter 4)

Atom	x	y	z	U(eq)
Ru	531(1)	7930(1)	1223(1)	36(1)
Cl	-35(1)	6526(1)	1222(1)	59(1)
P(1)	614(1)	7695(1)	562(1)	36(1)
P(2)	438(1)	8031(1)	1890(1)	37(1)
O(1)	-325(2)	8858(3)	1193(1)	51(1)
O(2)	-2823(5)	12144(6)	1161(3)	142(3)
O(3)	-2077(5)	13040(6)	912(4)	176(5)
N(1)	971(3)	9154(3)	1182(1)	39(1)
N(2)	548(3)	9905(3)	1149(1)	43(1)
N(3)	-2238(6)	12335(7)	1074(3)	119(3)
C(1)	1581(3)	7670(4)	1288(2)	40(1)
C(2)	1891(4)	6850(4)	1378(2)	54(2)
C(3)	2606(4)	6761(5)	1413(2)	58(2)
C(4)	3058(4)	7508(4)	1365(2)	50(2)
C(5)	3802(4)	7408(5)	1398(2)	64(2)
C(6)	4230(4)	8128(6)	1364(2)	74(2)
C(7)	3939(4)	8972(6)	1297(2)	68(2)
C(8)	3234(4)	9085(5)	1259(2)	58(2)
C(9)	2770(3)	8353(4)	1289(2)	45(2)
C(10)	2016(3)	8422(4)	1249(2)	41(1)
C(11)	1646(3)	9234(4)	1184(2)	42(1)
C(12)	-101(3)	9653(4)	1162(2)	41(1)
C(13)	-649(4)	10394(5)	1150(2)	50(2)
C(14)	-483(4)	11236(5)	1041(2)	66(2)
C(15)	-990(4)	11898(5)	1019(3)	82(3)
C(16)	-1651(5)	11677(6)	1114(3)	77(2)
C(17)	-1850(4)	10859(7)	1238(2)	81(3)

C(18)	-1331(4)	10180(5)	1248(2)	69(2)
C(19)	-215(3)	7583(4)	309(2)	40(1)
C(20)	-862(3)	7681(4)	483(2)	51(2)
C(21)	-1465(4)	7622(4)	276(2)	61(2)
C(22)	-1448(4)	7458(4)	-106(2)	66(2)
C(23)	-811(4)	7362(4)	-281(2)	61(2)
C(24)	-199(4)	7432(4)	-77(2)	54(2)
C(25)	1075(3)	6647(4)	462(2)	43(1)
C(26)	707(4)	5879(4)	371(2)	59(2)
C(27)	1050(5)	5083(5)	321(2)	77(2)
C(28)	1764(5)	5038(5)	359(2)	82(3)
C(29)	2142(4)	5774(5)	449(2)	68(2)
C(30)	1796(3)	6591(5)	510(2)	54(2)
C(31)	1051(3)	8536(4)	269(2)	37(1)
C(32)	1584(3)	8352(4)	19(2)	51(2)
C(33)	1842(4)	9024(5)	-217(2)	61(2)
C(34)	1572(4)	9866(4)	-199(2)	60(2)
C(35)	1035(4)	10050(4)	46(2)	59(2)
C(36)	785(4)	9396(4)	280(2)	51(2)
C(37)	851(3)	7183(4)	2186(2)	45(2)
C(38)	824(4)	6295(5)	2081(2)	59(2)
C(39)	1094(5)	5632(5)	2299(3)	81(3)
C(40)	1395(5)	5849(6)	2633(3)	85(3)
C(41)	1420(5)	6706(6)	2752(2)	81(2)
C(42)	1149(4)	7379(5)	2528(2)	67(2)
C(43)	809(4)	9079(4)	2046(2)	47(2)
C(44)	1534(4)	9168(5)	2076(2)	62(2)
C(45)	1837(5)	10000(7)	2163(2)	86(3)
C(46)	1405(7)	10745(6)	2210(3)	98(3)
C(47)	692(6)	10660(5)	2175(2)	84(3)
C(48)	387(4)	9836(4)	2092(2)	62(2)

C(49)	-459(3)	8033(4)	2079(2)	41(1)
C(50)	-579(4)	8162(4)	2461(2)	56(2)
C(51)	-1248(4)	8188(5)	2607(2)	66(2)
C(52)	-1807(4)	8081(5)	2383(3)	75(2)
C(53)	-1704(4)	7946(6)	2006(2)	84(3)
C(54)	-1040(4)	7919(5)	1858(2)	63(2)
N(4)	-456(6)	14020(7)	748(4)	158(5)
C(55)	-896(6)	14542(7)	716(3)	101(3)
C(56)	-1442(6)	15204(8)	690(4)	149(5)
N(5)	1712(13)	8796(17)	3338(10)	260(15)
C(57)	1386(10)	9418(12)	3249(6)	111(7)
C(58)	825(11)	10025(14)	3147(7)	130(8)

Table A.8 for *cis*-[Ru(L^1)$_3$(PPh_3)$_2$] (3) (Chapter 5)

Atom	x	y	z	U(eq)
Ru	2454(1)	6728(1)	2268(1)	27(1)
S(1)	3791(1)	7837(1)	3087(1)	36(1)
S(2)	1368(1)	5243(1)	1858(1)	37(1)
P(1)	3129(1)	7045(1)	1220(1)	31(1)
P(2)	1040(1)	7644(1)	1965(1)	33(1)
N(1)	4163(3)	5151(3)	2982(3)	35(1)
N(2)	3814(3)	6068(3)	2861(3)	30(1)
N(3)	2119(4)	6147(4)	3991(3)	39(1)
N(4)	1934(3)	6039(3)	3181(3)	33(1)
C(1)	4303(5)	3171(5)	3245(4)	48(2)
C(2)	4579(5)	2223(5)	3408(4)	49(2)
C(3)	4811(6)	1889(5)	4173(5)	64(2)
C(4)	5070(7)	987(6)	4335(6)	75(2)
C(5)	5103(7)	367(6)	3736(6)	79(3)
C(6)	4910(6)	659(5)	2985(6)	66(2)
C(7)	4652(5)	1611(5)	2791(4)	49(2)

C(8)	4481(5)	1978(5)	2017(5)	51(2)
C(9)	4628(6)	1443(6)	1388(5)	68(2)
C(10)	4505(6)	1821(7)	655(6)	76(3)
C(11)	4219(5)	2745(6)	524(5)	64(2)
C(12)	4067(5)	3301(5)	1125(4)	47(2)
C(13)	4186(4)	2940(4)	1868(4)	41(2)
C(14)	4084(4)	3535(4)	2508(4)	38(1)
C(15)	3797(4)	4532(4)	2409(4)	37(1)
C(16)	4374(4)	6781(4)	3316(3)	32(1)
C(17)	5356(4)	6748(4)	3928(3)	36(1)
C(18)	6095(5)	7512(5)	4013(4)	47(2)
C(19)	7013(5)	7522(6)	4607(5)	63(2)
C(20)	7193(5)	6785(6)	5121(4)	62(2)
C(21)	6462(5)	6033(6)	5046(4)	58(2)
C(22)	5543(5)	6001(5)	4452(4)	49(2)
C(23)	2755(2)	6511(6)	5630(4)	90(3)
C(24)	2901(2)	6545(5)	6413(4)	96(3)
C(25)	3173(3)	5696(6)	6835(6)	109(4)
C(26)	3298(4)	5828(7)	7623(7)	134(4)
C(27)	3184(5)	6698(9)	8023(6)	151(5)
C(28)	2915(4)	7458(8)	7519(5)	130(4)
C(29)	2761(2)	7424(5)	6695(4)	78(2)
C(30)	2492(3)	8278(5)	6289(5)	86(2)
C(31)	2359(4)	9144(7)	6594(7)	152(5)
C(32)	2091(5)	9911(6)	6098(7)	140(5)
C(33)	1959(5)	9796(7)	5294(7)	194(8)
C(34)	2098(4)	8882(7)	4968(6)	141(5)
C(35)	2357(3)	8131(5)	5439(5)	95(3)
C(36)	2482(3)	7259(5)	5089(3)	53(2)
C(37)	2317(5)	7023(4)	4263(4)	40(1)
C(38)	1440(4)	5232(4)	2844(3)	33(1)

C(39)	954(4)	4439(4)	3197(4)	39(1)
C(40)	831(6)	3518(5)	2855(5)	56(2)
C(41)	352(7)	2751(6)	3141(6)	76(3)
C(42)	-39(6)	2900(6)	3757(6)	74(3)
C(43)	57(5)	3803(6)	4094(5)	65(2)
C(44)	559(5)	4575(5)	3827(4)	52(2)
C(45)	3001(4)	6043(4)	499(4)	37(1)
C(46)	2094(5)	5451(4)	246(4)	42(2)
C(47)	1948(6)	4768(5)	-355(4)	54(2)
C(48)	2706(6)	4618(6)	-697(5)	64(2)
C(49)	3607(6)	5181(6)	-451(5)	72(2)
C(50)	3754(5)	5896(6)	130(4)	57(2)
C(51)	2696(4)	8040(4)	567(4)	40(1)
C(52)	2365(6)	7923(6)	-239(4)	62(2)
C(53)	2021(8)	8690(7)	-706(6)	85(3)
C(54)	2054(8)	9583(7)	-368(6)	87(3)
C(55)	2387(7)	9729(6)	432(6)	71(2)
C(56)	2698(5)	8951(4)	904(4)	47(2)
C(57)	4540(4)	7354(4)	1503(4)	38(1)
C(58)	4984(5)	8252(5)	1415(5)	57(2)
C(59)	6047(6)	8469(6)	1656(6)	75(3)
C(60)	6663(5)	7771(6)	1992(5)	65(2)
C(61)	6243(5)	6867(6)	2071(4)	55(2)
C(62)	5192(5)	6649(5)	1830(4)	45(2)
C(63)	1273(5)	8977(4)	2110(4)	42(2)
C(64)	2011(5)	9363(5)	2772(5)	54(2)
C(65)	2231(6)	10349(5)	2904(6)	72(2)
C(66)	1724(7)	10965(6)	2354(7)	88(3)
C(67)	993(7)	10600(6)	1709(6)	78(3)
C(68)	772(5)	9619(5)	1572(5)	59(2)
C(69)	71(4)	7515(4)	998(4)	39(2)

C(70)	-911(5)	7830(5)	896(5)	52(2)
C(71)	-1607(5)	7760(6)	166(6)	67(2)
C(72)	-1359(6)	7383(6)	-469(5)	73(3)
C(73)	-392(6)	7045(6)	-370(4)	67(2)
C(74)	303(5)	7135(5)	365(4)	51(2)
C(75)	187(4)	7370(5)	2594(4)	41(2)
C(76)	137(5)	7956(6)	3213(5)	62(2)
C(77)	-460(7)	7676(8)	3707(5)	79(3)
C(78)	-1040(6)	6804(8)	3561(6)	79(3)
C(79)	-1030(5)	6220(6)	2938(5)	63(2)
C(80)	-432(5)	6503(5)	2455(4)	50(2)

Table A.10 for *cis*-[Ru(L^1)$_4$(PPh_3)$_2$] (4) (Chapter 5)

	x	y	z	U(eq)
Ru	2289(1)	2270(1)	1100(1)	52(1)
S(1)	3099(2)	2772(2)	457(1)	62(1)
S(2)	1278(2)	1456(2)	1504(1)	64(1)
P(1)	3666(2)	2396(2)	1637(1)	51(1)
P(2)	1438(2)	3304(2)	1315(1)	56(1)
N(1)	2960(7)	690(7)	621(4)	74(3)
N(2)	2941(7)	1438(6)	674(3)	71(3)
N(3)	638(7)	1871(6)	166(3)	69(3)
N(4)	1038(6)	1883(5)	643(3)	54(3)
C(1)	2720(10)	-879(9)	578(4)	91(5)
C(2)	2689(13)	-1635(10)	575(6)	129(7)
C(3)	2793(11)	-2045(8)	992(6)	86(5)
C(4)	2722(12)	-2852(10)	984(6)	116(6)
C(5)	2795(11)	-3243(9)	1397(8)	115(6)
C(6)	2928(11)	-2889(12)	1843(7)	99(6)
C(7)	3000(11)	-3295(10)	2265(8)	109(6)
C(8)	3104(11)	-2962(11)	2705(7)	109(7)

C(9)	3208(9)	-2177(10)	2738(5)	92(5)
C(10)	3128(8)	-1748(10)	2319(6)	73(5)
C(11)	3174(9)	-947(9)	2315(5)	83(4)
C(12)	3111(9)	-533(7)	1914(5)	74(4)
C(13)	2947(9)	-880(7)	1447(4)	61(4)
C(14)	2926(9)	-1674(8)	1431(5)	64(4)
C(15)	2983(9)	-2081(10)	1862(6)	75(4)
C(16)	2862(9)	-472(8)	1010(5)	67(4)
C(17)	2871(9)	340(8)	1028(5)	79(4)
C(18)	3218(7)	1834(7)	328(4)	49(3)
C(19)	3616(10)	1599(7)	-130(4)	57(4)
C(20)	3264(9)	1961(7)	-551(4)	73(4)
C(21)	3622(12)	1777(9)	-983(4)	90(5)
C(22)	4350(14)	1255(11)	-979(7)	120(8)
C(23)	4659(11)	890(9)	-570(6)	109(6)
C(24)	4287(10)	1045(7)	-140(5)	77(4)
C(25)	-25(10)	2021(8)	-818(5)	91(5)
C(26)	-341(9)	2113(9)	-1303(5)	96(5)
C(27)	-109(9)	2730(10)	-1565(5)	75(5)
C(28)	-413(10)	2831(11)	-2063(5)	106(6)
C(29)	-189(15)	3463(13)	-2299(6)	122(8)
C(30)	394(12)	4024(13)	-2062(6)	97(6)
C(31)	633(14)	4650(12)	-2310(6)	112(7)
C(32)	1121(14)	5203(10)	-2079(6)	117(8)
C(33)	1492(10)	5142(9)	-1589(6)	102(6)
C(34)	1309(13)	4515(10)	-1324(6)	95(6)
C(35)	1644(10)	4376(9)	-829(5)	91(5)
C(36)	1404(10)	3769(9)	-596(5)	82(5)
C(37)	811(9)	3207(8)	-819(5)	65(4)
C(38)	472(9)	3291(9)	-1328(4)	64(4)
C(39)	742(11)	3947(9)	-1569(5)	74(5)

C(40)	545(8)	2567(8)	-570(4)	52(3)
C(41)	900(8)	2451(7)	-66(4)	66(4)
C(42)	682(8)	1394(6)	931(4)	54(3)
C(43)	-136(5)	861(5)	842(3)	67(4)
C(44)	-233(9)	418(8)	420(4)	95(9)
C(45)	-1019(9)	-65(8)	341(4)	97(9)
C(46)	-1683(7)	-98(6)	677(4)	110(6)
C(47)	-1576(9)	335(8)	1082(5)	166(16)
C(48)	-796(9)	817(8)	1164(4)	98(9)
C(44A)	-88(8)	150(7)	1059(4)	102(10)
C(45A)	-874(9)	-331(6)	974(4)	88(9)
C(47A)	-1724(8)	598(8)	466(5)	220(20)
C(48A)	-941(9)	1081(7)	550(5)	171(16)
C(49)	4632(9)	1795(7)	1478(4)	61(4)
C(50)	5126(9)	1843(8)	1079(4)	74(4)
C(51)	5812(10)	1358(9)	973(5)	81(5)
C(52)	6014(11)	721(9)	1245(6)	95(5)
C(53)	5497(12)	621(8)	1617(5)	104(6)
C(54)	4852(9)	1143(9)	1740(4)	79(5)
C(55)	4209(9)	3337(7)	1695(4)	64(4)
C(56)	3935(9)	3818(9)	2031(5)	83(4)
C(57)	4225(13)	4577(9)	2060(6)	106(6)
C(58)	4817(15)	4813(12)	1746(7)	134(8)
C(59)	5120(12)	4368(11)	1413(6)	114(7)
C(60)	4791(10)	3620(8)	1380(5)	95(5)
C(61)	3696(8)	2127(6)	2278(3)	47(3)
C(62)	4413(7)	2365(7)	2627(4)	55(3)
C(63)	4454(9)	2110(7)	3102(4)	70(4)
C(64)	3787(10)	1614(8)	3241(4)	74(4)
C(65)	3091(9)	1360(7)	2893(5)	75(4)
C(66)	3041(9)	1624(7)	2414(4)	67(4)

C(67)	1557(9)	4165(7)	962(4)	59(4)
C(68)	820(10)	4673(8)	820(5)	89(5)
C(69)	987(11)	5269(8)	539(5)	89(5)
C(70)	1888(12)	5407(8)	404(5)	87(5)
C(71)	2635(11)	4952(7)	563(5)	78(4)
C(72)	2446(9)	4331(7)	845(4)	67(4)
C(73)	123(8)	3157(7)	1223(4)	61(4)
C(74)	-363(10)	3182(7)	760(5)	69(4)
C(75)	-1324(12)	3013(8)	674(5)	95(5)
C(76)	-1816(11)	2802(9)	1054(7)	110(6)
C(77)	-1338(11)	2734(9)	1508(7)	110(6)
C(78)	-382(11)	2916(7)	1593(4)	81(5)
C(79)	1588(9)	3640(8)	1949(4)	62(4)
C(80)	1650(9)	4412(8)	2057(5)	79(4)
C(81)	1772(11)	4631(10)	2530(6)	110(6)
C(82)	1848(12)	4114(11)	2892(6)	112(6)
C(83)	1782(10)	3353(10)	2794(5)	92(5)
C(84)	1650(8)	3121(8)	2313(5)	72(4)
Cl(1)	6095(4)	3409(4)	208(2)	188(3)
Cl(2)	4720(5)	4079(4)	-465(2)	263(4)
C(85)	5146(14)	3356(14)	-190(7)	244(14)

List of Publications

Thesis Work

1. Synthesis of ruthenium(III) complexes with *N*-(2-pyridyl)-*N′*-(5-*R*-salicylidene)hydrazines: Physical properties and structural studies
   K. Nagaraju, R. Raveendran, Satyanarayan Pal, S. Pal
   Polyhedron 33 (2012) 52–59.
2. Ruthenium(III) cyclometallates: Regioselective metallation of 1-pyrenyl in 1-pyrenaldehyde 4-*R*-benzoylhydrazones
   K. Nagaraju, S. Pal
   J. Organomet. Chem. 737 (2013) 7–11.
3. *Ortho*-ruthenation of 1-naphthalenyl in 1-naphthaldehyde 4-*R*-benzoylhydrazones: Ruthenium(III) CNO pincer complexes
   K. Nagaraju, S. Pal
   J. Organomet. Chem. 745-746 (2013) 404–408.
4. Complexes of *cis*-$\{Ru(PPh_3)_2\}^{2+}$ with N,S-donor thiobenzhydrazones of polycyclic aromatic aldehydes: Synthesis, properties and structures
   K. Nagaraju, S. Pal
   Inorg. Chim. Acta (Submitted)

Other Publications

1. Non-oxo vanadium(IV) complexes with acetylacetone 4-*R*-benzoylhydrazones
   K. Nagaraju, A. Sarkar, Satyanarayan Pal, S. Pal
   J. Coord. Chem. 66 (2013) 77–88.
2. Cyclometallates of ruthenium(III) with 9-anthraldehyde aroylhydrazones
   K. Nagaraju, S. Pal (Manuscript under preparation)

Posters and Presentations

1. Synthesis of Ruthenium(III) Complexes with N-(2-Pyridyl)-5-R-Salicylidene)Hydrazines: Physical Properties and Structural Studies

   K. Nagaraju, R. Raveendran, Satyanarayan Pal, S. Pal

   Poster Presentation

   Modern Trends in Inorganic Chemistry, 2011 (**MTIC-XIII, 2011),** University of Hyderabad, Hederabad.

2. Synthesis, Structures and Properties of Ruthenium(III) and Ruthenium(II) Complexes with Some Aroylhydrazones and Thiobenzoylhydrazones

   K. Nagaraju, S. Pal

   Poster and Oral Presentation

   CHEMFEST-2013, University of Hyderabad, Hederabad.